universität wien

DISSERTATION / DOCTORAL THESIS

Titel der Dissertation /Title of the Doctoral Thesis

„Bacterial Ghosts as carriers of ice nucleation proteins“

verfasst von / submitted by

Johannes Kaßmannhuber, BSc MSc

angestrebter akademischer Grad / in partial fulfilment of the requirements for the degree of

Doctor of Philosophy (PhD)

Wien, 2017 / Vienna 2017

Studienkennzahl lt. Studienblatt / degree programme code as it appears on the student record sheet:	A 794 685 437
Dissertationsgebiet lt. Studienblatt / field of study as it appears on the student record sheet:	Biologie
Betreut von / Supervisor:	Ao. Univ. Prof. Dr. Angela Witte
Mitbetreut von / Co-Supervisor:	Univ. Prof. i. R. Werner Lubitz

Danksagung

Recht herzlich bedanken möchte ich mich bei Prof. Angela Witte und Prof. Werner Lubitz, einerseits für die Möglichkeit diese Dissertation zu verfassen und andererseits für Ihre tatkräftige Unterstützung, ihre Hilfe und ihr Engagement innerhalb dieser spannenden und interessanten Aufgabenstellung.

Des Weiteren möchte ich mich bei Bird-C GmbH & Co KG bedanken, die diese Arbeit finanziert hat, sowie bei Petra Lubitz, Lea Schöner, Mascha Rauscher, Abbas Muhammad, Marek Sramko, Beate Mayr, Pavol Kudela, Timo Langemann, Ela Herwig, Ivana Hodul, Laura Felgitsch und bei allen, die ich vergessen habe, für ihren Beitrag an dieser Arbeit und ihre Hilfe.

Meinen Eltern gilt besonderer Dank, ohne Sie wäre all dies nicht möglich gewesen, sowie meinen Geschwistern Lucas & Eva für ihre treue Unterstützung.

Zum Schluss möchte ich mich noch bei meinen Liebsten, Kathrin und unserem Paul bedanken, für ihre Geduld und die vielen Aufmunterungen.

Die Vernunft ahmt die Natur nach.

Thomas von Aquin

Weise ist der Mensch, wenn ihm alle Dinge so schmecken, wie sie wirklich sind.

Klassische Lehre von der Klugheit

Bacterial Ghosts as carriers of ice nucleation proteins

Contents

Abbreviations **10**
Objectives **12**
Summary **13**
Zielsetzung **15**
Zusammenfassung **16**

1 Introduction **18**
1.1 Ice nucleation 18
1.2 Bacterial ice nuclei 20
1.2.1 Ecology of ina$^+$ bacteria 21
1.2.2 Bacterial ice nucleation proteins 23
1.2.3 Applications of ina$^+$ bacteria 27
1.3 Bacterial antifreeze proteins 28
1.4 Bacterial Ghosts 30
1.4.1 Recombinant Bacterial Ghost system 31
1.4.2 Bacterial Ghost production 34
1.5 Ethyleneimine as inactivation agent for bacteria 35
1.6 References 36
2 Outer-membrane anchored INP on BGs envelope **44**
2.1 Publication. Functional display of ice nucleation protein InaZ on the surface of bacterial ghosts 44
2.2 Contribution to Publication 44
2.3 Ice nucleation activity of ina$^+$ *E. coli* C41 overnight cultures 58
2.3.1 Introduction 58
2.3.2 Results 58
2.3.3 Discussion 59
2.4 References 60
3 BGs carrying inner-membrane anchored INP **61**
3.1 Manuscript I. Freezing from the inside. Ice nucleation in *Escherichia coli* and *Escherichia coli* ghosts by inner membrane bound ice nucleation protein InaZ 61
3.2 Contribution to manuscript I 61
3.3 Manuscript I 62
4 BGs carrying truncated forms of InaZ **81**
4.1 BGs carrying INP288 81
4.1.1 Introduction 81
4.1.2 Construction of plasmid pBinp288 81
4.1.3 E-lysis studies and droplet-freezing assay 82
4.2 BGs carrying INP96 on the outer membrane 84
4.2.1 Introduction 84
4.2.2 Construction of plasmid pBNinaZ_inp96/his 84
4.2.3 Expression and E-lysis studies 86
4.3 BGs displaying OmpA-INP96 fusion protein 87
4.3.1 Introduction 87
4.3.2 Construction of plasmid pHS64inp96/his 87

4.3.3 E-lysis of *E. coli* C2988J (pGLysivb, pHS64inp96his) ... 88
4.4 BGs carrying cytoplasmic located INP96 integrated into S-layers SbsA and SbsB ... 89
4.4.1 Introduction ... 89
4.4.2 Construction of plasmid pUCsbsAinp96/his and pAKinp96/his ... 89
4.4.3 E-lysis ... 91
4.5 Discussion ... 92
4.6 References ... 93
5 Ethyleneimine (EI) inactivation of BG preparations ... 94
5.1 EI inactivation studies of *Bordetella bronchiseptica* BGs ... 94
5.1.1 Results ... 94
5.2 Ice nucleation activity of EI treated BGs carrying ice nucleation protein InaZ ... 97
5.2.1 Results ... 97
5.3 Discussion ... 100
5.4 References ... 101
5.5 Manuscript II. *Bordetella bronchiseptica* Bacterial Ghost vaccine for canines ... 102
5.5.1 Contribution to Manuscript II ... 102
5.5.2 Manuscript II (style *Vaccine* to be submitted) ... 103
6 Material and Methods ... 122
6.1 Material ... 122
6.2 Bacterial strains ... 122
6.3 Growth media ... 123
6.4 Antibiotics ... 123
6.5 Buffers & Solutions ... 123
6.6 Cloning ... 124
6.7 PCR ... 124
6.8 CaCl2 / RbCl2 competent cells ... 124
6.9 Transformation of CaCl2 / RbCl2 competent cells ... 125
6.10 Growth and E-lysis of ice nucleation active bacteria ... 125
6.11 Expression- and lysis-study in small scale ... 125
6.12 Monitoring and determination of E-lysis efficiency ... 126
6.13 β-propiolactone-treatment after E-lysis process ... 126
6.14 Ethyleneimine-treatment after E-lysis process ... 126
6.15 Mid-scale *B. bronchiseptica* BG production ... 127
6.16 Sterility testing of BGs ... 128
6.17 Protein sample preparation ... 128
6.18 Protein sample preparation of lysed culture ... 128
6.19 Gel-Electrophoresis of proteins ... 128
6.20 Production of antibodies ... 128
6.21 Western blot ... 129
6.22 Production of INP antibodies ... 129
6.23 Ice-nucleating activity measurements ... 129
6.24 References ... 130
7 Appendix ... 131
7.1 Summary of produced BG constructs ... 131
7.2 Supplementary data for chapter 2.1 ... 131

Abbreviations

Ab	antibodies
AF	anti-freeze
AFP	antifreeze protein
BG	bacterial ghost
bp	base pairs
BPL	β-propiolactone
C	celsius
cfu	colony forming units
Da	dalton
DC	dendritic cells
dH2O	deionized water
DNA	deoxyribonucleic acid
Dox	doxorubicin
EcN	*Escherichia coli* Nissle 1917
EHEC	enterohemorrhagic *Escherichia coli*
EI	ethylenemine
FCM	flow cytometry measurement
f_{ice} %	fraction of frozen droplets in percent
FSC	forward scatter
g	gram
GMO	genetically modified organism
h	hours
HRP	horseradish peroxidase
IBP	ice-binding Protein
Ig	immunoglobulin
IM	inner membrane
IN	ice nucleus
ina-	ice nucleation active minus
ina^+	ice nucleation active
INP	ice nucleation protein
IRI	ice recrystallization inhibition
k	kilo
L,l	liter
LB	Luria-Bertani medium
LBv	’vegetarian’ Luria-Bertani medium
LE	lysis efficacy
LI	time point of E-lysis induction
LPS	lipopolysaccharide
LR	lysis rate
M	Mol
m	milli

M	mega
MBP	maltose binding protein
MCS	multiple cloning site
min	minute
MP	melting point
n	nano
nm	nanometer
OD_{600}	optical density at 600 nm
OM	outer membrane
ORF	open reading frame
PBS	phosphate buffered saline
PCR	polymerase chain reaction
pH	potentia hydrogenii
rbs	ribosome binding site
RE	restriction enzyme
RNA	ribonucleic acid
RT	real-time
s	second
SSC	side scatter
TFF	tangential flow filtration
T_{50}	temperature of 50 % frozen droplets
THF	thermal hysteresis protein
V	volt
WB	western blot
µ	micro
Ω	ohm
°	degree

Objectives

Bacterial ghosts (BGs) are defined as empty cell envelops derived from Gram-negative bacteria produced by controlled expression of the cloned gene *E* of bacteriophage ΦX174. BGs represent the bacterial cell-envelope composition at the time point of their production. BGs are composed of the three distinct Gram-negative cell-layers, cytoplasmic membrane, peptidoglycan within the periplasmic space and the bacterial outer-membrane

The aim of this thesis was to insert the bacterial ice nucleation protein (INP) InaZ of *Pseudomonas syringae* on the surface of the outer-membrane of *E. coli* BGs and to expose it on the inner-membrane facing the internal lumen of the BGs. The ability of different constructed INP-BGs to act as ice nuclei catalyzing heterogeneous ice formation of supercooled ultra-pure water had to be investigated by droplet-freezing assay to evaluate and compare the efficiency of orienting water molecules into an ice-like structure.

Another aim of this thesis was to produce for the first time BGs from the animal pathogen *Bordetella bronchiseptica* and inactivate E-lysis escape mutants with ethyleneimine (EI). The EI inactivated BGs were used as vaccine candidate for kennel cough in dogs and were immunogenetically compared to a commercial vaccine also inactivated with EI.

The structural functionality of ice nucleation of INP *E. coli* BGs after EI or β-propriolactone (BPL) inactivation had to be compared.

Summary

The thesis “Bacterial ghosts as carriers of ice nucleation proteins” describes the development of different

Bacterial Ghosts (BGs) carrying the *P. syringae* ice nucleation protein (INP) InaZ and truncated forms of it at the different compartments of the cell envelope like outer and inner membrane. INP-BGs revealed similar to higher ice nucleation (IN) activity compared to their corresponding living *E. coli* parental strains. IN activity was determined by a droplet-freezing assay, for which a cooling device was constructed for detection of expressed INP.

BG outer-membrane anchored INP

Antibodies against INP had been produced and used for the detection of different recombinant expressed INP in *E. coli*. For the production of BGs displaying INP on their surface two different E-lysis plasmids have been used and both reached E-lysis efficiencies (LE) of 99.9 %. By Western blot analysis the stability of INP during E-mediated lysis process could be demonstrated. INP-BGs produced under different conditions have been shown to act as type II ice nuclei with first freezing activity at -6°C, whereas first droplet freezing activity of the parental living *E. coli* cells were detected at -5.5°C. Moreover, by extension of INP expression it could be demonstrated that living *E. coli* cells could also exhibit type I IN activity with highest nucleation temperatures at -2°C.

BG inner-membrane anchored INP

In order to bind INP to the inner membrane (IM) of *E. coli* a truncated form of InaZ was fused to N-terminal and C-terminal membrane anchoring motifs. Thereby, the resulting INP fusion proteins could be anchored either (i) with the amino-terminal sequence, (ii) the carboxy-terminal sequence, or (iii) with both end sequences to the IM. The different INP fusion proteins were produced in *E. coli* C41 and induced expression of the lysis gene *E* generated corresponding INP-BGs. For all three variants LE >99.7 % could be achieved and the presence of IM anchored INP was confirmed by Western blot analysis. The tested INP-BG variants carrying IM anchored INP showed first droplet freezing events between -6°C and -8°C. First droplet freezing of the parental living *E. coli* cells was detected at temperatures between -7°C and -9°C.

Other forms of truncated InaZ derived INP constructs

S-layer proteins SbsA and SbsB have been used as carriers of a truncated form of InaZ (INP96). INP96 corresponds to aa 176 - 273 of the 1200aa long InaZ. To display INP96 on the surface of BGs, an OmpA-INP96 sandwich fusion was generated, where INP96 is inserted into the second surface exposed region. Moreover, the INP N-terminal domain acting as outer-membrane anchor has been successfully used to display INP96 on the surface of BGs. As INPs are thought to be larger variants of antifreeze proteins, a C-terminal truncated InaZ variant, INP288 (aa 1 – 470 of InaZ), was constructed. Possible antifreeze activity could not be confirmed by droplet freezing assay.

EI inactivation of BG preparations from *Bordetella bronchiseptica*

This investigation was performed to produce for the first time BGs from *B. bronchiseptica*. Also for the first time, ethyleneimine (EI) was used to inactivate E-lysis escape mutants of *B. bronchiseptica* and *E. coli*. EI inactivation was also used for the production of INP-BGs and their IN activity was compared to β-propriolactone (BPL) inactivation of INP-BGs of *E. coli*. It could be demonstrated that BPL inactivated INP-BGs exhibited a better IN activity.

Dogs vaccinated with newly developed *B. bronchiseptica* BGs inactivated with EI demonstrated significant protection from spontaneous coughing, duration of coughing, and induced coughing scores.

Zielsetzung

Bacterial Ghosts (BGs) sind definiert als leere Zellhüllen, welche von Gram-negativen Bakterien abstammen und durch kontrollierte Expression des klonierten Gens *E* vom Bakteriophagen ΦX174 erzeugt werden. BGs spiegeln die vollständige Zellschichtzusammensetzung des Vorgänger-Bakteriums zum Zeitpunkt ihrer Herstellung wider. Folglich bestehen BGs aus den drei verschiedenen Gram-negativen Zellschichten, der cytoplasmatischen Membran, dem Peptidoglycan im periplasmatischen Raum und der bakteriellen äußeren Membran.

Das Hauptziel dieser Arbeit war, das bakterielle Eisnukleationsprotein (INP) InaZ von *Pseudomonas syringae* an der Oberfläche der äußeren Membran von *E. coli* BGs zu verankern, sowie an deren inner Membran, dem internen Lumen der BGs zugewandt. Durch Tröpfchen-Gefrier-Versuche wurde die Fähigkeit der unterschiedlich konstruierten INP-BGs als Eiskeime zu wirken und somit die heterogene Eisbildung von unterkühltem Wasser zu katalysieren, untersucht, um deren Effizienz Wassermoleküle in einer eisartigen Struktur anzuordnen, bewerten und vergleichen zu können.

Ein weiteres Ziel dieser Arbeit war die BG Produktion des Tierpathogenen Bakteriums *Bordetella bronchiseptica* sowie die Inaktivierung von E-Lyse überlebenden Mutanten durch Ethyleneimin (EI).

Die inaktivierten BGs wurden als Impfstoffkandidat an Zwingerhusten leidenden Hunden getestet. Darüber hinaus wurde die Eisnukleationsaktivität von EI und β-Propriolacton (BPL) inaktivierten INP-BGs verglichen.

Zusammenfassung

Die Doktorarbeit “Bacterial ghosts as carriers of ice nucleation proteins” beschreibt die Herstellung verschiedener Bacterial Ghosts (BGs), welche das Eisnukleationsprotein (INP) InaZ aus *P. syringae* und verkürzte Formen davon an der äußeren und inneren Membran tragen. INP-BGs zeigten eine ähnlich hohe bzw. höhere Eisnukleationsaktivität verglichen mit ihren lebenden *E. coli* Vorfahren. Durch eine eigens konstruierte Kühlvorrichtung wurde die Eisnukleationsaktivität der INP tragenden Konstrukte durch Tröpfchen-Gefrier-Versuche bestimmt.

BGs mit außer-Membran verankertem INP

Zunächst wurden Antikörper gegen INP produziert, um INP in den unterschiedlichen rekombinanten *E. coli* Stämmen nachzuweisen. Für die Produktion von BGs, die das INP auf der BG-Oberfläche tragen, wurden zwei verschiedene E-Lyse-Plasmide verwendet und mit beiden wurde eine E-Lyseeffizienz von 99,9 % erreicht. Durch Western-Blot-Analyse konnte die Stabilität von INP während des E-vermittelten Lyseprozesses nachgewiesen werden. Es wurde gezeigt, dass die zwei verschieden produzierten ina$^+$ BGs als Typ II Eiskeime wirken mit einer ersten Gefrieraktivität bei -6°C. Die erste Gefrieraktivität lebender ina$^+$ *E. coli* Zellen wurde bereits bei -5,5°C nachgewiesen. Bei extensiver INP-Expression konnte eine Typ I Nukleationsäktivität von ina+ *E. coli* Zellen erreicht werden.

BGs mit inner-Membran verankertem INP

Um INP an die innere Membran (IM) zu binden, wurde eine verkürzte Form von InaZ mit verschiedenen IM Verankerungsmotiven fusioniert. Die resultierenden INP-Fusionsproteine wurden (i) mit der aminoterminalen Sequenz, (ii) der carboxyterminalen Sequenz oder (iii) mit beiden Endsequenzen an die cytoplasmatische Membran verankert. Die verschiedenen INP-Fusionsproteine wurden in *E. coli* C41 hergestellt, anschließend wurde die Expression des Lysegens *E* induziert, um die davon abgeleiteten INP-BGs zu gewinnen. Für alle drei Varianten konnte eine LE von > 99,7% erreicht werden und das Vorhandensein des verankerten INP wurde durch Western Blot Analyse bestätigt. Die getesteten INP-BG Varianten mit IM verankertem INP zeigten erste Gefriereignisse zwischen -6°C und -8°C. Die ersten gefrorenen Tropfen der lebenden INP-*E. coli* Zellen wurden bei Temperaturen zwischen -7°C und -9°C nachgewiesen.

Weitere Konstruktionen verkürzter Formen von InaZ

S-Layer-Proteine SbsA und SbsB wurden als Träger von INP96, einer verkürzten Form von InaZ (entspricht InaZ von Aminosäure 176 – 273) verwendet. Um INP96 an der BG-Oberfläche zu verankern, wurde eine OmpA-INP96-Fusion konstruiert. Darüber hinaus wurde die INP-N-terminale Domäne, die als Außenmembrananker dient, erfolgreich verwendet, um INP96 auf der Oberfläche von BGs zu verankern. Da INPs als größere Varianten von Frostschutzproteinen angesehen werden können, wurde eine C-terminale verkürzte InaZ-Variante INP288 (As 1 – 470 von InaZ) konstruiert,

deren Frostschutzaktivität mittels Tröpfchen-Gefrier-Versuchen jedoch nicht nachgewiesen werden konnte.

EI Inaktivierung von *Bordetella bronchiseptica* BG Präparationen

Im Zuge dieser Arbeit wurden zum ersten Mal *Bordetella bronchiseptica* BGs produziert und deren E-Lyse überlebenden Mutanten mittels Ethyleneimin (EI) inaktiviert. EI Inaktivierung wurde auch zur Herstellung von *E. coli* INP-BGs verwendet und mit β-Propriolacton (BPL) behandelten *E. coli* INP-BGs bzgl. Eisnukleationsaktivität verglichen.

Zudem waren mit *B. bronchiseptica* BGs geimpfte Hunde signifikant höher gegen spontan- und induziertem Husten geschützt als die Placebo-Gruppe und zeigten zudem eine geringere Dauer des Hustenleidens.

1 Introduction

1.1 Ice nucleation

When aqueous solutions cooled below their melting point (MP) remain liquid they are in a metastable state known as supercooled [1].Therefore, at atmospheric pressure pure liquid water does not spontaneously freeze at 0°C [2]. Under laboratory conditions and in the absence of any impurities ultra-pure water can be supercooled up to -48°C [3] designated as 'supercooling threshold temperature' [2]. In the state of supercooled water, naturally small ice-crystals (embryo ice crystals) are formed [4]. Embryo ice crystals are – "*thermodynamically unstable aggregates of water molecules in a structure that favors further development into stable ice"* [5] – composed of a minimum of 275 water molecules [6] and have a cubic or hexagonal structure [7, 8].The critical embryo size – "*where probability of growth and probability of decay becomes equal"* [5] – reflects the metastable equilibrium of supercooled liquid, where a minimal increase in size by assembling water molecules on their surface or by contact with each other can lead to ice nucleation [4, 5]. By definition, ice nucleation (IN) is the "*formation of a thermodynamically stable body of ice from a metastable phase (vapor or liquid)"* [9]. The conventional model describes nucleation of water as stepwise aggregation of water molecules into ice-like features (embryo ice crystals) – because of the electrostatic attraction of the polar parts – until the critical size is exceeded [1, 10]. However, the mechanism of phase transition from water to ice is still not fully understood and of great scientific interest. The mechanism of ice nucleation is generally divided into homogeneous and heterogeneous nucleation.

Homogeneous ice nucleation occurs "*without any foreign substance aiding the process"* of ice formation [5]. During homogeneous freezing, at the critical embryo ice crystal size the ratio of cubic and hexagonal shaped crystals is balanced at 50 % [11]. Additionally, homogeneous freezing occurs only at highest supercooled and supersaturated conditions, atmospheric water for example freezes homogeneously below -38°C [12].

Heterogeneous freezing is defined as "*ice nucleation aided by the presence of a foreign substance so that nucleation takes place at a lesser supersaturation or supercooling than is required for homogeneous ice nucleation"* [5]. These foreign solid aerosol particles, so-called ice nuclei, organize water molecules into an ice-like structure and trigger ice formation at temperatures between 0°C and -35°C [13, 14]. "*For homogeneous ice formation at -5°C, 45,000 water molecules are required in an embryo ice crystal though this number can drop to 600 or lower when ice nucleators are present"* [15].

Further, heterogeneous IN is subdivided into four modes (**Fig. 1**).

(1) "*Immersion freezing, where the ice nuclei is incorporated in a liquid body and initiates nucleation from inside the droplet*" [12].

(2) "*Condensation freezing, where water droplets are formed by condensation around a cloud condensation nucleus* (CCN), *which acts simultaneously as ice nuclei*" [16].

(3) Contact freezing is caused by an ice nuclei upon contact with a droplet surface [12, 17] and

(4) deposition freezing, where IN occurs directly from water vapor upon an ice nuclei surface [5, 12].

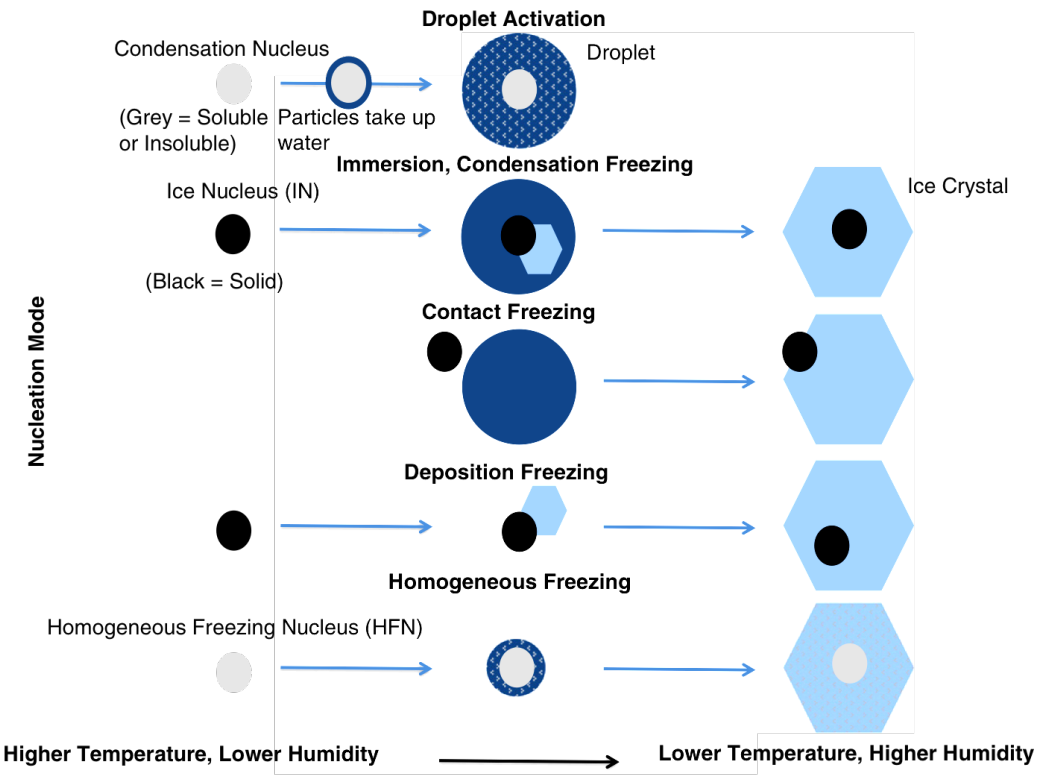

Figure 1. Schematic diagram of water nucleation published by Cziczo and Froyd (2014) [12].

Therefore, aerosol particles largely influence the properties of tropospheric clouds and the global water-cycle by functioning as CCN and IN forcing the growth of frozen cloud droplets leading to precipitation (**Fig. 1** and **Fig. 2**). [18, 19]. Pratt *et al.* (2009) examined the chemical composition of cloud ice crystal residues, where ~50% of the residue were identified as mineral dust, ~33% as biological material and the remaining percentage are salt, soot and organic carbon-nitrate [20].

These atmospheric identified biological particles are for example bacteria, pollen or fungal spores (**Fig. 2**). [21]. In association with dust or seawater the biological material is thought to rise into the atmosphere and become part of the hydrological-cycle [22, 23]. Since clouds also act as a protective screen of the earth by reflecting solar radiation with a cooling effect on the earth-atmosphere system, the indirect influence of aerosol particles on the climate is of great scientific interest [19].

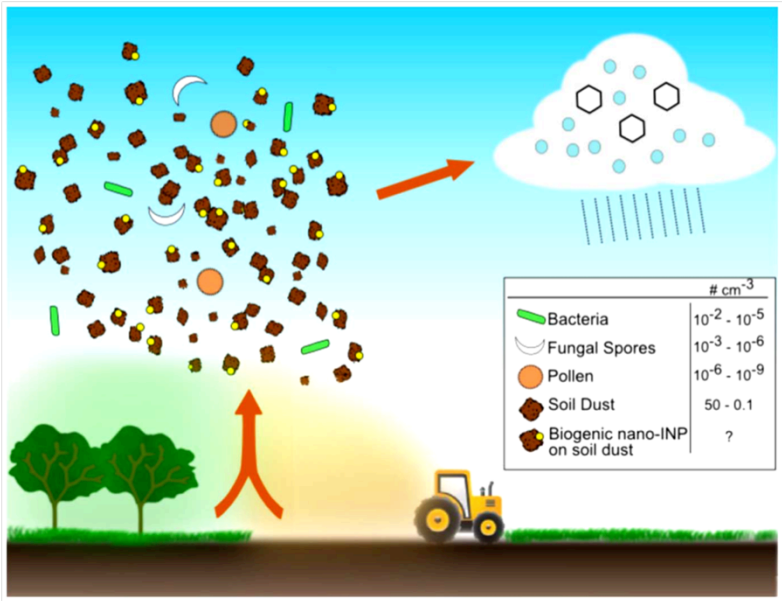

Figure 2. *"Illustration of the hypothetical distribution of biogenic particles in association with soil dust to the troposphere and their impact to cloud properties*", published by O'Sullivan et al. (2015) [22].

1.2 Bacterial ice nuclei

In 1972, Schnell and Vali published their discovery of atmospheric effective ice nuclei active at warm subzero temperatures on decomposed leaves [24]. Two years later, Maki *et al.* (1974) identified *Pseudomonas syringa*e isolated from decaying leaves of *Alnus tenuifolia* causing ice nucleation at temperatures of about -2°C [25]. Up to the present, the plant pathogen *Pseudomonas syringae* represents one of the most efficient ice nucleation active (ina^+) bacterial ice nucleus known, initiating plant damaging ice formation at temperatures of about -2°C [26, 27]. Ina^+ bacteria are taxonomically scattered about all three orders of *Gammaproteobacteria* and have the property to catalyze heterogeneous ice formation of supercooled water by orienting water molecules into an ice-like structure. [28-32]. In general, ina^+ bacteria are Gram-negative, epiphytic and pathogenic like *Pseudomonas syringae, Pseudomonas putidia, Erwinia herbicola, Erwinia ananas, Xanthomonas campestris, or Pantoea ananatis* among many others [25, 26, 33-41].

1.2.1 Ecology of ina$^+$ bacteria

As already mentioned, many of the known ice nucleating bacteria colonize the phyllosphere and cause frost injuries of leaves and crops at subzero temperatures which would not occur in the absence of bacterial ice nuclei[42]. In a snap bean field for example an average number of 2.7 x 10^6 ina$^+$ *P. syringae* g^{-1} leaf was detected [43]. In the early years of the discovery of ina$^+$ bacteria, they were found in association with leaves. Therefore, the focus of finding further ina$^+$ species was more or less restricted to the agricultural ecosystem, until 1978, when David Sands from the Montana State University thought that he solved the problem of crop damage caused by *P. syringae* with a copper treatment in a 3.6 square kilometers wheat field[44]. *"As the disease returned three weeks later"* [44], Sands got into a plane and on a height of 2,500 meters where he collected ina$^+$ *P. syringae* on selective agar plates [45]. He assumed that atmospheric bacterial IN can cause precipitation and consequently colonize new plants [45]. This process Sands described as bioprecipitation (**Fig. 3**). His hypothesis of bioprecipitation seemed to be proven true among others by a study of Hirano *et al.* (1996), where they demonstrated that a bean field which has been exposed to rain harbors 1,000-fold more *P. syringae* bacteria within two days compared to the rain-protected neighboring bean field [46].

Morris *et al.* (2008) isolated ina$^+$ *P. syringae* out of a large sample quantity from agricultural and non-agricultural sources [47]. Beside the property to nucleate ice formation, strains isolated from non-agricultural sources show the same pathogenic characteristics like strains collected from agricultural environment [47]. The non-agricultural sources included firn snow from highly alpine area, lake water above 2,100-meter sea level, stream water, rain water and wild plants above 2,000 meter, where *P. syringae* was found in cfu concentrations of hundreds to several thousand per liter [47]. Some non-agricultural sources like freshly fallen snow at 1,200 meter in La Clusaz, France (1.3 x 10^5 cfu l^{-1} meltwater), or leaves of *primula officinalis* collected at 2,100-meter altitude in Talant, France (8.1 x 10^4 cfu g^{-1}) [47] showed concentrations of *P. syringae* which are comparable to some sources of agricultural areas [48]. Moreover, "*85 % of all isolated P. syringae strains were ice nucleation active"* [47]. Beside the mentioned habitats, ina$^+$ bacteria have also been isolated from marine water as well as from arctic seawater [49, 50].

By wind and air currents, the tiny and lightweight bacteria primarily from land masses but also from aquatic environment can be transported easily as aerosols into the atmosphere to the elevation of clouds [43, 51]. The global average emission rate of bacteria – observed by concentration measurements of atmospheric bacteria containing particles and global simulation models – are reported to be in the range of 10^4 - 10^5 m^{-3}, or 50-220m^{-2} s^{-1} [43, 51].

On account of the different habitats in which ice nucleating *P. aeruginosa* bacteria were found, bioprecipitation seems to function as a *feedback cycle which is closely related to the earth water cycle, in which water is evaporated and elevated into the atmosphere and returns to the ground by precipitation* (**Fig. 3**) [47]. The same is valid for many other ina$^+$ bacteria, for example, *Erwinia*

herbicola or several ina^{+} *Pantoea* sp., which have been isolated from soil, plants, rainwater, snow and air [31, 52-54].

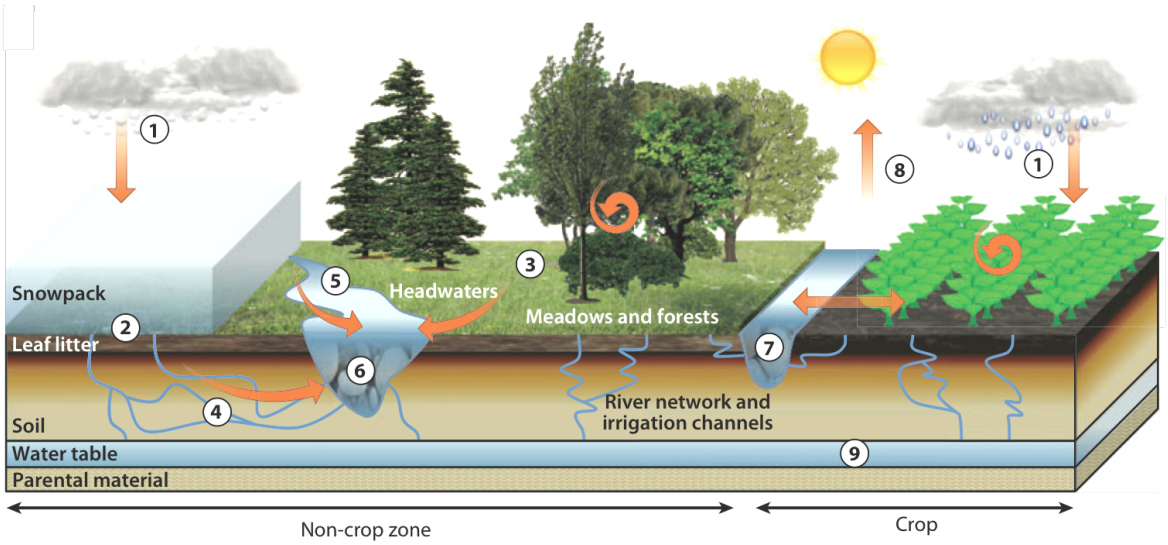

Figure 3. Illustration of the hypothetical life cycle of *P. syringae* (probable as well for other in the atmosphere , in clouds and precipitation detected bacteria) which is closely linked to the water-cycle, published by Morris *et al.* (2013) [55]. *"The spatial scales of the life history of Pseudomonas syringae. (a) At the landscape scale, P. syringae is deposited on the (1) ground and on plants by rain and snowfall. In subalpine and alpine environments, P. syringae survives in (2) snowpack that insulates the ground surface and in (3) leaf litter and the covering grasses. During snowmelt or rainfall, a fraction of these populations follows the (4) subsurface and (5) surface water flow that feeds into the alpine river network. (6) P. syringae is transported in the water column and can integrate epilithic biofilms. Epiphytic populations of P. syringae on wild plants washed from leaves with rain and dew runoff can also follow this path. In agricultural ecosystems, similar processes are involved. In addition to spread from agricultural sources, P. syringae can move into cultivated plant stands with precipitation (1) and (7) irrigation water from rivers. (8) Populations from plants are aerosolized and transported into the troposphere. (9) Some water flows deep through the soil and goes to groundwater"* [55].

Over the past decade science was getting more and more interested in the effect of bacteria on clouds precipitation and formation and the possible influence on the global climate. Considering the fact that concentrations of microbial ice nuclei in the lower part of the troposphere are assumed to be similar to non-biological derived ice nuclei, it is reasonable to suggest the bacterial influence [56, 57]. As already mentioned above, ice nucleation active bacteria have the property to catalyze heterogeneous ice formation of supercooled water (**Fig. 4**). Laboratory experiments simulating cloud conditions in a cloud chamber performed by Möhler *et al.* (2008) demonstrated that *P. syringae*, *Pseudomonas viridiflava* and *E. herbicola* are able to promote ice formation at relatively warm temperatures between -7°C and -11°C in the condensation or immersion mode [14]. Furthermore, Attard et al. (2012) demonstrated that ina+ *P. syringae* strains after treatment with UV radiation, NO_2 and O_3 gases – naturally occurring in atmospheric conditions – maintain their ice nucleation activity [58].

Bauer *et al.* (2003) found that airborne ice-active bacteria are involved in cloud formation acting as cloud condensation nuclei (CCN) (**Fig. 4**) at supersaturations between 0.07 % and 0.11 %, whereas insoluble but wettable aerosol particles of equivalent size would not have activated cloud condensation at such low supersaturations [59]. The authors attribute this phenomenon to the bacterial size and the physico-chemical nature of the bacterial outer membrane [59]. The bacterial concentration in

tropospheric clouds ranges from 10^2 to 10^5 cells ml^{-1}, where in theory "*a single ice-nucleating bacterium within a cloud can induce precipitation and thus cause its own deposition*" [60].

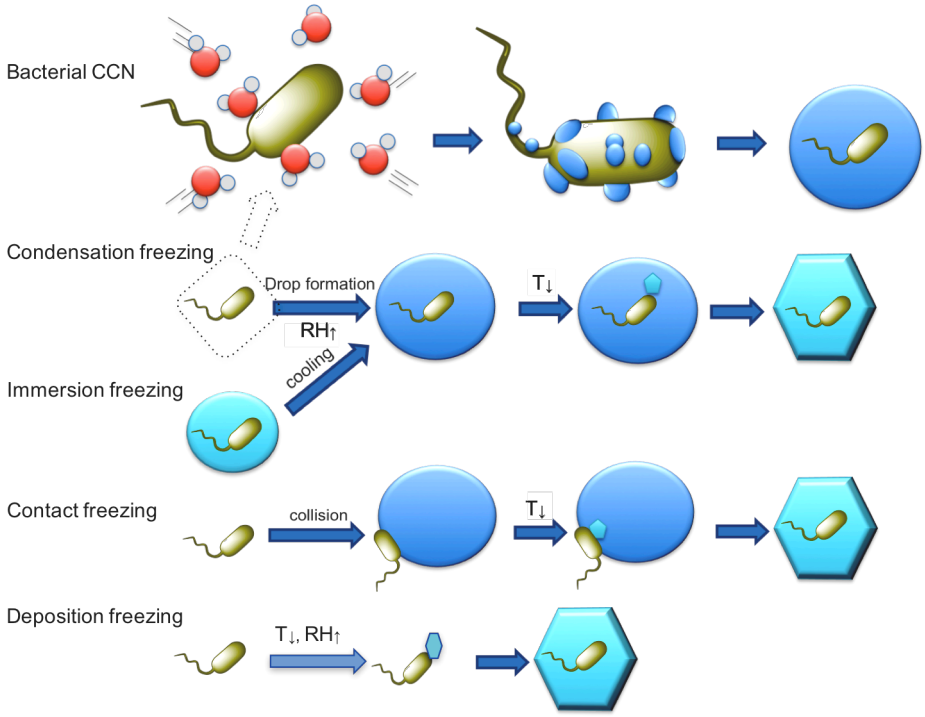

Figure 4. Possible modes of ina+ bacteria influencing cloud glaciation. T↓: temperature decrease; RH↑: relative humidity increase. Adapted from Lohmann (2017, ETH Zürich)[61].

1.2.2 Bacterial ice nucleation proteins

Bacterial ice nucleation proteins (INPs) are bound to the outer cell membrane and enable bacteria to act as ice nuclei. Beside its contribution to the bacterial pathogenicity, the biological function of INPs is considered to direct ice formation into the extracellular space at warm subzero temperatures to provide adaption time for the bacterium to freezing stress [33]. Furthermore, the resulting osmotic imbalance due to the extracellular ice formation results in an above-average water outflow from the cell to lower the intracellular ice nucleation point [62]. With respect to the characterization of INPs, *P. syringae* is known to produce several INPs which are well characterized, i.e., InaZ, InaV, InaQ, InaQ, or InaK [63-67].

Bacterial INPs – which are strongly homologous – range in size from 120-150 kDa and are composed of three characteristic protein domains, a highly repetitive central domain with several tandem consensus octapeptides (AGYGSTxT) (x is non-repetitive residue), and non-repetitive N- and C-terminal domains [63, 68]. The relatively hydrophobic N-terminal domain (approximately15 % of the protein) is assumed to bind to phosphatidylinositol as a lipid and polysaccharides and functions as membrane anchor [33, 65, 69, 70]. Whereas, the function of the hydrophilic C-terminal domain is not completely understood, but is believed to have an important role in stabilizing the INP conformation preventing the tandem repeats from unfolding [33, 66, 71].

The largest repetitive element of the central domain consists of 48 high-fidelity residues subdivided into three mid-fidelity repeats of 16 residues (AGYGSTxTAxxxSLx), which can be further broken down into two low-fidelity octapeptides [70]. The central domain is predicted to form a ß-helical fold secondary structure (**Fig. 5A**) where its nucleation sites mimic an ice like surface, which is able to bind water molecules and functions as template orientating water molecules into a lattice structure leading to the formation of ice [30, 66, 71, 72]. Site directed mutations of the central domain, which delete or add a 48-codon repeat-element but maintain the residual repetitive segments showed little effect on the ice nucleation phenotype [73]. However, if the periodicity of regular repeat pattern is disrupted a reduction in nucleation activity was ascertained, as a consequence of reducing nucleation sites [63, 73]. The repetitive elements are rich of threonine (T) and serine (S), where for example the highly conserved SLTA and TQTA residues of the *Pseudomonas borealis* INP (PbINP) were shown to create flat and relatively hydrophobic surfaces (despite the overall hydrophilicity of the repeating domain) containing several hydrogen bond donors and acceptors (**Fig. 5B**) [30, 74]. These sites are assumed to function as nucleation sites of the INP mimicking the "*basal plane of ice through their hydroxyl groups in combination with captured, clathrate waters incorporated into the protein surface*" [30]. Furthermore, the inward facing conserved serine and glutamine (Q) residues (hydrophilic) in the INP modelled structure of Garnham *et al.* (2011) – which are located in opposite corners of the structure – connect the adjacent coil via hydrogen bonds and therefore stabilize the ß-helical structure (**Fig. 5B**) [74].

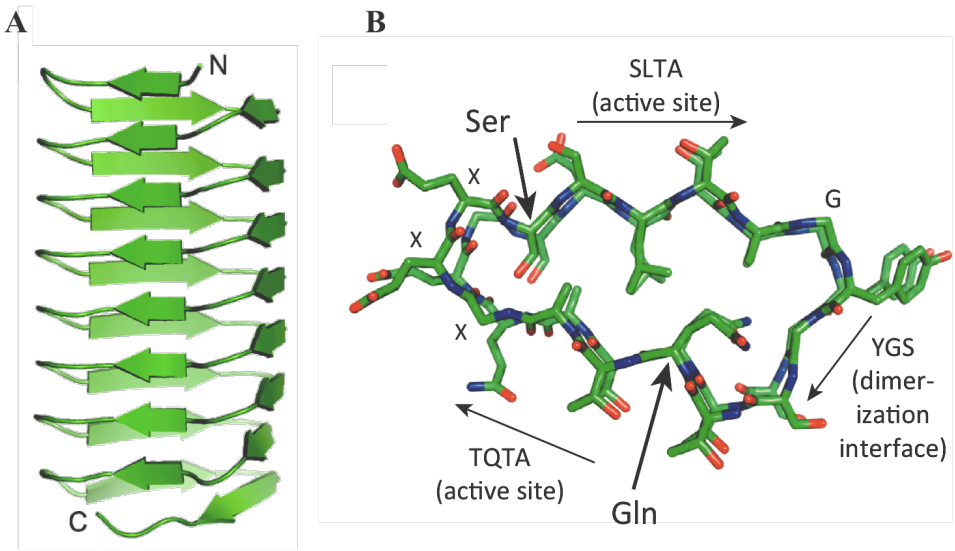

Figure 5. Predicted model of the *Pseudomonas borealis* INP by Garnham *et al.* (2011) [74] **A.** ß-helical model *P. syringe* INP. **B.** *"Cross section through the Pseudomonas syringae INP central repeat region, showing the putative ice-forming (active) sites (residues SLTA and TQTA), the putative dimerization interface (residues YGS), and internal Ser and Gln ladders"* [75].

The ice nucleation sites of INPs are asumed to act primarily as ice-binding sites (IBS) *"to mimic the surface of ice by ordering water molecules in an ice-like structure that serves as an ice embryo"* [76]. The mechanism of ice-binding of INPs is assumed to be best explained by the 'Anchored Clathrate Water Hypothesis' (ACW), as hydrogen bonds alone seem not to be sufficient to explain this

phenomenon [77, 78]. Also Pandey *et al.* (2016) accentuate, that "*the fact of surface sites matching ice templates and the presence of hydrophilic sites (by matching bonds) commonly assumed to promote ice nucleation are not sufficient to explain the IN properties of P. syringae*" [30]. The outward-projecting threonine (T) of the nucleation sites forms hydrogen bonds with its hydrophilic hydroxyl group and clathrate water molecules, which are located on the ice-like waters of the quasi liquid layer; concurrently, clathrate waters are hydrogen bound to the INP backbone and constrained around the threonine hydrophobic methyl group [75, 79, 80] (**Fig. 6**). Subsequent, the constrained clathrate water molecules are merged with the ice-like waters of the quasi liquid layer by the hydrophobic groups and form ice [75, 79, 80].

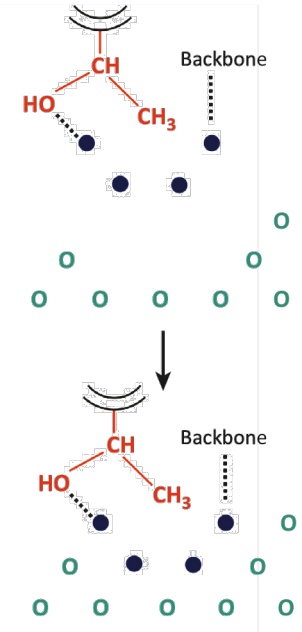

Figure 6. Mechanism of how INP absorbs to ice by the anchored clathrate water hypothesis illustrated by Davies (2014). *"The ice-binding site (IBS) of an INP is represented by the single threonine residue in red. Water molecules in the ice lattice or quasi-liquid layer above ice are shown as blue circles. Clathrate waters around the IBS are dark blue dots. Ice-like clathrate waters around hydrophobic groups on the IBS hydrogen bond to the protein backbone and side chain groups (top). These clathrate waters merge with the quasi-liquid layer waters and become ice (bottom)"* [75].

Briefly summarized, the ACW hypothesis integrates elements of the hydrogen-bonding hypothesis and the hydrophobic effect mechanism, where the function of the hydrophobic surface is to constrain, position and anchor the clathrate water molecules into the ice-like quasi liquid layer [75, 76]

Interestingly, not every cell in a population of an ice nucleation active bacterial strain is ice nucleation active [28]. Single cells in a culture of ina^{+} bacteria *P. syringae* exhibit heterogeneity in ice nucleation activity ranging from -2°C to -12°C, where only every millionth cell represents an ice nuclei active at -2°C [26, 81]. Generally, bacterial ice nuclei causing ice formation at colder subzero temperatures are numerically more present compared to nuclei active at warmer temperatures [26, 81]. Govindarajan and Lindow (1988) studied the size of ice nuclei of *P. syringae* causing the variety of ice active temperatures within a population by γ-radiation analysis. Their data indicate that a single INP has little ice nucleation activity, whereas homogeneous formed aggregates of monomers are large enough to orientate high numbers of water molecules and catalyze ice formation at temperatures just below 0°C [81]. The smallest ice nucleant they measured – active at -12°C – had a molecular mass of approximately 150 kDa representing a single INP molecule, suitable to the 150 kDa *P. syringae* ice

active InaZ [81, 82]. The largest ice nucleant of 19,000 kDa – representing an INP oligomer – on a single *P. syringae* bacterium was ice active at -2°C [81]. Therefore, the effectiveness of ice nucleation activity is depending on the INP aggregation state, in which a minimal size composed of 53 monomers is necessary for ice nucleation activity at -2°C [81]. The aggregation of single INP molecules to large plane structures enhancing the number of ice active sites has also been verified by immunofluorescence and transmission electron microscopy [83, 84]. The mechanism of aggregation has not yet been fully understood, but for *Pb*INP the GYGS sites are thought to be responsible for the protein dimerization (**Fig. 5B**) [74]. Here, the serine and tyrosine residues might cause a intercalated hydrogen-bond network with the neighboring serine and tyrosine residues of the dimerization site [74]. According to the heterogeneity in ice formation activity within a population and the general different activity of the known INPs, bacterial ice nuclei are classified according to their functional nucleation temperature into three different types; typ I (class A) acts at -5°C or warmer, type II (class B) from -5 to -7°C and type III (class C) below -7°C [85, 86]. Kozloff *et al.* (1991) and Turner *et al.* (1991) demonstrated in their studies that these different INP aggregate classes within a population exhibit chemically different compositions (**Fig. 7**) [69, 87].

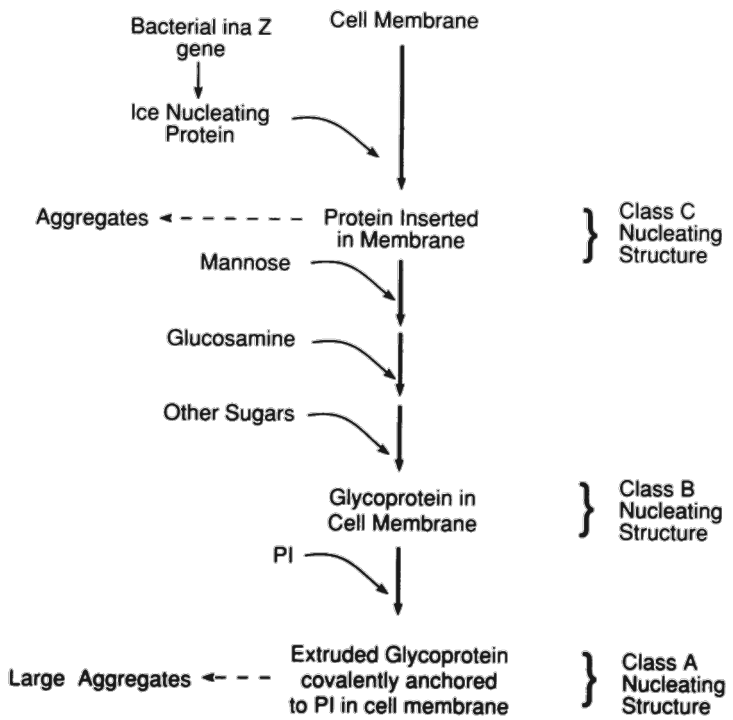

Figure 7. Proposed mechanism of the INP anchoring formation illustrated by Kozloff *et al.* (1991) and its concurrent formation from class C to class B and to class A [69]. *"Side-to-side aggregation is thought to involve the substituted sugars, and PI* (phosphatidylinositol) *provides a mobile anchor to the cell membrane"* [69].

Furthermore, intermediary or mixed structures were identified as well [69, 87]. The lowest nucleation activity indicates class C structure, where the core protein is inserted to the membrane and suggested – in its intermediate form – to be linked to a few mannose residues through an *N*-glycan bond to the amide nitrogen of N-terminal asparagine residues [69, 87]. In class B structure mannose is bound as a

complex mannan and glucosamine as well as galactose and probably galactosamine are linked via O-glycan bond to the threonine and serine residues of the repetitive INP domain [69, 87]. These additional O-glycan linked sugars are suggested to play an important role in the formation of large INP lipoglycoprotein aggregates through binding and cross-linking reactions [69]. Only class A structure possesses phosphatidylinositol (PI), where the inositol residue of PI attaches to the N-terminal asparagine linked mannan complex [69, 88] Hence, the INP is anchored as lipoglycoprotein to the outer membrane by the hydrophobic diaglycerol residue of PI [69]. Burke and Lindow (1990) estimated that the movement of PI anchored INP through the outer membrane could be energetically efficient for the formation of large ice nucleation complexes [89].

1.2.3 Applications of ina$^+$ bacteria

Qualities of INPs attract interest in the range of bioengineering application, therefore effective bacterial ice nuclei are already used by snowmaking industry (Snomax®). Recombinant bacterial INPs were already functionally expressed in Gram-negative non-ice nucleation active *Escherichia coli*, as well as in plants [90, 91]. INPs are also used for molecular biological applications using ice-nucleation activity as a reporter gene system[92]. In addition, the N-terminal domain of INPs, which link the protein to the outer cell membrane, is used as cell surface display system. Enzymes like triphenylmethane reductase or carbonic anhydrase as well as the HIV-1 protein gp120 were functionally displayed on the cell surface using the INP N-terminal anchoring system. [93-97] Bacterial ice nucleation has also been tested for diagnostic purposes (Bacterial ice nucleation diagnostic, BIND), where an ice nucleation active (*ina*) gene is introduced into *Salmonella* bacteriophage P22, acting as ina$^+$ reporter phage to detect *Salmonella* food contaminations [98]. Infected *Salmonella* cells expressing ice nucleation activity can be detected by an freezing indicator dye, which changes color when the contaminated sample starts to freeze [98]. The BIND assay has been used to detect *S. typhimurium*, *S. gallinarium*, *S. enteriditis*, or *S. typhi* in foods like milk, egg or meat [96].

1.3 Bacterial antifreeze proteins

Bacterial antifreeze proteins (AFPs) show the contrary effect of INPs. AFPs protect the organism from freezing temperatures and have been found in *Micrococcus cryophilus*, *Rhodococcus erythropolis*, *Marinomonas primoryensis*, *Flavobacterium xanthum* and many more [(99-102)]. Like INPs, bacterial AFPs possess IBSs *"which organize water molecules into a regular ice-like lattice that matches, at a minimum, the primary prism and basal planes of ice"* [(80)]. Recently, the ice-binding mechanism of INPs (as described in chapter 1.2.2) is thought to be the same for bacterial AFPs [(33)]. AFPs also known as thermal hysteresis proteins (THPs) bind to embryo ice crystals and have the ability to control the shape and the size of ice crystals with the result of ice growth [(33, 99)]. AFPs control ice crystal growth through their thermal hysteresis activity and/or their ability of ice recrystallization inhibition [(103, 104)] Therefore, antifreeze proteins are characterized *inter alia "by their ability to prevent ice from growing upon cooling below the bulk melting point",* causing a gap between the melting and freezing point known as thermal hysteresis (TH) (**Fig. 8 A**) [(105)]. The temperature below the thermal hysteresis activity of an AFP, where ice crystal growth starts, is referred to as hysteresis freezing point [(105)]. The TH caused by AFPs can be laboratory determined by a nanoliter osmometer connected to a microscope (**Fig. 8 B**).

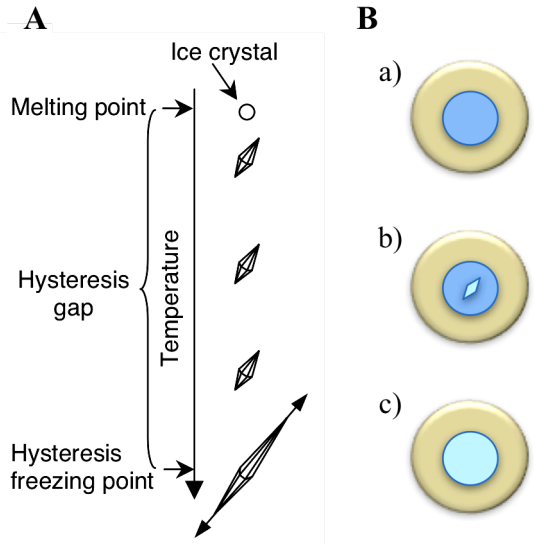

Figure 8. A. Illustration of the thermal hysteresis phenomenon published by Kristiansen and Zachariassen (2005) [(105)]. **B.** Observation of thermal hysteresis by a nanoliter osmometer – reproduced from Lorv *et al.* (2014) [(33)]. *"A water drop harboring AFPs cooled to its melting point is absent of ice crystals* (a). *With further cooling ice crystals are seen to neither grow or melt* (hysteresis gap) (b). *At subzero temperatures beyond the gap* (starting at hysteresis freezing point) *ice formation occurs fulgurous and is blocking the microscope light"* (c) [(33)].

For instance, the AFP of *Marinomonas primoryensis* (*Mp*AFP) – at micromolar concentration level – has a TH of 2°C [(106)]. Beside TH, bacterial AFPs have the ability of ice recrystallization inhibition (IRI) [(37)]. Hence, *AFPs hinder the restructuring of ice into larger ice crystal structures within a frozen solution* [(107)]. It is assumed that IRI activity of AFPs avoid the movement of melt water among ice crystals necessary for recrystallization leading to a destabilization of the small ice crystals [(107)].

AFPs exhibit a greater diversity in size compared to INPs from bacteria ranging from 23-164 kDa [108-112]. Up to now, *Mp*AFP represents an exception with its molecular size of ~ 1.5 MDa, it is 100 times larger than typical bacterial AFPs and resembles the AFPs of insects [101, 106]. However, only ~ 2 % of the entire protein possesses antifreeze activity [80].

As antifreeze activity is also dependent on AFP concentration [113] it is not astonishing that most of the identified AFPs are secreted to the extracellular environment where they inhibit ice formation [34, 100, 114].The highly active AFP of the antarctic bacterium *Flavobacterium xanthum* (*Fl*AFP) was located in the cytoplasmic space with high ice recrystallization inhibition activity [102]. The *Mp*AFP is the only known AFP which is located at the outer membrane, suggesting that the AFP-like domain serves to transiently bind the bacterium to ice where nutritional resources are more abundant [80].

Some bacteria like *Pseudomonas borealis* DL7, *Chryseobacterium* sp. GL8, *Pseudomonas fluorescens* KUAF-68, or *Pseudomonas putidia* GR12-2 demonstrate both, ice-nucleation activity and antifreeze activity [32, 34, 110]. For instance, the lipoglycoprotein AfpA (164 kDa) secreted by the rhizobacterium *Pseudomonas putidia* GR12-2 exhibits antifreeze activity and low ice nucleation activity at -10°C and shares similarity in its amino acid sequence to the IBS of some bacterial INPs like inaV [115]. Moreover, Kobashigawa *et al.* (2005) showed that a recombinant INP composed of two repetitive 48-residues (INP96) from the *P. syringae* InaZ exhibits ice-binding ability and slight antifreeze activity [4]. In contrast, *Pseudomonas fluorescens* KUAF-68 produces a secreted AFP of 80 kDa and an INP of 120 kDa encoded by different genes [110]. The cooperative function of simultaneous antifreeze and ice nucleation activity is speculated to improve freeze tolerance [33]. The INPs direct freezing to the bacterial cell surrounding environment, whereas the secreted AFPs inhibit ice recrystallization leading to a minimization of freeze-thaw stress [112].

Up to now, only the structure of *Mp*AFP and AfpA is characterized [33]. The ice binding site of *Mp*AFP form a Ca^{2+} ß-solenoid structure, in which Ca^{2+} is necessary for the proper folding of each XGTGND turn and structure stability [79, 106]. Similar to *Mp*AFP, AfpA is also thought to need Ca^{2+} ions for its GXGXD calcium binding turns [33]. According to the identified ß-solenoid structure of *Mp*AFP modeling structure studies suggested the ß-helical model of *P. syringe* INP, but on a much larger scale [74]. Due to the similar characteristics of AFP and INP one could argue that INPs might be large versions of AFPs.

1.4 Bacterial Ghosts

Bacterial ghosts (BGs) are defined as empty cell envelopes derived from a Gram-negative bacterium and perfectly mimic the ancestor's cell-membrane composition at the time point of their production via controlled expression of lysis gene *E* [116, 117]. The conversion of a single living bacterium into a BG is a rapid process in the range of milliseconds[117] and can be characterized by puncturing the bacterium cell envelope from the inside to the outside expelling its cytoplasmic content to the surrounding medium (**Fig. 9 A**).

The lysis function of gene *E* from the *Escherichia coli* bacteriophage ΦX174 was discovered in 1966[118], which codes for a 91aa polypeptide and forms in its oligomeric conformation a single transmembrane tunnel structure at the adhesion sites of the bacterial inner membrane (IM) and outer membrane (OM)[119] leading to expulsion of the cytoplasmic contents (**Fig. 9 B**) [120, 121]. Protein E fuses the IM and OM resulting in a sealed periplasmatic space at the sites of the lysis tunnel [117, 120]. The size of the E-specific transmembrane lysis tunnel is fluctuating between 40 - 200 nm and is located in areas of potential cell division sites predominantly in the middle of the cell (**Fig. 9 C**) or at polar sites (**Fig. 9 A**) [117].

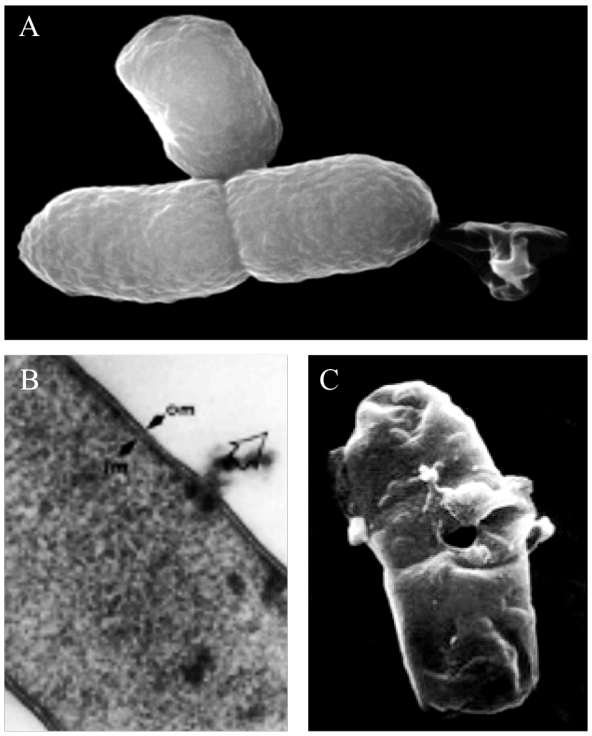

Figure 9. Electron microscopy images during E-mediated lysis. **A.** *"Formation of the E-specific lysis tunnel through which the cytoplasmic content is expelled to the outside medium including the bacterial nucleic acids content, ribosomes soluble proteins and other solutes"* [128] – reproduced from Ebensen *et al.* (2004) [129]. **B.** Protein E forms a transmembrane tunnel structure. **C.** BG with an E-Lysis tunnel at the central division site. Images B and C are reproduced from Witte *et al.* (1992) [117].

Consequently, BGs are composed of the three distinct Gram-negative cell-membrane layers, the cytoplasmic membrane, peptidoglycan and the bacterial outer-membrane with its specific LPS pattern

and capsule substances external to it. Hence, any protein, lipid, polysaccharide and complex structures derived from the cell envelope complex of a living bacterium is retained in BGs[117, 122].

The BG production system is most probably universally applicable in Gram-negative bacteria as BGs have been already successfully produced by plasmid controlled E-mediated lysis out of various Gram-negative bacteria, like for example *Actinobacillus pleuropneumoniae*, *Bordetella bronchiseptica*, *Erwinia cypripedii*, *Helicobacter pylori*, *Klebsiella pneumoniae*, *Mannheimia haemolytica*, *Pasteurella multocida*, *Pseudomonas putida*, *Pseudomonas aeruginosa, Pectobacterium cypripedii, Ralstonia eutropha*, *Salmonella typhimurium* and *Vibrio cholerae* [123]. Moreover, BGs produced from different pathogenic and non-pathogenic bacteria, which perfectly mimic the envelop-complex of the derived form, have been shown to be highly immunogenic and able to stimulate the innate as well as the adaptive immune system [124-127].

1.4.1 Recombinant Bacterial Ghost system

The extended BG platform technology uses the perfectly suited characteristics of BGs functioning as carriers and delivery vesicles of active compounds, foreign proteins, target antigens or DNA. The recombinant BG system is using all spaces of a ghost including IM and OM, periplasmic space and the internal lumen.

The internal lumen of BGs can be filled with chemical compounds, DNA, proteins or enzymes and sealed with membrane vesicles fused at the site of E-lysis tunnel [130-132]. Another mode of locating proteins of interest in the cytoplasmic lumen is their incorporation into self-assembling surface layer (S-layer) proteins, where each multiple recombinant S-layer protein assembles into a sheet-like lattice structure, which have been shown by electron microscopy studies to be retained within the inner lumen of the BGs cytoplasmic space [133, 134]. The genes of *Bacillus stearothermophilus* S-layer proteins SbsA – self-assembling into a hexagonal (p6) lattice[135] – and SbsB – self-assembling into an oblique (p2) lattice[136] – have been used for the production engineered S-layer lattices located in the BGs cytoplasmic lumen [137]. Truppe *et al.* (1997) demonstrated that PHB-synthase and Lux-AB incorporated to SbsA and SbsB, respectively, fully preserved their enzymatic activity [138]. Additionally, it was shown that the hexagonal structure of SbsA exhibits a higher quantitative capacity to integrate foreign proteins compared to SbsB, however, the oblique SbsB structure tolerates the inclusion of larger inserts [139, 140]. Furthermore, proteins of interest can be fused to the inner side of the cytoplasmic membrane of the cell envelope by the hydrophobic membrane spanning domains of the truncated E (E´) and L (L´) proteins of the bacteriophages ΦX174 and MS2, respectively [141-143]. The protein of interest can be fused to the amino-terminal E` sequence, the carboxy-terminal L´ sequence, or to both sequences in order to be anchored to the inner membrane [127].

Proteins of interest can additionally be embedded within the sealed periplasmic space of BGs when they are exported via their fusion to the maltose binding protein (MBP) MalE or GIII-signal sequence

prior to E-mediated lysis [137, 144]. Also recombinant S-layer proteins fused to MBP can be exported to the periplasmic space, demonstrated by Cui *et al.* (2010)[145]. They integrated the Zona pellucida 3 protein (ZP3) into SbsA and successfully exported the MBP-SbsA-ZP3 fusion protein to the periplasmic space of *E. coli* followed by E-lysis for production of recombinant BGs as vaccine delivery vehicles [145].

Target proteins fused to outer membrane proteins (OMP) like OmpA can also be anchored to the surface of BGs. Jechlinger *et al.* (2005) cloned the gene coding for the Hepatitis B virus core 149 protein (HBcAg-149) into the *ompA* sequence encoding the third loop of the OMP, which is directed outwards, presenting the antigen on the cell surface [146]. The produced recombinant BGs carrying the monomeric membrane-fused HBcAg-149 antigens have been shown to initiate high immune response in mice [146].

Below an illustration (**Fig. 10**) published by Muhmmad *et al.* (2012) summarizes the wide spectrum of the recombinant BG system localizing target antigens (TA).

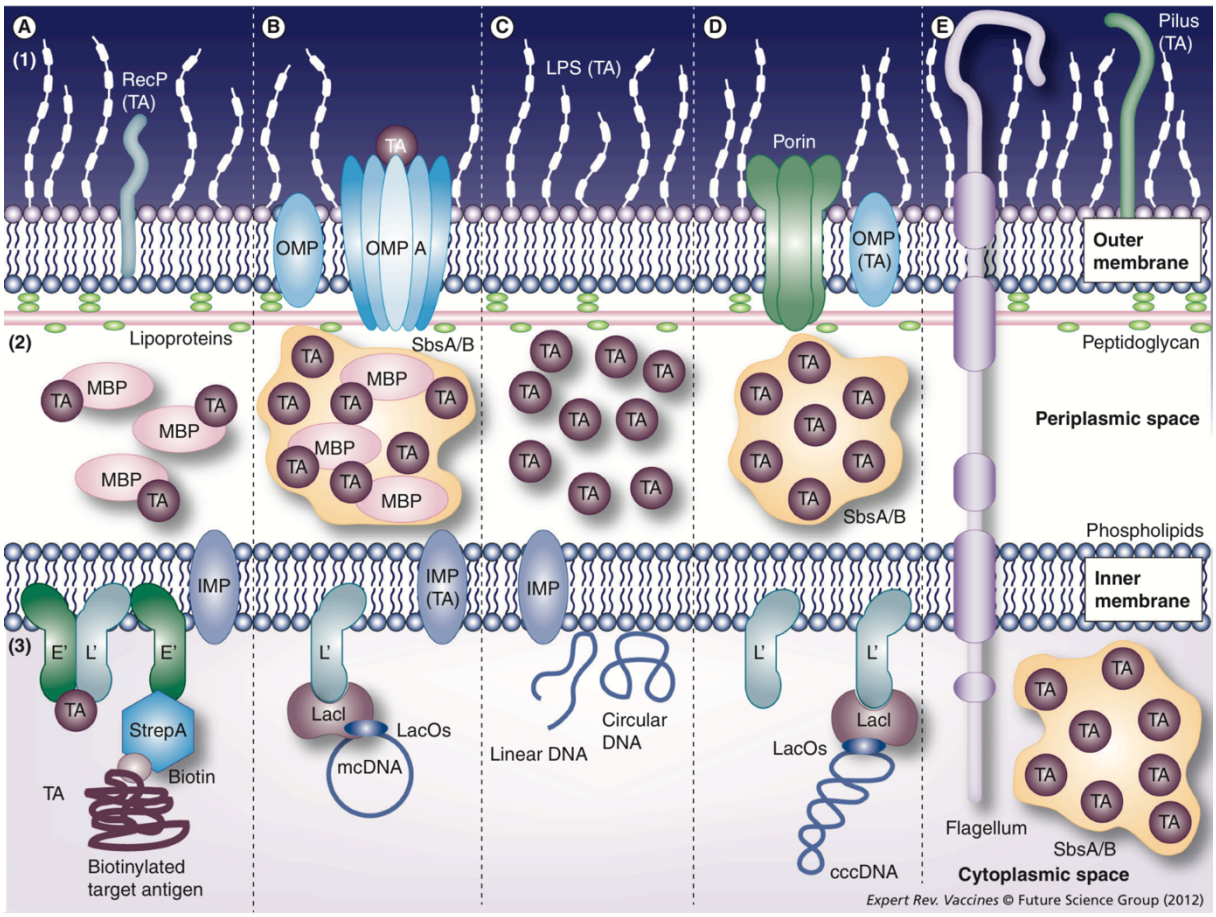

Figure 10. Diversity of target antigen (TA) locations in the different areas of the bacterial ghost envelope, published by Muhammad *et al.* (2012) [137]. *"**(A)** (1) RecP acting as a TA; (2) export of TA to sealed periplasmic space as maltose-binding protein (MBP) fusion; (3) protein TA anchored into the inner membrane via E', L', or E' and L' anchor sequences, or attachment of biotinylated TA to E'-membrane-anchored StrepA. **(B)** (1) Presentation of TA as a fusion protein on the outer membrane surface with OMP A; (2) export of TA to the sealed periplasmic space as MBP–SbsA or –SbsB S-layer fusion proteins; (3) mcDNA carrying the LacOs anchored to the inner membrane via L'-membrane- anchored LacI or IMP acting as TA. **(C)** (1) LPS acting as a TA; (2) export of TA to the sealed periplasmic space using a signal sequence that is cleaved off after transport (e.g., GIII, MBP signal sequence); (3) loading of bacterial lumen with linear and circular DNA plasmids, making BG a carrier for DNA vaccines. **(D)** (1) OMP acting as a TA; (2) export of TA to the sealed periplasmic space as SbsA or SbsB S-layer fusion proteins using a signal sequence that is cleaved off after transport (e.g., GIII, MBP signal sequence); (3) DNA carrying the LacOs anchored to the inner membrane via L'-membrane anchored LacI (LacI–L') repressor molecule. **(E)** (1) Pilus acting as a TA; (2) the periplasmic space; (3) cytoplasmic space lled up with recombinant S-layer proteins carrying foreign TA. cccDNA: Covalently closed circular DNA; E': Membrane anchor sequence of the N-terminal part of lysis protein E derived from bacteriophage FX174; IMP: Inner membrane protein; L': Membrane anchor sequence of the C-terminal part of lysis protein L derived from bacteriophage MS2; LacI: The lac repressor; LacO: Lac operator sequence; LPS: Lipopolysaccharide; MBP: Maltose-binding protein; mcDNA: Minicircle DNA; OMP: Outer membrane protein; RecP: Recombinant or induced pilus; StrepA: Streptavidine; TA: Target antigen."* [137].

1.4.2 Bacterial Ghost production

Protein E-mediated lysis leads to BG formation and has been shown to be not only dependent on expression of *E* but also on several other factors like growth phase of the cell, intact membrane potential, its regulation of the autolytic system, cell division or pH and osmotic pressure of the growth medium [147-150]. *E. coli* cells grown to stationary phase were demonstrated to be resistant to E-mediated lysis, but when fresh growth medium was added to the culture (in a ratio of ~ 1:3) E-lysis occurred immediately [151]. Therefore, the output of BG production in respect of lysis efficiency and production amount requires controllable growth and lysis conditions.

In 2010, Langemann *et al.* (2010) published a fermentation process for the production of *E. coli* ghosts using the lysis plasmid pGLysivb[128], where gene *E* is under transcriptional control of the temperature-sensitive *c*I857 repressor gene and mutated - λp_{Rmut}- operator system [152, 153].

The fermentation process is divided into three phases: a 90 min growth phase (**Fig. 11**), E-lysis induction via a temperature shift from 35°C to 42°C (**Fig. 11**) followed by an E-lysis phase of 120 min and downstream processing [128]. During growth phase at 35°C and a pH of 7.2 dissolved oxygen (dO_2) saturation can be regulated by stirring and aeration rate, whereas after lysis induction the dO_2 control is turned off to follow the lysis process by increasing dO_2 (**Fig. 11** (b) and (c)).

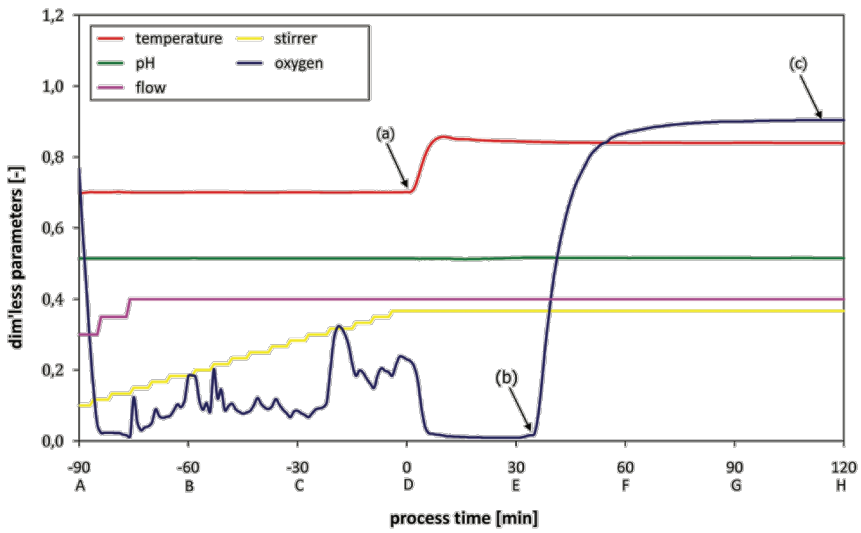

Figure 11. Example fermentation protocol of *E. coli* carrying lysis plasmid pGLysivb, showing all relevant process parameters during growth and lysis phase, published by Langemann *et al.* (2010). *(a) "lysis induction by temperature up-shift, (b) lysis onset as indicated by dO2 up-shift, (c) stationary dO2 plateau indicating end of lysis phase"* [128].

Additionally, dielectric spectroscopy measurements (also known as permittivity measurements) have been implemented as on-line monitoring tool to follow the E-lysis process in real time [154]. Here, the loss of the cell membrane potential – a consequence of E- mediated lysis –is indicated by reduced permittivity signals [154]. Moreover, the E-lysis process can be monitored via fluorescence-based flow cytometry measurement (FCM), which allows an on-line process control to follow BG formation and to evaluate the ratio to non-lysed bacteria [155].

By using tangential flow filtration (TFF) through a hollow fiber cartridge with a membrane pore size of 0.2 µm the BG product is concentrated, washed with sterile de-ionized water (dH_2O) and harvested from the fermenter. The inactivation agent β-propriolactone (BPL) is used to inactivate any surviving E-lysis escape mutants from BG production [128]. The DNA-alkylating agent mainly reacts with purine residues and induces nicks within and between the DNA strands leading to cell death [156]. To remove any remains of the inactivation-process, the BPL-treated BG product is then washed with sterile dH_2O by diafltration in a 0.2 µm pore size TFF module [128]. In the end, the broth is ~50-fold concentrated and >99 % of the medium is exchanged [128]. The final lyophilized BG product is *"stable at room temperature for many years"* [128]. The yield of the BG production process with ~5 g L^{-1} biomass at time point of lysis induction and >99 % lysis efficiency (LE) can be enhanced by fed-batch production 8 to 10-fold with a LE of >98 % [154]. Moreover, fed-batch procedures have been performed for the production of recombinant BGs, like BGs carrying IM-anchored β-galactosidase [157]. Beside the effect of avoiding nutrient limitations resulting in extended log-phase and higher cell densities when cells are cultivated in a fed-batch, the yield of recombinant proteins can be improved as well.

1.5 Ethyleneimine as inactivation agent for bacteria

More than 30 years ago Ethyleneimine (EI) was introduced for inactivation of viruses [158]. Nowadays, EI especially in its binary form (BEI) is widely used for virus inactivation within the production of killed virus vaccines [159]. EI acts by alkylating nucleic acids by modification of purines resulting in replication arrest and has been reported not to harm proteins [160-163]. *The nucleophilic substitution reaction performed by N7-guanine causes an opening of the BEI ring and guanine becomes alkylated* (**Fig. 12**) [159].

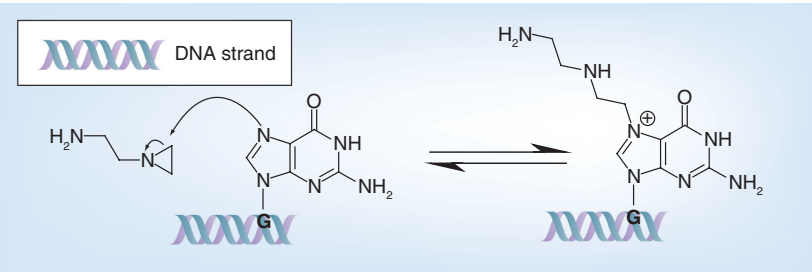

Figure 12. Reaction mechanism of BEI with guanine base of DNA or RNA published by Delrue *et al.* (2012) [159].

In the same mode of action adenine is alkylated by BEI [164]. Moreover, EI has been demonstrated to fully inactivate *Shigella flexneri* without limiting the antigenic and immunogenic quality of their outer membrane vesicles [165]. Also *Pasteurella haemolytica* in a suspension of 10^{10} $cells^{-ml}$ was reported to be fully inactivated by EI without minimizing antigenic properties [166]. In the presented work it was an aim to inactivate remaining live *Bordetella bronchiseptica* and *E. coli* after BG production.

1.6 References

1. **Zachariassen KE, Kristiansen E.** 2000. Ice Nucleation and Antinucleation in Nature. Cryobiology **41:**257-279.
2. **Hew CL, Yang DS.** 1992. Protein interaction with ice. Eur J Biochem **203:**33-42.
3. **Moore EB, Molinero V.** 2011. Structural transformation in supercooled water controls the crystallization rate of ice. Nature **479:**506-508.
4. **Kobashigawa Y, Nishimiya Y, Miura K, Ohgiya S, Miura A, Tsuda S.** 2005. A part of ice nucleation protein exhibits the ice-binding ability. FEBS Lett **579:**1493-1497.
5. **Vali G, DeMott PJ, Möhler O, Whale TF.** 2015. Technical Note: A proposal for ice nucleation terminology. Atmos Chem Phys **15:**10263-10270.
6. **Pradzynski CC, Forck RM, Zeuch T, Slavicek P, Buck U.** 2012. A fully size-resolved perspective on the crystallization of water clusters. Science **337:**1529-1532.
7. **Zaragoza A, Conde MM, Espinosa JR, Valeriani C, Vega C, Sanz E.** 2015. Competition between ices Ih and Ic in homogeneous water freezing. J Chem Phys **143:**134504.
8. **Takahashi T.** 1982. On the role of cubic structure in ice nucleation. Journal of Crystal Growth **59:**441-449.
9. **Vali G, DeMott P, Möhler O, Whale TF.** 2014. Ice nucleation terminology. Atmospheric Chemistry and Physics Discussions **14:**22155-22162.
10. **Franks F.** 2003. Nucleation of ice and its management in ecosystems. Philosophical Transactions of the Royal Society of London Series A: Mathematical, Physical and Engineering Sciences **361:**557-574.
11. **Ickes L, Welti A, Hoose C, Lohmann U.** 2015. Classical nucleation theory of homogeneous freezing of water: thermodynamic and kinetic parameters. Physical Chemistry Chemical Physics **17:**5514-5537.
12. **Cziczo DJ, Froyd KD.** 2014. Sampling the composition of cirrus ice residuals. Atmospheric Research **142:**15-31.
13. **Lundheim R.** 2002. Physiological and ecological significance of biological ice nucleators. Philos Trans R Soc Lond B Biol Sci **357:**937-943.
14. **Möhler O, Georgakopoulos DG, Morris CE, Benz S, Ebert V, Hunsmann S, Saathoff H, Schnaiter M, Wagner R.** 2008. Heterogeneous ice nucleation activity of bacteria: new laboratory experiments at simulated cloud conditions. Biogeosciences **5:**1425-1435.
15. **McCorkle AM.** 2009. Natural Ice-Nucleating Bacteria Increase the Freezing Tolerance of the Intertidal Bivalve Geukensia demissa. DigitalCommons@Connecticut College, Biology Honors Papers.
16. **Fukuta N, Schaller RC.** 1982. Ice Nucleation by Aerosol Particles. Theory of Condensation-Freezing Nucleation. Journal of the Atmospheric Sciences **39:**648-655.
17. **Li T, Donadio D, Ghiringhelli LM, Galli G.** 2009. Surface-induced crystallization in supercooled tetrahedral liquids. Nat Mater **8:**726-730.
18. **Koop T, Mahowald N.** 2013. Atmospheric science: The seeds of ice in clouds. Nature **498:**302-303.
19. **Lohmann U, Feichter J.** 2005. Global indirect aerosol effects: a review. Atmos Chem Phys **5:**715-737.
20. **Pratt KA, DeMott PJ, French JR, Wang Z, Westphal DL, Heymsfield AJ, Twohy CH, Prenni AJ, Prather KA.** 2009. In situ detection of biological particles in cloud ice-crystals. Nature Geosci **2:**398-401.
21. **Hoose C, Kristjánsson JE, Chen J-P, Hazra A.** 2010. A Classical-Theory-Based Parameterization of Heterogeneous Ice Nucleation by Mineral Dust, Soot, and Biological Particles in a Global Climate Model. Journal of the Atmospheric Sciences **67:**2483-2503.
22. **O'Sullivan D, Murray BJ, Ross JF, Whale TF, Price HC, Atkinson JD, Umo NS, Webb ME.** 2015. The relevance of nanoscale biological fragments for ice nucleation in clouds. Sci Rep **5:**8082.
23. **Wilson TW, Ladino LA, Alpert PA, Breckels MN, Brooks IM, Browse J, Burrows SM, Carslaw KS, Huffman JA, Judd C, Kilthau WP, Mason RH, McFiggans G, Miller LA, Najera JJ, Polishchuk E, Rae S, Schiller CL, Si M, Temprado JV, Whale TF, Wong JP,**

Wurl O, Yakobi-Hancock JD, Abbatt JP, Aller JY, Bertram AK, Knopf DA, Murray BJ. 2015. A marine biogenic source of atmospheric ice-nucleating particles. Nature **525:**234-238.

24. **Schnell RC, Vali G.** 1972. Atmospheric Ice Nuclei from Decomposing Vegetation. Nature **236:**163-165.
25. **Maki LR, Galyan EL, Chang-Chien MM, Caldwell DR.** 1974. Ice nucleation induced by pseudomonas syringae. Appl Microbiol **28:**456-459.
26. **Lindow SE, Arny DC, Upper CD.** 1982. Bacterial ice nucleation: a factor in frost injury to plants. Plant Physiol **70:**1084-1089.
27. **Lindow SE, Hirano SS, Barchet WR, Arny DC, Upper CD.** 1982. Relationship between Ice Nucleation Frequency of Bacteria and Frost Injury. Plant Physiol **70:**1090-1093.
28. **Gurian-Sherman D, Lindow SE.** 1993. Bacterial ice nucleation: significance and molecular basis. Faseb j **7:**1338-1343.
29. **Warren G, Wolber P.** 1991. Molecular aspects of microbial ice nucleation. Mol Microbiol **5:**239-243.
30. **Pandey R, Usui K, Livingstone RA, Fischer SA, Pfaendtner J, Backus EH, Nagata Y, Frohlich-Nowoisky J, Schmuser L, Mauri S, Scheel JF, Knopf DA, Poschl U, Bonn M, Weidner T.** 2016. Ice-nucleating bacteria control the order and dynamics of interfacial water. Sci Adv **2:**e1501630.
31. **Hill TCJ, Moffett BF, DeMott PJ, Georgakopoulos DG, Stump WL, Franc GD.** 2014. Measurement of Ice Nucleation-Active Bacteria on Plants and in Precipitation by Quantitative PCR. Appl Environ Microbiol **80:**1256-1267.
32. **Wilson SL, Kelley DL, Walker VK.** 2006. Ice-active characteristics of soil bacteria selected by ice-affinity. Environ Microbiol **8:**1816-1824.
33. **Lorv JS, Rose DR, Glick BR.** 2014. Bacterial ice crystal controlling proteins. Scientifica (Cairo) **2014:**976895.
34. **Sun X, Griffith M, Pasternak JJ, Glick BR.** 1995. Low temperature growth, freezing survival, and production of antifreeze protein by the plant growth promoting rhizobacterium Pseudomonas putida GR12-2. Can J Microbiol **41:**776-784.
35. **Lindow SE, Arny DC, Upper CD.** 1978. Erwinia herbicola: A Bacterial Ice Nucleus Active in Increasing Frost Injury to Corn. Phytopathology **68:**523-527.
36. **Phelps P, Giddings TH, Prochoda M, Fall R.** 1986. Release of cell-free ice nuclei by Erwinia herbicola. J Bacteriol **167:**496-502.
37. **Kawahara H.** 2008. Cryoprotectants and Ice-Binding Proteins, p 229-246. *In* Margesin R, Schinner F, Marx J-C, Gerday C (ed), Psychrophiles: from Biodiversity to Biotechnology doi:10.1007/978-3-540-74335-4_14. Springer Berlin Heidelberg, Berlin, Heidelberg.
38. **Abe K, Watabe S, Emori Y, Watanabe M, Arai S.** 1989. An ice nucleation active gene of Erwinia ananas. Sequence similarity to those of Pseudomonas species and regions required for ice nucleation activity. FEBS Lett **258:**297-300.
39. **Zhao JL, Orser CS.** 1990. Conserved repetition in the ice nucleation gene inaX from Xanthomonas campestris pv. translucens. Mol Gen Genet **223:**163-166.
40. **Muryoi N, Matsukawa K, Yamade K, Kawahara H, Obata H.** 2003. Purification and properties of an ice-nucleating protein from an ice-nucleating bacterium, Pantoea ananatis KUIN-3. J Biosci Bioeng **95:**157-163.
41. **Miller AM, Figueiredo JE, Linde GA, Colauto NB, Paccola-Meirelles LD.** 2016. Characterization of the inaA gene and expression of ice nucleation phenotype in Pantoea ananatis isolates from Maize White Spot disease. Genet Mol Res **15:**15017863.
42. **Hirano SS, Upper CD.** 2000. Bacteria in the leaf ecosystem with emphasis on Pseudomonas syringae-a pathogen, ice nucleus, and epiphyte. Microbiol Mol Biol Rev **64:**624-653.
43. **Morris CE, Conen F, Alex Huffman J, Phillips V, Poschl U, Sands DC.** 2014. Bioprecipitation: a feedback cycle linking earth history, ecosystem dynamics and land use through biological ice nucleators in the atmosphere. Glob Chang Biol **20:**341-351.
44. **Ogden LE.** 2014. Life in the Clouds. BioScience doi:10.1093/biosci/biu144
45. **Christner B.** 2012. Cloudy with a Chance of Microbes. Microbe Magazine **7:**70-75.

46. **Hirano SS, Baker LS, Upper CD.** 1996. Raindrop Momentum Triggers Growth of Leaf-Associated Populations of Pseudomonas syringae on Field-Grown Snap Bean Plants. Appl Environ Microbiol **62:**2560-2566.
47. **Morris CE, Sands DC, Vinatzer BA, Glaux C, Guilbaud C, Buffiere A, Yan S, Dominguez H, Thompson BM.** 2008. The life history of the plant pathogen Pseudomonas syringae is linked to the water cycle. ISME J **2:**321-334.
48. **Lindow SE, Arny DC, Upper CD.** 1978. Distribution of ice nucleation-active bacteria on plants in nature. Appl Environ Microbiol **36:**831-838.
49. **Kawahara H, Ikugawa H, Obata H.** 1996. Isolation and Characterization of a Marine Ice-nucleating Bacterium, Pseudomonas sp. KUIN-5, Which Produces Cellulose and Secretes It in the Culture Broth. Bioscience, Biotechnology, and Biochemistry **60:**1474-1478.
50. **Loomis SH, Zinser M.** 2001. Isolation and identification of an ice-nucleating bacterium from the gills of the intertidal bivalve mollusc Geukensia demissa. J Exp Mar Bio Ecol **261:**225-235.
51. **Burrows SM, Butler T, Jöckel P, Tost H, Kerkweg A, Pöschl U, Lawrence MG.** 2009. Bacteria in the global atmosphere – Part 2: Modeling of emissions and transport between different ecosystems. Atmos Chem Phys **9:**9281-9297.
52. **Stephanie, Waturangi DE.** 2011. Distribution of Ice Nucleation-Active (INA) Bacteria from Rain-water and Air. HAYATI Journal of Biosciences **18:**108-112.
53. **Paradis S, Boissinot M, Paquette N, Bélanger SD, Martel EA, Boudreau DK, Picard FJ, Ouellette M, Roy PH, Bergeron MG.** 2005. Phylogeny of the Enterobacteriaceae based on genes encoding elongation factor Tu and F-ATPase β-subunit. International Journal of Systematic and Evolutionary Microbiology **55:**2013-2025.
54. **Watanabe K, Sato M.** 1998. Detection of Variation of the R-Domain Structure of Ice Nucleation Genes in Erwinia herbicola-Group Bacteria by PCR-RFLP Analysis. Current Microbiology **37:**201-209.
55. **Morris CE, Monteil CL, Berge O.** 2013. The life history of Pseudomonas syringae: linking agriculture to earth system processes. Annu Rev Phytopathol **51:**85-104.
56. **Després VR, Huffman JA, Burrows SM, Hoose C, Safatov AS, Buryak G, Fröhlich-Nowoisky J, Elbert W, Andreae MO, Pöschl U, Jaenicke R.** 2012. Primary biological aerosol particles in the atmosphere: a review. 2012 **64:**
57. **DeLeon-Rodriguez N, Lathem TL, Rodriguez RL, Barazesh JM, Anderson BE, Beyersdorf AJ, Ziemba LD, Bergin M, Nenes A, Konstantinidis KT.** 2013. Microbiome of the upper troposphere: species composition and prevalence, effects of tropical storms, and atmospheric implications. Proc Natl Acad Sci U S A **110:**2575-2580.
58. **Attard E, Yang H, Delort AM, Amato P, Pöschl U, Glaux C, Koop T, Morris CE.** 2012. Effects of atmospheric conditions on ice nucleation activity of Pseudomonas. Atmos Chem Phys **12:**10667-10677.
59. **Bauer H, Giebl H, Hitzenberger R, Kasper-Giebl A, Reischl G, Zibuschka F, Puxbaum H.** 2003. Airborne bacteria as cloud condensation nuclei. Journal of Geophysical Research: Atmospheres **108:**n/a-n/a.
60. **Amato P.** 2012. Clouds Provide Atmospheric Oases for Microbes. Microbe Magazine **7:**119-123.
61. **Lohmann U.** 2017. Modes of ice formation in clouds. http://www.iac.ethz.ch/group/atmospheric-physics/research/ice-nucleation.html. Accessed
62. **Oude Vrielink AS, Aloi A, Olijve LL, Voets IK.** 2016. Interaction of ice binding proteins with ice, water and ions. Biointerphases **11:**018906.
63. **Green RL, Warren GJ.** 1985. Physical and functional repetition in a bacterial ice nucleation gene. Nature **317:**645-648.
64. **Schmid D, Pridmore D, Capitani G, Battistutta R, Neeser J-R, Jann A.** 1997. Molecular organisation of the ice nucleation protein InaV fromPseudomonas syringae. FEBS Letters **414:**590-594.
65. **Li Q, Yan Q, Chen J, He Y, Wang J, Zhang H, Yu Z, Li L.** 2012. Molecular characterization of an ice nucleation protein variant (inaQ) from Pseudomonas syringae and the analysis of its transmembrane transport activity in Escherichia coli. Int J Biol Sci **8:**1097-1108.

66. **Kajava AV, Lindow SE.** 1993. A model of the three-dimensional structure of ice nucleation proteins. J Mol Biol **232:**709-717.
67. **Jung HC, Lebeault JM, Pan JG.** 1998. Surface display of Zymomonas mobilis levansucrase by using the ice-nucleation protein of Pseudomonas syringae. Nat Biotechnol **16:**576-580.
68. **Kawahara H.** 2002. The structures and functions of ice crystal-controlling proteins from bacteria. J Biosci Bioeng **94:**492-496.
69. **Kozloff LM, Turner MA, Arellano F.** 1991. Formation of bacterial membrane ice-nucleating lipoglycoprotein complexes. J Bacteriol **173:**6528-6536.
70. **Kawahara H.** 2013. Characterizations of Functions of Biological Materials Having Controlling-Ability Against Ice Crystal Growth, in Advanced Topics on Crystal Growth, Dr. Sukarno Ferreira (Ed.). INTECH doi:10.5772/54535
71. **Graether SP, Jia Z.** 2001. Modeling Pseudomonas syringae ice-nucleation protein as a beta-helical protein. Biophys J **80:**1169-1173.
72. **Wolber P, Warren G.** 1989. Bacterial ice-nucleation proteins. Trends Biochem Sci **14:**179-182.
73. **Green RL, Corotto LV, Warren GJ.** 1988. Deletion mutagenesis of the ice nucleation gene from Pseudomonas syringae S203. Mol Gen Genet **215:**165-172.
74. **Garnham CP, Campbell RL, Walker VK, Davies PL.** 2011. Novel dimeric beta-helical model of an ice nucleation protein with bridged active sites. BMC Struct Biol **11:**36.
75. **Davies PL.** 2014. Ice-binding proteins: a remarkable diversity of structures for stopping and starting ice growth. Trends Biochem Sci **39:**548-555.
76. **Bar Dolev M, Braslavsky I, Davies PL.** 2016. Ice-Binding Proteins and Their Function. Annu Rev Biochem **85:**515-542.
77. **Nutt DR, Smith JC.** 2008. Dual function of the hydration layer around an antifreeze protein revealed by atomistic molecular dynamics simulations. J Am Chem Soc **130:**13066-13073.
78. **Smolin N, Daggett V.** 2008. Formation of ice-like water structure on the surface of an antifreeze protein. J Phys Chem B **112:**6193-6202.
79. **Garnham CP, Campbell RL, Davies PL.** 2011. Anchored clathrate waters bind antifreeze proteins to ice. Proc Natl Acad Sci U S A **108:**7363-7367.
80. **Guo S, Garnham CP, Whitney JC, Graham LA, Davies PL.** 2012. Re-evaluation of a bacterial antifreeze protein as an adhesin with ice-binding activity. PLoS One **7:**e48805.
81. **Govindarajan AG, Lindow SE.** 1988. Size of bacterial ice-nucleation sites measured in situ by radiation inactivation analysis. Proc Natl Acad Sci U S A **85:**1334-1338.
82. **Wolber PK, Deininger CA, Southworth MW, Vandekerckhove J, van Montagu M, Warren GJ.** 1986. Identification and purification of a bacterial ice-nucleation protein. Proc Natl Acad Sci U S A **83:**7256-7260.
83. **Mueller GM, Wolber PK, Warren GJ.** 1990. Clustering of ice nucleation protein correlates with ice nucleation activity. Cryobiology **27:**416-422.
84. **Welch JF, Speidel, H. K.** 1989. Visualization of potential bacterial ice nucleation sites. Cryo Letters **10:**309-314.
85. **Ruggles JA, Nemecek-Marshall M, Fall R.** 1993. Kinetics of appearance and disappearance of classes of bacterial ice nuclei support an aggregation model for ice nucleus assembly. J Bacteriol **175:**7216-7221.
86. **Turner MA, Arellano F, Kozloff LM.** 1990. Three separate classes of bacterial ice nucleation structures. J Bacteriol **172:**2521-2526.
87. **Turner MA, Arellano F, Kozloff LM.** 1991. Components of ice nucleation structures of bacteria. J Bacteriol **173:**6515-6527.
88. **Kozloff LM, Turner MA, Arellano F, Lute M.** 1991. Phosphatidylinositol, a phospholipid of ice-nucleating bacteria. J Bacteriol **173:**2053-2060.
89. **Burke MJ, Lindow SE.** 1990. Surface properties and size of the ice nucleation site in ice nucleation active bacteria: Theoretical considerations. Cryobiology **27:**80-84.
90. **Orser C, Staskawicz BJ, Panopoulos NJ, Dahlbeck D, Lindow SE.** 1985. Cloning and expression of bacterial ice nucleation genes in Escherichia coli. J Bacteriol **164:**359-366.
91. **Baertlein DA, Lindow SE, Panopoulos NJ, Lee SP, Mindrinos MN, Chen TH.** 1992. Expression of a bacterial ice nucleation gene in plants. Plant Physiol **100:**1730-1736.

92. **Lindgren PB, Frederick R, Govindarajan AG, Panopoulos NJ, Staskawicz BJ, Lindow SE.** 1989. An ice nucleation reporter gene system: identification of inducible pathogenicity genes in Pseudomonas syringae pv. phaseolicola. Embo j **8:**1291-1301.
93. **van Bloois E, Winter RT, Kolmar H, Fraaije MW.** 2011. Decorating microbes: surface display of proteins on Escherichia coli. Trends Biotechnol **29:**79-86.
94. **Gao F, Ding H, Feng Z, Liu D, Zhao Y.** 2014. Functional display of triphenylmethane reductase for dye removal on the surface of Escherichia coli using N-terminal domain of ice nucleation protein. Bioresour Technol **169:**181-187.
95. **Fan LH, Liu N, Yu MR, Yang ST, Chen HL.** 2011. Cell surface display of carbonic anhydrase on Escherichia coli using ice nucleation protein for CO(2) sequestration. Biotechnol Bioeng **108:**2853-2864.
96. **Pattnaik PB, V. K.; Sunita Grover; Niyaz Ahmed.** 1997. Bacterial ice nucleation: prospects and perspectives. Current Science **72:**316-320.
97. **Kwak YD, Yoo SK, Kim EJ.** 1999. Cell surface display of human immunodeficiency virus type 1 gp120 on Escherichia coli by using ice nucleation protein. Clin Diagn Lab Immunol **6:**499-503.
98. **Wolber PK, Green RL.** 1990. Detection of bacteria by transduction of ice nucleation genes. Trends Biotechnol **8:**276-279.
99. **Venketesh S, Dayananda C.** 2008. Properties, potentials, and prospects of antifreeze proteins. Crit Rev Biotechnol **28:**57-82.
100. **Duman JG, Olsen TM.** 1993. Thermal Hysteresis Protein Activity in Bacteria, Fungi, and Phylogenetically Diverse Plants. Cryobiology **30:**322-328.
101. **Gilbert JA, Davies PL, Laybourn-Parry J.** 2005. A hyperactive, Ca2+-dependent antifreeze protein in an Antarctic bacterium. FEMS Microbiol Lett **245:**67-72.
102. **Kawahara H, Iwanaka Y, Higa S, Muryoi N, Sato M, Honda M, Omura H, Obata H.** 2007. A novel, intracellular antifreeze protein in an antarctic bacterium, Flavobacterium xanthum. Cryo Letters **28:**39-49.
103. **Scotter AJ, Marshall CB, Graham LA, Gilbert JA, Garnham CP, Davies PL.** 2006. The basis for hyperactivity of antifreeze proteins. Cryobiology **53:**229-239.
104. **Raymond JA, DeVries AL.** 1977. Adsorption inhibition as a mechanism of freezing resistance in polar fishes. Proc Natl Acad Sci U S A **74:**2589-2593.
105. **Kristiansen E, Zachariassen KE.** 2005. The mechanism by which fish antifreeze proteins cause thermal hysteresis. Cryobiology **51:**262-280.
106. **Garnham CP, Gilbert JA, Hartman CP, Campbell RL, Laybourn-Parry J, Davies PL.** 2008. A Ca2+-dependent bacterial antifreeze protein domain has a novel beta-helical ice-binding fold. Biochem J **411:**171-180.
107. **Yu SO, Brown A, Middleton AJ, Tomczak MM, Walker VK, Davies PL.** 2010. Ice restructuring inhibition activities in antifreeze proteins with distinct differences in thermal hysteresis. Cryobiology **61:**327-334.
108. **Singh P, Hanada Y, Singh SM, Tsuda S.** 2014. Antifreeze protein activity in Arctic cryoconite bacteria. FEMS Microbiology Letters **351:**14-22.
109. **Gilbert JA, Hill PJ, Dodd CE, Laybourn-Parry J.** 2004. Demonstration of antifreeze protein activity in Antarctic lake bacteria. Microbiology **150:**171-180.
110. **Kawahara H, Nakano Y, Omiya K, Muryoi N, Nishikawa J, Obata H.** 2004. Production of two types of ice crystal-controlling proteins in Antarctic bacterium. J Biosci Bioeng **98:**220-223.
111. **Raymond JA, Christner BC, Schuster SC.** 2008. A bacterial ice-binding protein from the Vostok ice core. Extremophiles **12:**713-717.
112. **Xu H, Griffith M, Patten CL, Glick BR.** 1998. Isolation and characterization of an antifreeze protein with ice nucleation activity from the plant growth promoting rhizobacterium Pseudomonas putida GR12-2. Canadian Journal of Microbiology **44:**64-73.
113. **Fletcher GL, Hew CL, Davies PL.** 2001. Antifreeze proteins of teleost fishes. Annu Rev Physiol **63:**359-390.
114. **Yamashita Y, Nakamura N, Omiya K, Nishikawa J, Kawahara H, Obata H.** 2002. Identification of an antifreeze lipoprotein from Moraxella sp. of Antarctic origin. Biosci Biotechnol Biochem **66:**239-247.

115. **Muryoi N, Sato M, Kaneko S, Kawahara H, Obata H, Yaish MW, Griffith M, Glick BR.** 2004. Cloning and expression of afpA, a gene encoding an antifreeze protein from the arctic plant growth-promoting rhizobacterium Pseudomonas putida GR12-2. J Bacteriol **186:**5661-5671.
116. **Schon P, Schrot G, Wanner G, Lubitz W, Witte A.** 1995. Two-stage model for integration of the lysis protein E of phi X174 into the cell envelope of Escherichia coli. FEMS Microbiol Rev **17:**207-212.
117. **Witte A, Wanner G, Sulzner M, Lubitz W.** 1992. Dynamics of PhiX174 protein E-mediated lysis of Escherichia coli. Arch Microbiol **157:**381-388.
118. **Hutchison CA, 3rd, Sinsheimer RL.** 1966. The process of infection with bacteriophage phi-X174. X. Mutations in a phi-X Lysis gene. J Mol Biol **18:**429-447.
119. **Blasi U, Linke RP, Lubitz W.** 1989. Evidence for membrane-bound oligomerization of bacteriophage phi X174 lysis protein-E. J Biol Chem **264:**4552-4558.
120. **Witte A, Wanner G, Blasi U, Halfmann G, Szostak M, Lubitz W.** 1990. Endogenous transmembrane tunnel formation mediated by phi X174 lysis protein E. J Bacteriol **172:**4109-4114.
121. **Witte A, Blasi U, Halfmann G, Szostak M, Wanner G, Lubitz W.** 1990. Phi X174 protein E-mediated lysis of Escherichia coli. Biochimie **72:**191-200.
122. **Witte A, Wanner G, Lubitz W, Holtje JV.** 1998. Effect of phi X174 protein E-mediated lysis on murein composition of Escherichia coli. FEMS Microbiol Lett **164:**149-157.
123. **Mayr UB, Walcher P, Azimpour C, Riedmann E, Haller C, Lubitz W.** 2005. Bacterial ghosts as antigen delivery vehicles. Adv Drug Deliv Rev **57:**1381-1391.
124. **Lubitz P, Mayr UB, Lubitz W.** 2009. Applications of bacterial ghosts in biomedicine. Adv Exp Med Biol **655:**159-170.
125. **Marchart J, Dropmann G, Lechleitner S, Schlapp T, Wanner G, Szostak MP, Lubitz W.** 2003. Pasteurella multocida- and Pasteurella haemolytica-ghosts: new vaccine candidates. Vaccine **21:**3988-3997.
126. **Marchart J, Rehagen M, Dropmann G, Szostak MP, Alldinger S, Lechleitner S, Schlapp T, Resch S, Lubitz W.** 2003. Protective immunity against pasteurellosis in cattle, induced by Pasteurella haemolytica ghosts. Vaccine **21:**1415-1422.
127. **Szostak MP, Hensel A, Eko FO, Klein R, Auer T, Mader H, Haslberger A, Bunka S, Wanner G, Lubitz W.** 1996. Bacterial ghosts: non-living candidate vaccines. J Biotechnol **44:**161-170.
128. **Langemann T, Koller VJ, Muhammad A, Kudela P, Mayr UB, Lubitz W.** 2010. The Bacterial Ghost platform system: production and applications. Bioeng Bugs **1:**326-336.
129. **Ebensen T, Paukner S, Link C, Kudela P, de Domenico C, Lubitz W, Guzman CA.** 2004. Bacterial ghosts are an efficient delivery system for DNA vaccines. J Immunol **172:**6858-6865.
130. **Paukner S, Kohl G, Jalava K, Lubitz W.** 2003. Sealed bacterial ghosts--novel targeting vehicles for advanced drug delivery of water-soluble substances. J Drug Target **11:**151-161.
131. **Paukner S, Kohl G, Lubitz W.** 2004. Bacterial ghosts as novel advanced drug delivery systems: antiproliferative activity of loaded doxorubicin in human Caco-2 cells. Journal of Controlled Release **94:**63-74.
132. **Paukner S, Kudela P, Kohl G, Schlapp T, Friedrichs S, Lubitz W.** 2005. DNA-loaded bacterial ghosts efficiently mediate reporter gene transfer and expression in macrophages. Mol Ther **11:**215-223.
133. **Kuen B, Koch A, Asenbauer E, Sara M, Lubitz W.** 1997. Molecular characterization of the Bacillus stearothermophilus PV72 S-layer gene sbsB induced by oxidative stress. J Bacteriol **179:**1664-1670.
134. **Kuen B, Sara M, Lubitz W.** 1996. Heterologous expression and self-assembly of the S-layer protein SbsA of Bacillus stearothermophilus in Escherichia coli. Mol Microbiol **19:**495-503.
135. **Howorka S, Sara M, Lubitz W, Kuen B.** 1999. Self-assembly product formation of the Bacillus stearothermophilus PV72/p6 S-layer protein SbsA in the course of autolysis of Bacillus subtilis. FEMS Microbiol Lett **172:**187-196.

136. **Sara M, Sleytr UB.** 1994. Comparative studies of S-layer proteins from Bacillus stearothermophilus strains expressed during growth in continuous culture under oxygen-limited and non-oxygen-limited conditions. J Bacteriol **176:**7182-7189.
137. **Muhammad A, Champeimont J, Mayr UB, Lubitz W, Kudela P.** 2012. Bacterial ghosts as carriers of protein subunit and DNA-encoded antigens for vaccine applications. Expert Rev Vaccines **11:**97-116.
138. **Truppe M, Howorka, S., Schroll, G., Lechleitner, S., Kuen, B., Resch, S. and Lubitz, W.** 1997. Biotechnological applications of recombinant S-layer proteins rSbsA and rSbsB from Bacillus stear- othermophilus PV72. FEMS Microbiol Rev **20:**88-91.
139. **Riedmann EM, Kyd JM, Smith AM, Gomez-Gallego S, Jalava K, Cripps AW, Lubitz W.** 2003. Construction of recombinant S-layer proteins (rSbsA) and their expression in bacterial ghosts--a delivery system for the nontypeable Haemophilus influenzae antigen Omp26. FEMS Immunol Med Microbiol **37:**185-192.
140. **Riedmann EM, Lubitz W, McGrath J, Kyd JM, Cripps AW.** 2011. Effectiveness of engineering the nontypeable Haemophilus influenzae antigen Omp26 as an S-layer fusion in bacterial ghosts as a mucosal vaccine delivery. Hum Vaccin **7 Suppl:**99-107.
141. **Szostak M, Wanner G, Lubitz W.** 1990. Recombinant bacterial ghosts as vaccines. Res Microbiol **141:**1005-1007.
142. **Szostak MP, Mader H, Truppe M, Kamal M, Eko FO, Huter V, Marchart J, Jechlinger W, Haidinger W, Brand E, Denner E, Resch S, Dehlin E, Katinger A, Kuen B, Haslberger A, Hensel A, Lubitz W.** 1997. Bacterial ghosts as multifunctional vaccine particles. Behring Inst Mitt 191-196.
143. **Witte A, Reisinger GR, Sackl W, Wanner G, Lubitz W.** 1998. Characterization of Escherichia coli lysis using a family of chimeric E-L genes. FEMS Microbiol Lett **164:**159-167.
144. **Lubitz W, Witte A, Eko FO, Kamal M, Jechlinger W, Brand E, Marchart J, Haidinger W, Huter V, Felnerova D, Stralis-Alves N, Lechleitner S, Melzer H, Szostak MP, Resch S, Mader H, Kuen B, Mayr B, Mayrhofer P, Geretschlager R, Haslberger A, Hensel A.** 1999. Extended recombinant bacterial ghost system. J Biotechnol **73:**261-273.
145. **Cui X, Duckworth JA, Lubitz P, Molinia FC, Haller C, Lubitz W, Cowan PE.** 2010. Humoral immune responses in brushtail possums (Trichosurus vulpecula) induced by bacterial ghosts expressing possum zona pellucida 3 protein. Vaccine **28:**4268-4274.
146. **Jechlinger W, Haller C, Resch S, Hofmann A, Szostak MP, Lubitz W.** 2005. Comparative immunogenicity of the hepatitis B virus core 149 antigen displayed on the inner and outer membrane of bacterial ghosts. Vaccine **23:**3609-3617.
147. **Witte A, Brand E, Mayrhofer P, Narendja F, Lubitz W.** 1998. Mutations in cell division proteins FtsZ and FtsA inhibit phiX174 protein-E-mediated lysis of Escherichia coli. Arch Microbiol **170:**259-268.
148. **Witte A, Lubitz W.** 1989. Biochemical characterization of phi X174-protein-E-mediated lysis of Escherichia coli. Eur J Biochem **180:**393-398.
149. **Witte A, Lubitz W, Bakker EP.** 1987. Proton-motive-force-dependent step in the pathway to lysis of Escherichia coli induced by bacteriophage phi X174 gene E product. J Bacteriol **169:**1750-1752.
150. **Lubitz W, Halfmann G, Plapp R.** 1984. Lysis of Escherichia coli after infection with phiX174 depends on the regulation of the cellular autolytic system. J Gen Microbiol **130:**1079-1087.
151. **Blasi U, Henrich B, Lubitz W.** 1985. Lysis of Escherichia coli by cloned phi X174 gene E depends on its expression. J Gen Microbiol **131:**1107-1114.
152. **Jechlinger W SM, Witte A, Lubitz W.** 1999. Altered temperature induction sensitivity of the lambda pR/cI857 system for controlled gene E expression in Escherichia coli. FEMS Microbiol Lett **173:**347–352.
153. **Haidinger W, Mayr UB, Szostak MP, Resch S, Lubitz W.** 2003. Escherichia coli Ghost Production by Expression of Lysis Gene E and Staphylococcal Nuclease. Applied and Environmental Microbiology **69:**6106-6113.

154. **Meitz A, Sagmeister P, Lubitz W, Herwig C, Langemann T.** 2016. Fed-Batch Production of Bacterial Ghosts Using Dielectric Spectroscopy for Dynamic Process Control. Microorganisms **4:**
155. **Langemann T, Mayr UB, Meitz A, Lubitz W, Herwig C.** 2016. Multi-parameter flow cytometry as a process analytical technology (PAT) approach for the assessment of bacterial ghost production. Appl Microbiol Biotechnol **100:**409-418.
156. **Perrin P, Morgeaux S.** 1995. Inactivation of DNA by beta-propiolactone. Biologicals **23:**207-211.
157. **Suhrer I, Langemann T, Lubitz W, Weuster-Botz D, Castiglione K.** 2015. A novel one-step expression and immobilization method for the production of biocatalytic preparations. Microb Cell Fact **14:**180.
158. **Warrington RE, Cunliffe HR, Bachrach HL.** 1973. Derivatives of aziridine as inactivants for foot-and-mouth disease virus vaccines. Am J Vet Res **34:**1087-1091.
159. **Delrue I, Verzele D, Madder A, Nauwynck HJ.** 2012. Inactivated virus vaccines from chemistry to prophylaxis: merits, risks and challenges. Expert Rev Vaccines **11:**695-719.
160. **Aarthi D, Ananda Rao K, Robinson R, Srinivasan VA.** 2004. Validation of binary ethyleneimine (BEI) used as an inactivant for foot and mouth disease tissue culture vaccine. Biologicals **32:**153-156.
161. **Bahnemann HG.** 1976. Inactivation of viruses in serum with binary ethyleneimine. J Clin Microbiol **3:**209-210.
162. **Bahnemann HG.** 1990. Inactivation of viral antigens for vaccine preparation with particular reference to the application of binary ethylenimine. Vaccine **8:**299-303.
163. **Brown F.** 2001. Inactivation of viruses by aziridines. Vaccine **20:**322-327.
164. **Broo K, Wei J, Marshall D, Brown F, Smith TJ, Johnson JE, Schneemann A, Siuzdak G.** 2001. Viral capsid mobility: a dynamic conduit for inactivation. Proc Natl Acad Sci U S A **98:**2274-2277.
165. **Camacho AI, Souza-Reboucas J, Irache JM, Gamazo C.** 2013. Towards a non-living vaccine against Shigella flexneri: from the inactivation procedure to protection studies. Methods **60:**264-268.
166. **Bauer K, Wittmann G, Mussgay M, Irion E, Geilhausen H.** 1977. Ethyleneimine inactivated microorganisms. US patent 4036952.

2 Outer-membrane anchored INP on BGs envelope

In a concept study the ability to induce ice formation by BGs from *Escherichia coli* carrying ice nucleation protein InaZ from *Pseudomonas syringae* in their outer membrane has been investigated in chapter 2.2. To produce ice nucleation active (ina$^+$) BGs, two different *E*-lysis plasmids were evaluated in combination with the INP expression vector. The two *E*-lysis plasmids were used in combination with ice nucleation plasmid pBINP to evaluate differences in the quality of catalyzing ice nucleation in the produced ina$^+$ BGs. Furthermore, nucleation efficiency of produced ina$^+$ BGs was compared to their living ancestors. In chapter 2.3 *E. coli* C41 cultures expressing InaZ for 15h were tested for type I nucleation activity. All material and methods used in this chapter are described in section "Materials and Methods".

2.1 Publication. Functional display of ice nucleation protein InaZ on the surface of bacterial ghosts

2.2 Contribution to Publication

The author of the thesis designed and performed all the experiments – except the FCM analysis and INP purification – evaluated the data, created the figures and contributed to writing the accepted manuscript.

Processing status:

Accepted for publishing in Bioengineered:

Kassmannhuber J, Rauscher M, Schöner L, Witte A, Lubitz W. 2017. Functional Display of Ice Nucleation Protein InaZ on the Surface of Bacterial Ghosts. Bioengineered.

http://dx.doi.org/10.1080/21655979.2017.1284712

Received 09 Dec 2016, Accepted 17 Jan 2017, Accepted author version posted online: 25 Jan 2017, Published online: 25 Jan 2017

BIOENGINEERED
2017, VOL. 0, NO. 0, 1–13
http://dx.doi.org/10.1080/21655979.2017.1284712

Taylor & Francis
Taylor & Francis Group

RESEARCH PAPER

Functional display of ice nucleation protein InaZ on the surface of bacterial ghosts

Johannes Kassmannhuber[a,b], Mascha Rauscher[a], Lea Schöner[a], Angela Witte[c], and Werner Lubitz[a]

[a]BIRD-C GmbH; Vienna, Austria; [b]Centre of Molecular Biology; University of Vienna; Vienna, Austria; [c]Department of Microbiology, Immunobiology and Genetics, Max F. Perutz Laboratories, University of Vienna, Vienna, Austria

ABSTRACT
In a concept study the ability to induce heterogeneous ice formation by Bacterial Ghosts (BGs) from *Escherichia coli* carrying ice nucleation protein InaZ from *Pseudomonas syringae* in their outer membrane was investigated by a droplet-freezing assay of ultra-pure water. As determined by the median freezing temperature and cumulative ice nucleation spectra it could be demonstrated that both the living recombinant *E. coli* and their corresponding BGs functionally display InaZ on their surface. Under the production conditions chosen both samples belong to type II ice-nucleation particles inducing ice formation at a temperature range of between −5.6 °C and −6.7 °C, respectively. One advantage for the application of such BGs over their living recombinant mother bacteria is that they are non-living native cell envelopes retaining the biophysical properties of ice nucleation and do no longer represent genetically modified organisms (GMOs).

ARTICLE HISTORY
Received 9 December 2016
Revised 16 January 2017
Accepted 17 January 2017

KEYWORDS
bacterial ghosts; ice nucleation; ice nucleation protein

Introduction

Ice nucleation proteins (INPs) of ice nucleation active (ina$^+$) bacteria have the property to catalyze heterogeneous ice formation of supercooled water by orienting water molecules into an ice-like structure.[1-3] INPs are integrated to the outer cell membrane of Gram-negative bacteria where they form large multimers,[4-6] or can be released into the surrounding environment known as extracellular ice nucleating material.[7,8] Generally, ina$^+$ bacteria are Gram-negative, epiphytic and pathogenic as *Pseudomonas syringae, Pseudomonas putidia, Erwinia herbicola, Erwinia ananas, Xanthomonas campestris, or Pantoea ananatis* among others.[7-17] The well characterized plant pathogen *Pseudomonas syringae* represents one of the most efficient INA bacterial ice nucleus known, initiating plant damaging ice formation at temperatures of −2°C.[11,18] Aside from the habitat of an epiphytic plant pathogen, *Pseudomonas syringae*, as well as other INA bacteria were found in clouds, rain, snow and streams indicating that they are disseminated with the earth hydrological cycle.[19-22] Airborne ice-active bacteria are involved in cloud condensation – acting as cloud condensation nuclei (CCN) – and precipitation.[23,24]

Recombinant bacterial INPs were already functionally expressed in Gram-negative non-ice nucleation active *Escherichia coli*, as well as in plants.[25,26] INPs are also used for molecular biologic applications, using ice-nucleation activity as a reporter gene system.[27] In addition, the N-terminal domain of INPs, which link the protein to the outer cell membrane is used as cell surface display system.[28-30]

In this concept study the ice nucleation protein Z (InaZ) of *Pseudomonas syringae* was expressed in *E. coli* which were further processed to Bacterial Ghosts (BGs). BGs are empty cell envelopes of Gram-negative bacteria produced by the expression of cloned gene *E* of bacteriophage Phix174[31-35] The conversion of a single living bacterium into a BG is a rapid process in the range of milliseconds[35] and can be characterized by puncturing the bacterium cell envelope from the inside to the outside expelling its cytoplasmic content to the surrounding medium. Electron micrographs of this process can be depicted from the original description in 1990[33] and a more recent one using this E-mediated lysis of *E. coli* for cryo-electron tomography of membrane protein complexes within the native cell envelope complex remaining intact after E-mediated lysis.[34]

Any protein, lipid, polysaccharide and complex structures derived from the molecular building blocks

CONTACT Werner Lubitz werner.lubitz@bird-c.at BIRD-C GmbH, Vienna, Austria

of the cell envelope complex of a living bacterium (either natural or recombinant expressed) is retained in BGs.[35,36] The formation of the E-specific transmembrane tunnel structure seals the periplasmic space retaining all constituents of this compartment with a minimal loss of less than 10% as compared with 90% of constituents from the cytoplasmic space measured by marker enzyme release and electron microscopic studies during the E-lysis process.[33,37,38] The loss of cytoplasm including its nucleic acids content, ribosomes, soluble proteins and other solutes is compensated by an influx of water through the envelope shell which is freely permeable for water.[35] The advantage of BGs over their living mother bacteria is that they are non-living but contain a native cell envelope with their biophysical and biochemical characteristics.[34,35]

BGs represent a versatile alternative to bacteria when properties of the cell envelope are in the focus of interest as they represent the state and composition of the cell envelope at the time point of their production. In this communication it was investigated whether recombinant proteins introduced into the envelope complex of *E. coli* such as INP also retain their functional properties in the BG envelope. So far surface changes in BGs have only been tested immunologically by inserting foreign antigens sequences into a loop of OmpA facing the outside of the outer membrane of *E. coli* but not functionally for the biophysical integrity of structural components.[39] Inserting INP into the cell envelope of *E. coli* and measuring its ice nucleation activities is the first example reporting the structural and functional stability of a recombinant protein being inserted into the outer membrane of BGs.

Results

E-mediated lysis for production of ice nucleation-active bacterial ghosts

To produce BGs carrying INPs genes *inaZ* and *E*, carried on different plasmids were transformed into *E. coli* C41. Briefly, 2 E-lysis plasmids have been used for this study (Fig. 1), pGLysivb which carries lysis gene *E* fused with an *in vivo* biotinylation sequence under transcriptional control of a *c*I857 repressor gene and mutated - λp_{Rmut}- operator system[40,41] and pGLMivb which represents a modification of pGLysivb where *E*-mediated cell lysis is controlled by *LacIq* / P_{TAC} repressor / promoter system. To express ice nucleation protein InaZ, in the follow called INP, its full length

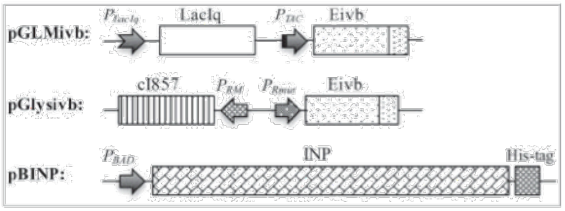

Figure 1. Partial map of plasmids used for production of BGs carrying INP.

sequence was fused to a C-terminal His-tag sequence located in plasmid pBINP downstream of the arabinose inducible P_{BAD} promoter (Fig. 1). Induction of INP was constitutive for the overnight culture of *E. coli* C41 (pBINP) clones used for E-lysis studies with plasmids pGLysivb and pGLMivb. The chemical and temperature inducible *E*-lysis plasmids were tested for lysis efficiency in combination with the INP expressed from pBINP in *E. coli* strain C41. With lysis plasmid pGLMivb expression of gene *E* is driven by the IPTG inducible P_{TAC} promotor, whereas with plasmid pGLysivb E-mediated lysis is induced by a temperature upshift of the culture from 23°C to 42°C under control of temperature-sensitive λ P_{Rmut} – cI857 promoter – repressor system. *E. coli* C41 was selected to produce INP-BGs as this strain is able to maintain cellular vitality despite recombinant membrane protein overexpression. [42]

In *E. coli* C41 carrying pBINP, expression of INP was induced by the addition of 0.2% arabinose to the culture medium. The culture was grown at 23°C as it has been shown that temperatures below 25°C have beneficial effects on ice nucleation activity.,[25,43] When the culture reached an optical density at 600 nm (OD_{600}) of 0.55–0.6 E-specific lysis was induced either by a temperature up-shift from 23 to 42°C (pGlysivb), or by addition of 0.5 mM IPTG (pGLMivb) and is referred to time point (Tp) 0 min in the corresponding growth curves (Fig. 2). The growth and lysis of the bacteria was monitored by measuring the OD_{600}, flow cytometry, light microscopy and by determination of colony forming units (cfu) analysis (Figs. 2–4).

During the growth phase of *E. coli* C41 carrying pBINP elongation of the cell body was observed in some of the bacteria. This elongation was unspecific in regard of INP expression as *E. coli* C41 cells carrying plasmid pBAD24 (the backbone plasmid of pBINP) and the lysis plasmid pGLysivb exhibit the same phenotype (Fig. 4).

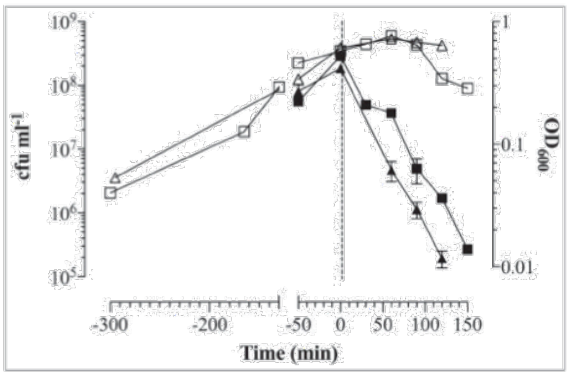

Figure 2. Growth and E-lysis of *E. coli* C41 carrying plasmids for expression of INP and BG production. *E. coli* C41 (pBINP, pGLMivb) (quad) and *E. coli* C41 (pBINP, pGLysivb) (triangle) cultures were grown in LBv supplemented with 0.2% arabinose to induce INP expression at 23°C from plasmid pBINP. At time point zero (illustrated by vertical sketched line) E-mediated lysis was induced from pGLysivb by temperature shift from 23°C to 42°C and from pGLMivb by addition of 0.5 mM IPTG. Open symbols indicate OD_{600} values of growth and lysis phase. During E-lysis colony forming units (closed symbols) were determined to calculate lysis efficiency. After 120 min (*E. coli* C41 [pBINP, pGLysivb]) and 150 min (*E. coli* C41 [pBINP, pGLMivb]) BG production was completed. Data were obtained from 3 independent experiments. Error bars indicate standard errors.

The E-lysis process of *E. coli* C41 (pBINP, pGLysivb) and *E. coli* C41 (pBINP, pGLMivb) was also monitored online via fluorescence-based flow cytometry (FCM) (Fig. 3), which allows an almost online process control to discriminate the ratio of full non-lysed bacteria and BGs already formed.[44] In a FCM sample of bacterial culture the use of the phospholipids staining dye RH414 enables the visualization of bacteria and the discrimination of non-cellular background. DiBAC4(3), which enters depolarized cell membranes and binds to intracellular proteins or membranes, provides an assessment of bacterial cell viability.[45] During E-lysis process of *E. coli* C41 (pBINP, pGLysivb) and *E. coli* C41 (pBINP, pGLMivb) BGs exhibit a strong DiBAC4(3) fluorescence signal and a complete shift of DiBAC-negative living cells (G1) to DiBAC-positive BGs (G2), can be detected at the end of lysis (Fig. 3). The lysis of the temperature inducible C41(pBINP, pGLysivb) culture and the chemically induced C41 (pBINP, pGLMivb) culture reached their time point of 99.9% lysis efficiency (LE) at 120 min and 150 min after lysis induction, respectively (Fig. 2). The presence of INP in C41 bacteria did not affect E-mediated lysis when compared with C41 bacteria carrying plasmid pBAD24 and lysis plasmid pGLysivb (Data not shown).

To inactivate *E*-lysis escape mutants and non-lysed bacteria at time of harvest, the cultures were further incubated for 2h at 23°C with 0.17% β-propiolactone. This standard procedure for inactivation of any nucleic acids remaining in BG preparations[45] ensures that BGs carrying INP and BGs without INP which were used in the following for the droplet-freezing assay did not contain any viable cells.

The attempts to trace pBINP encoded INP by its C-terminal His-tag were not successful and made it necessary to raise antibodies against INP. For this purpose, a N-terminal truncated version of INP (-NINP) was used and purified. -NINP was injected into rabbits to produce INP specific antibodies (see Materials and Methods) and with this antiserum Western blot analysis was performed to detect the presence of expressed INP at time point of E-lysis induction (0min) and after β-propiolactone treatment of harvested INP-BG samples (Fig. 5). The calculated molecular weight (M_r) of the 1200 aa long INP is 118,6 kDa and the band visible at 120 kDa in samples of full *E. coli* C41 bacteria with expressed INP and BGs derived from them (Fig. 5, lane 1 to 4) corresponds to the full length INP. Furthermore, an additional protein band at 87 kDa was detected in the INP bearing samples of *E. coli* C41 (pBINP, pGLMivb) and *E. coli* C41 (pBINP, pGLysivb). These 2 prominent bands were not detected in *E. coli* C41 carrying the backbone plasmid pBAD24 for the INP expression plasmid pBINP (Fig. 5, lane 5 to 6). As ATG and corresponding positional Shine-Dalgarno (SD) sequences for a truncated 87kDa INP could not be detected in the nucleotide sequence of *inaZ* it is most likely that the lower migrating protein band represents an INP degradation product. Such a INP degradation product has also been reported for InaV [46]

Ice nucleation activity of BGs carrying INP (INP-BGs)

Ice-nucleating activity of full bacteria and BGs carrying INP, produced from *E. coli* C41 with lysis plasmid pGLysivb (INP-BG-pLy) or pGLMivb (INP-BG-pLM) respectively, was determined by a droplet-freezing assay (for details see Material and Methods). Living *E. coli* C41 cells carrying INP and lysis plasmid pGLysivb (C41-INP) not induced for lysis were used as a positive control. Living *E. coli* C41 cells carrying pBAD24

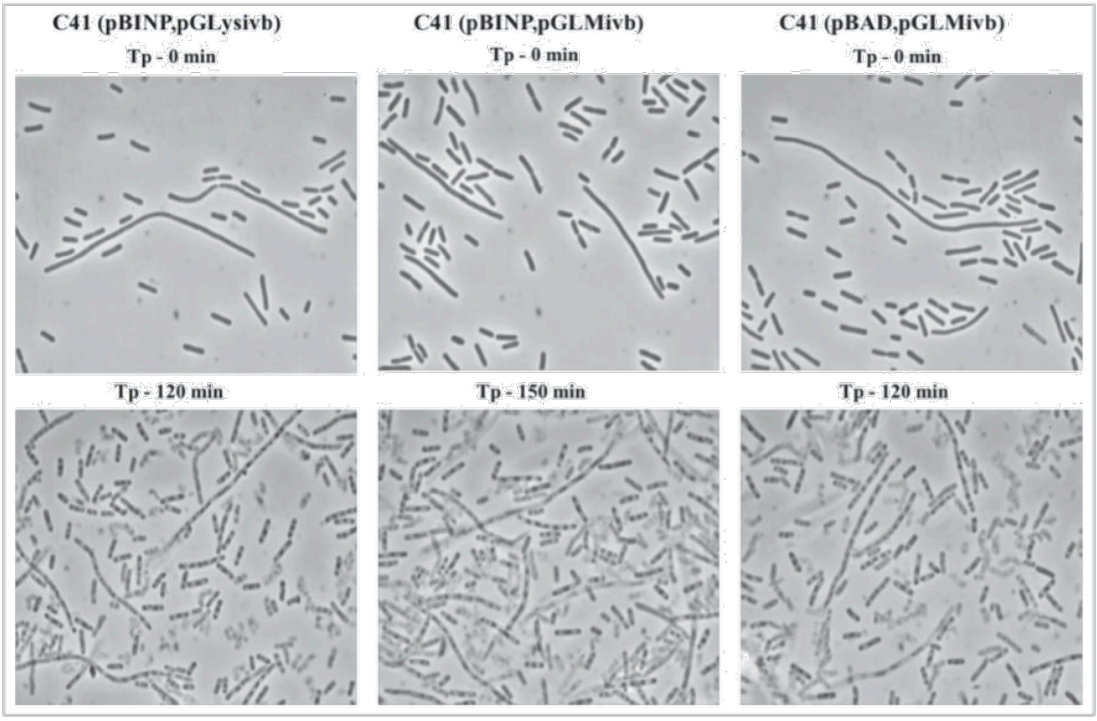

Figure 3. Light microscopy pictures of E. coli C41 (pBINP, pGLysivb), E. coli C41 (pBINP, pGLMivb), and E. coli C41 (pBAD, pGLysivb) strains at time point of lysis induction (Tp - 0min) and end point of E-mediated lysis after 120 min and 150 min, respectively (Tp - 120 min, Tp - 150 min).

and pGLysivb (C41–24-pLy) as well as their BG derived form (BG), carrying no INP were included as a negative control.

As the heterogeneous freezing of a droplet of ultra-pure water at a given temperature is determined by the most active ice nucleus inside the droplet (meaning that only these nuclei is detectable [4,11]) a series of dilutions from each suspension was tested. The particular freezing temperatures of the tested droplets plotted against the temperature, was used to determine the median freezing temperature T_{50} (Fig. 6B) and cumulative ice nucleation spectra (Fig. 7) of the samples. T_{50} is the temperature at which 50% of the droplets placed on the cooling device are frozen and was calculated out of the freezing spectra of each tested suspension containing 5×10^8 cells ml^{-1} (Fig. 6A).

Both independent prepared INP-BG samples (INP-BG-pLM and INP-BG-pLy) showed a very close T_{50} values of −6.9°C and −6.7°C respectively, with first freezing events starting at −6.0°C. With living of *E. coli* C41 carrying INP (C41-INP) the first freezing event was noted at −5.5°C. The T_{50} value for this group was calculated to be at −5.6°C. The T_{50} for *E. coli* C41 cells (C41–24-pLy) and corresponding BGs carrying no INP was at −20.1°C and −18.9°C, respectively. The first frozen droplets detected for C41–24-pLy and C41 BGs were at −14°C, therefore the ice nucleation activity of INP-BGs was monitored up to a temperature decrease of −13°C not to detect INP unspecific induction of ice formation. For further characterization of the ice nucleation activity of INP-BGs the cumulative number N(T), of ice nuclei ml^{-1} active at a given temperature (Fig. 7A) and the nucleation frequency (NF) (Fig. 7B) were determined. The NF, obtained by normalizing the number of ice nuclei ml^{-1} for the number of cells in the original suspension, describes the fraction of cells in the suspension enfolding active ice nucleation sites at a given temperature.[25] For both INP-BGs, ice nucleation was detected at −6°C, with a nucleation frequency of 3×10^{-8} for INP-BG-pLM and $1{,}9 \times 10^{-7}$ for INP-BG-pLy. As the temperature decreased from −6°C to −7°C, the total number of ice nucleation active sites per cell at −7°C for INP-BG-pLM compared with INP-BG-pLy varies significantly 5×10^{-5}

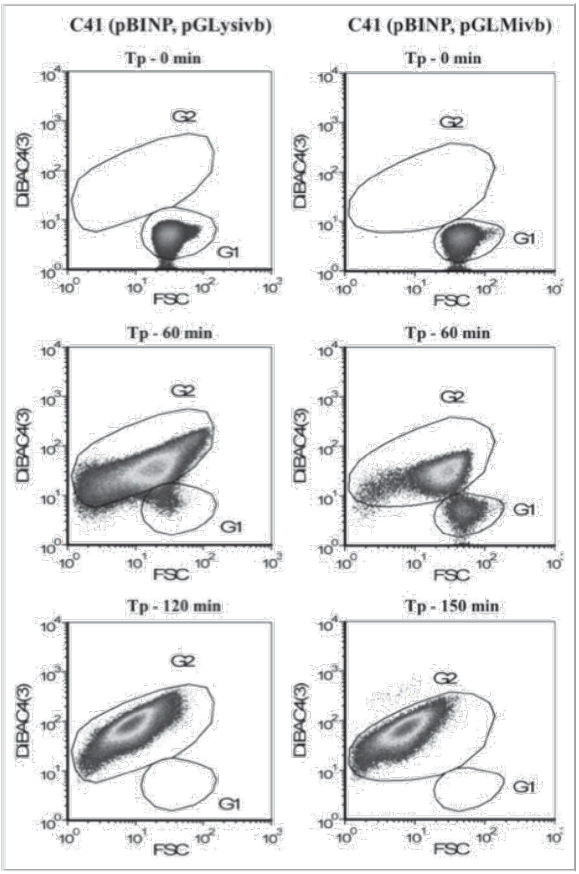

Figure 4. Flow cytometry density dot plots showing E-lysis process of E. coli C41 (pBINP, pGLysivb) and E. coli C41 (pBINP, pGLMivb) strains. Illustrated populations are discriminated from non-cellular background via Rh414 staining. Dot plots illustrate fluorescence intensity with Dibac4(3) vs. FSC–forward scatter; G1: living cells, G2: BGs. Tp - 0 min: indicates time point of lysis induction; Tp - 60 min: 60 min after lysis induction; Tp - 120 min: end of lysis phase for E. coli C41 (pBINP, pGLysivb); Tp - 150 min: end of lysis phase for E. coli C41 (pBINP, pGLMivb).

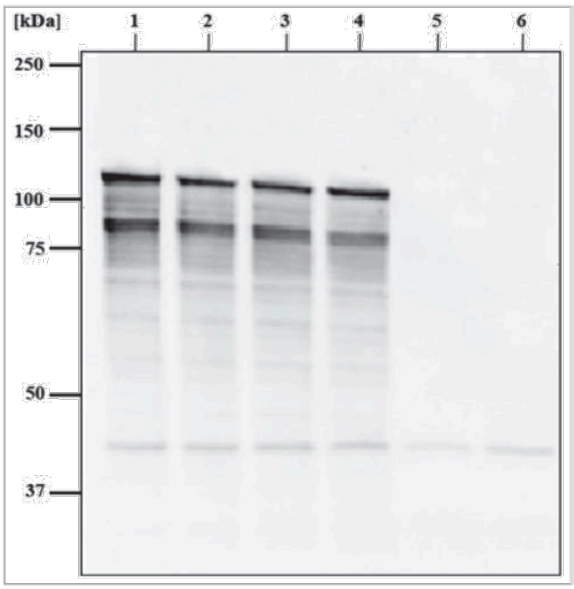

Figure 5. Western blot analysis of *E. coli* C41 expressing INP and harboring E-lysis plasmid pGLysivb or pGLMivb, respectively, and their derived BGs. Samples were taken at time point of E-lysis induction (Tp - 0 min) and after β-propiolactone treatment of BG samples. Western blotting was performed with rabbit anti-H-NINP serum and anti-rabbit IgG horseradish peroxidase conjugated antibodies. Lane1: *E. coli* C41 (pBINP, pGLMivb); lane 2: INP-BG-pLM, BG derived form of *E. coli* C41 (pBINP, pGLMivb); lane 3: *E. coli* C41 (pBH-NINPL, pGLysivb); lane 4: INP-BG-pLy, BG derived form of *E. coli* C41 (pBINP, pGLysivb); lane 5: *E. coli* C41 (pBAD, pGLysivb); lane 6: BG, BG derived form of *E. coli* C41 (pBAD, pGLysivb). Positions of molecular size marker proteins are indicated in kilodaltons (kDa).

and 3.3×10^{-6}, respectively. At a temperature of $-10°C$ both types of INP-BGs exhibit closer NF activity values of 1.6×10^{-4} for INP-BG-pLy and 3×10^{-4} for INP-BG-pLM. With further decrease in temperature down to $-13°C$, NF of INP-BG-pLM and INP-BG-pLy was 6.3×10^{-4} and 6.4×10^{-4}. Ice nucleation activity of living *E. coli* C41 carrying INP (C41-INP) was detected at higher temperature ($-5.5°C$) with an obviously higher NF of 1.2×10^{-5} which increased to 3.3×10^{-4} at $-7°C$. When temperature decreased to-13°C, an increase in NF up to 1.3×10^{-3} for C41-INP was detected.

Discussion

This communication is the first report of *E. coli* BGs carrying INP on their cell surface (INP-BGs). INP-BGs are able to lower the freezing point of ultra-pure water to a considerable content. The efficiency of bacteria nucleating ice-formation at a certain temperature can be subdivided into 3 distinct classes, type I acts at $-5°C$ or warmer, type II from -5 to $-7°C$ and type III below $-7°C$.[47,48] According to this classification model the T_{50} value of INP-BGs determined in this study are belonging to type II (Fig. 6B) and with additional type III ice nucleation BGs in the samples (Fig. 7). Negative control BGs without INP and live *E. coli* C41 bacteria alone exhibit a T_{50} value of $-18.9°C$ and $-20.1°C$, respectively (Fig 7).

Recombinant live bacteria *E. coli* C41 expressing INP on their surface also belong with their T_{50} value to type II ina$^+$ particles, however, they possess slightly

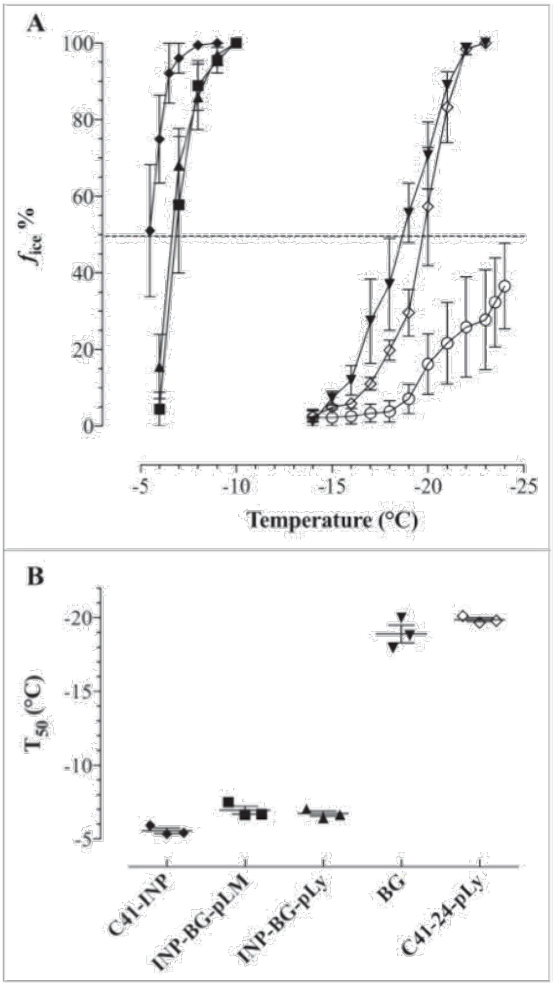

Figure 6. Average number of freezing spectra (A) and median freezing temperatures (T_{50}) (B) of INP-BGs living *E. coli* C41 and *E. coli* C41 BGs. *E.coli* C41 (pBINP, pGLMivb) (INP-BG-pLM) (■) C41 (pBINP, pGLysivb) (INP-BG-pLy) (▲), *E.coli* C41(pBINP, pGLysivb) cells carrying INP (C41-INP) (◆), *E.coli* C41(pBAD24, pGLysivb) ghosts (BGs) (▼) and C41 (pBAD24, pGLysivb) cells (C41–24-pLy) (◇). 210×10 μl droplets of ROTISOLV® water (◯) were included as unspecific control. (A) Ice nucleation curve plotted as number fraction of frozen droplets in percent (f_{ice} %) at any temperature. (B) T_{50}, temperature where 50% of all droplets are frozen. Forty-five 10 μl droplets of each suspension containing 5×10^8 cells ml^{-1} were tested by droplet freezing. Average numbers are obtained from 3 independent experiments. Error bars represent the standard errors.

more ice catalyzing sites active at temperature of −6 to −7°C than the corresponding INP-BGs (Fig. 7). This difference might be explained by the fact that although the rod shaped bacterial cell envelope in BGs is retained it lacks the inner cytoplasmic turgor which makes the live bacteria chock-full which could provide a better positioning of neighboring INPs for ice nucleation. The crucial question, what makes a good ice nucleation center seems to depend on the coupling of surface crystallinity and hydrophilicity.[49] Recently, the idea of ice templating by INPs has been proven experimentally showing that hydrogen bonding at the water-bacteria contact induce structural order and drive phase transitions of water in bacterial hydration shell.[3]

Former findings that a growth temperature of 30°C and higher of bacteria expressing INP had significant negative effects on the number of active ice nuclei were also investigated.[25,43] INP-BGs were produced with 2 different lysis plasmids (pGLMivb and pGLysivb) controlling E-lysis by a chemical and temperature-sensitive promotor system, respectively. INP-BGs produced with pGLMivb were kept at 23°C for the whole production process whereas INP-BGs produced with pGLysivb were shifted to 42°C for 2h for the E-induced lysis. When the 2 different INP-BGs were compared for their ice-nucleation activity INP-BGs-pGLy (2h at 42°C) showed nearly the same ice nucleation frequency at −6°C. However, at −7°C INP-BGs-pGLM kept at 23°C exhibit a significant difference in the number of ice nucleation active sites per cell compared with INP-BGs-pGLy with NF of 5×10^{-5} versus 3.3×10^{-6} (Fig. 7). This observation indicates a slight negative effect of higher temperature on nucleation frequency of INP-BGs. A bit more the differences were detectable with the living INP bacteria (C41-INPC) with respect to the T_{50} value at lower temperature of −5.6°C (Fig. 6) and the (higher) total number of ice nuclei per cell at the first droplet freezing temperature (Fig. 7). Posttranslational modifications of INP are supposed to modify the stability of INP accumulations.[6,50] Independent from potential temperature effect on INP formation and the firm cell-envelope of living cells mentioned above host cell phospholipase is induced by protein E.[51] This enzymatic activity makes the envelope membranes more fluid at the E-mediated lysis tunnel area and could account for the −1°C difference detected in the T_{50} value of INP-BGs and live C41-INP parent bacteria.

Full length INP and a major INP degradation product have been detected with the rabbit antibodies raised against purified InaZ protein truncated with its N-terminal anchoring sequence (Fig. 5). The comparison of INP in *E. coli* C41 bacteria before and after E- mediated lysis show the same intensity of the INP specific bands in the live bacteria and their

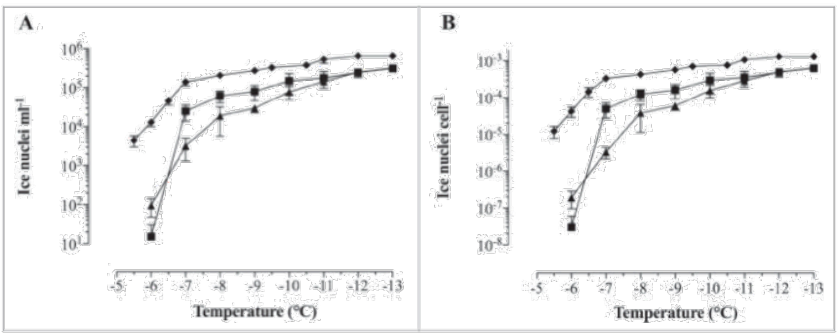

Figure 7. Cumulative concentration of ice nucleation activity for INP-BGs and *E. coli* C41-INP. *E. coli* C41 (pBINP, pGLysivb) (▲) and *E. coli* C41 (pBINP, pGLMivb) (■) - BGs. Not lysed *E. coli* C41 (pBINP, pGLysivb) (◆) harvested before lysis induction. (A) Average Number of ice nuclei ml^{-1} at a given temperature N(T). (B) Average of Nucleation frequency (NF) expressed as ice nuclei $cell^{-1}$. Data obtained from 3 independent experiments. Error bars represent the standard errors.

corresponding BGs. The chemical induced BGs seem to have a little bit better expression of INP and this could also explain the difference of number of ice nuclei at −7°C discussed above. Other studies observed ice nucleation activity for recombinant ice nucleation active *E. coli* similar to the *P. syringae* wild type strain acting as typ I ice nuclei (below −5°C).[25,52] In the latter case INP of ina^+ *E. coli* was expressed during logarithmic and stationary growth phase of the bacteria[46,53] whereas E-protein mediated lysis requires active growth and cell division of the host bacteria limiting the INP expression time considerably.[54-56]

It should be mentioned that the experiments described in this communication did not have the aim to optimize the expression rates nor the quantity of INP per BG. Fed-Batch production of BGs could significantly increase the level of INP per BG and the total yield of INP-BG.[57]

The investigations performed were rather concept studies to answer the question whether BGs have the ability to induce ice nucleation at all. BGs from a recombinant Gram-negative bacterium as in our case *E. coli* C41 carrying INP could have the advantage over live parent bacteria that they are non-living and most important that they are no longer genetically modified organisms (GMOs) but only products thereof. In this respect they do not represent any biohazard in modifying microbial communities and escape arguments against GMOs in all different aspects. In addition β-propiolactone (BPL) treatment (which alkylates nucleic acids) of the produced BGs inactivate E-lysis escape mutants assuring a total safe BG preparation.[45] The ability of INA BGs to lower the freezing time and temperature of goods could give an edge over its commercial competitors improving the economics and safety of snow making.

In the past BGs have been used for various purposes such as vaccines, carrier and targeting vehicles, miniature bioreactors and have been produced from a range of Gram-negative bacteria, as for example *Salmonella tryphimurium, Actinobacillus pleuropneumoniae, Klebsiella pneumoniae, Vibrio cholera, Mannheimia haemolytica, Bordetella bronchiseptica, Shigella flexneri, Ralstonia eutropha, Pectobacterium cypripedii* and various pathogenic and non-pathogenic E. coli strains including probiotic *E.coli* Nissle 1917.[58-60] The use of INP-BGs from non-pathogenic *E. coli* strains or other harmless bacterial strains could find applications for advanced freezing processes and texturing of frozen food, water solubility of BG adsorbed compounds, BG ice nucleation in the atmosphere, cloud formation or artificial rain. One particular advantage for the latter 2 applications could be that BGs represent a light version of bacteria having lost almost $^3/_4$ of their weight when compared with the live parent bacteria. Therefore, INP-BGs should be able to use atmospheric transport ways more efficiently than their heavy brothers and sisters. Even if biologic ice nucleation in clouds on a global scale is in the uppermost estimate of 0.6%[61] INP-BGs could find their niche in local applications competing with the use of toxic chemicals for cloud seeding or as both cloud condensing nuclei and heterogeneous ice nuclei for the production of clouds and precipitation.[23]

Beside various commercial applications of INP-BGs mentioned above it is anticipated that INP-BGs could also be a valuable tool to further investigate the molecular mechanisms governing biologic ice growth. In a

recent study BGs have been used for cryo-electron tomography (cryoET) of native E. coli envelope membranes.[34] CryoET has become a powerful tool for direct visualization of 3D structures of membrane protein complexes smaller than 300 nm at molecular resolution within native cell membranes. This application of cryoET for structural and functional studies of membrane protein complexes could become applied to INP. Furthermore, genetic engineered *E. coli* BGs as carrier of INP could extend the tool box for systematic studies in basic science manipulating various cell envelope structures such as lipids, polysaccharides and other which influence the efficiency of the biologic ice nucleation process.[50,62]

Materials and methods

Strains, plasmids and media

The *E. coli* strain K-12 5-α (New England BioLabs, NEB) has been used for routine cloning and *E. coli* C41(DE3) (Lucigen) for INP-BG production. Bacterial cultures were grown in animal protein-free, vegetable variant of Luria-Bertani (LBv: 10.0 g/l soy peptone (Carl Roth), 5.0 g/l yeast extract (Carl Roth), and 5.0 g/l NaCl). Appropriate antibiotics were supplemented to maintain the respective plasmids. The final concentration of antibiotics was as follows: ampicillin, 100 μg ml^{-1}; gentamycin, 20 μg ml^{-1}. The plasmids pBAD24[63] and pGLysivb[40,41] used in this study have been described previously. Lysis plasmid pGLMivb was obtained from Bird-C plasmid collection and represents a modification of lysis plasmid pGLysivb, where the temperature inducible λpR-cI857 promoter repressor system is exchanged by a chemical inducible LaqIq-repressor-P_{tac}-promoter system. Plasmid pEX-A2INP (Eurofins Genomics) harbors a chemically synthesized 3600 bp *inaZ* gene encoding INP of *Pseudomonas syringae*.[64]

Plasmid construction

To express, the INP under control of P_{BAD} promoter the *inaZ* gene was cloned into the plasmid pBAD24. The sequence of *inaZ* without the termination codon was amplified by PCR where plasmid pEX-A2INP was used as template and primers inaZ-fwd and inaZ-his-rev to introduce terminal restriction sites *EcoRI* (5′- end) and *HindIII* (3′-end), as well as a 6x-His tag coding sequence and 2 termination codons at the 3′-end. Sense: (inaZ-fwd) 5′-GTACCGGAATTCAAT GAATCTCGACAAGGC- 3′; anti-sense: (inaZ-his-rev) 5′- CTGGGAAGCTTTTA TTAATGGTGATGGTGAT GGTGAGAGCCGGATCCCTTTACCTCTATCCAGT CATC -3′. The amplified PCR fragment was cloned into the corresponding sites of the bacterial expression vector pBAD24, resulting in plasmid pBINP.

To construct pBH-NINP, expressing a N-terminal His-tagged truncated INP (H-NINP) lacking 485 bp of the 525 bp long N-terminal domain sequence, a 3174 bp PCR product was produced by PCR amplification using plasmid pEX-A2INP as template. Following primers were used: his-inaZ-fwd (5′-GTACC GGAATTCA ATGCACCATCACCATCACCATGG ATCCGGCTCTATGAATCTCGACAAGGC-3′) to introduce terminal 6x-His tag coding sequence and *EcoRI*- restriction site at 5′-end; inaZ-rev: (5′-GACCC AAGCTTCTACTTTACCTCTATCCAGTCATC-3′) for a 3′-end *HindIII* site. The amplified PCR product and plasmid pBAD24 were digested with appropriate restriction enzymes and ligated into their corresponding sites to get pBH-NINP.

Growth, E-lysis and inactivation of bacteria

E. coli C41 harboring pBINP and E-lysis plasmid were grown in LBv supplemented with suitable antibiotics and 0.2% L-arabinose at 23°C to induce constitutive expression of the ice nucleation protein sequence under control of P_{BAD}. When the culture reached an optical density at 600 nm (OD_{600}) of 0.6 E-mediated lysis was initiated. Expression of gene *E* in lysis plasmid pGLysivb was induced by a temperature up-shift of the growing cultures from 23°C to 42°C. Whereas the expression of gene *E* from lysis plasmid pGLMivb in cultures kept at 23°C was induced with 0.5 mM isopropyl-D-1-thiogalactopyranoside (IPTG). After the completion of E-lysis process, the cell harvest was washed 4 times with 1x Vol. of sterile de-ionized water (dH_2O) by centrifugation and suspended in 1x Vol of sterile dH_2O. To inactivate any surviving E-lysis escape mutants from BG production, 0.17% (v/v) of the DNA-alkylating agent β-propiolactone (BPL, 98.5%, Ferak) was added to the washed harvest and kept for 120 min at 23°C with agitation. This mixture was washed twice with 1x Vol. of sterile dH_2O and once with ROTISOLV® water (Carl Roth) and finally resuspended in 1/10x Vol. ROTISOLV®.

Monitoring and determination of E-lysis efficiency

The BG production was monitored by light-microscopy (Leica DM R microscope, Leica Microsystems), by checking the optical density at 600nm (OD_{600}) and fluorescence-activated flow cytometry according to Langemann et al.[44,45] Flow cytometry (FCM) was performed using a CyFlow® SL flow cytometer (Partec) with a 488-nm blue solid-state laser. The membrane potential-sensitive dye DiBAC4(3) (abs./em.: 493/516 nm, FL1,) was used for the evaluation of cell-viability. Fluorescent dye RH414 (abs./em. 532/760 nm) was used for staining phospholipid membranes and discriminating non-cellular background. 1 ml samples were diluted to provide appropriate cell counts and stained with 1.5 μl DiBAC4(3) (0.5mM) and 1.5 μl RH414 (2 mM), both from AnaSpec. Collected data was analyzed using FloMax V 2.52 (CyFlow SL; Quantum Analysis) and presented as 2D density dot plots illustrating forward scatter (FSC) against DiBAC fluorescence signal (FL1, DiBAC). To determine the colony forming units (cfu) during growth and lysis of *E. coli* C41 expressing INP bacterial samples were collected at different time points, diluted with saline and 50 μl samples were plated as triplicates on Plate Count Agar (Carl Roth) using a WASP spiral plater (Don Whitley Scientific). The plates were incubated at 36°C overnight and analyzed the next day using ProtoCOL SR 92000 colony counter (Synoptics Ltd). Lysis efficiency (LE) is defined as ratio of BGs after complete lysis to total cell counts and can be calculated by using following equation:

$$LE = \left(1 - \frac{cfu_{(t)}}{cfu_{(t_0)}}\right) \times 100\% \qquad (1)$$

where, t_0 is the time point of lysis induction (LI) and t is any time after LI.

Production of INP antibodies

N-terminal His-tagged INP lacking the N-terminal domain (H-NINP) was expressed from pBH-NINP in *E. coli* C41and H-NINP affinity purification of the protein was performed under denaturing conditions by using a nickel- agarose column (QIAGEN) according to the manufacturer's instructions. With this protein fraction custom made INP specific polyclonal serum was produced by Moravian Biotechnology in rabbits after 4 rounds of immunization.

Western blot analysis

Pellets (5×10^{-8} cells or BGs ml^{-1}) were resuspended in 1x SDS gel-loading buffer, boiled for 5 min and electrophoretically separated on Bolt™ 8% Bis-Tris Plus gel by using XCell SureLock™ Mini-Cell electrophoresis system (Thermo Fisher Scientific). The proteins were then transferred to nitrocellulose membrane (GE Healthcare) with transfer buffer (25 mM Tris, 192 mM glycine, 20% methanol) using the XCell II™ Blot Module (Thermo Fisher Scientific). The membrane was placed in TBST (20 mM Tris-HCl, pH 7.5, 100 mM NaCl, 0.05% Tween-20) with 5% milk powder (Carl Roth) overnight at 4°C. Immunodetection was performed using rabbit polyclonal α-H-INP antibody serum followed by α-rabbit IgG-HRP (GE Healthcare). Detection was performed with an Amersham ECL Western blot detection kit (GE Healthcare) and developed with ChemiDoc™ XRS (Bio-Rad).

Ice-nucleating activity measurements

The ability to nucleate ice formation was measured by droplet freezing assay using a modified device based on a method of Vali.[65] The cooling unit was constructed with the help of instruction notes by Quick-Ohm (Quick-Ohm Küpper). Hence, to detect ice nuclei in the suspensions to be tested (each suspension was adjusted to a concentration of 5×10^8 cells ml^{-1} determined by FCM) active at lower temperatures, a series of tenfold dilutions from each suspension (ranging from 5×10^8 cells ml^{-1} to 5×10^4 cells ml^{-1}) was tested resulting in respective ice nucleus spectrum. Forty-five 10 μl droplets if not indicated otherwise of each dilution were distributed on a sterile aluminum plate coated with a hydrophobic film. The plate surface was washed with acetone before coating and flushed with a stream of filtered air before the sample droplets were placed. The plate was surrounded by styrofoam and covered by a plexiglas plate for isolation. The temperature of the working plate was decreased by 2 in series circuited 2-stage Peltier elements of the type TEC2–127–63–04, controlled by a QC-PC-C01C temperature controller (Quick-Ohm Küpper). The temperature controller was energized by a 10 kΩ potentiometer (M22S-R10K, Eaton). To measure the surface temperature of the plate a small precision temperature sensor TS-NTC-103A (B+B Thermo – Technik) was affixed, which is connected to

the controller and the controller-display QC-PC-D-100 (Quick-Ohm Küpper). The plate surface can be cooled by the Peltier elements to a maximum temperature of −24.5°C. The temperature variation of the plate surface determined by a Voltcraft PL-120 T1 thermometer and a type K temperature sensor (1xK NL 1000, B+B Thermo – Technik) was ± 0.4°C. Samples were tested for its ice nucleation activity from −2 to −13°C at a constant rate of 0.5 or 1°C decrements. After a 30 sec dwell time at each temperature the Plexiglas plate was removed and the number of frozen droplets was recorded by a Panasonic Luminex DMC-FS3 digital camera.

The different samples were compared by the median freezing temperature (T_{50}), which represents the temperature where 50% of all droplets are frozen. The T_{50} was calculated with the equation reported by Kishimoto et al.[66]

$$T_{50} = \frac{T_1 + (T_2 - T_1)(2^{-1}n - F_1)}{(F_2 - F_1)} \quad (2)$$

where F1 and F2 are the number of frozen drops at temperature T1 and adjacent temperature T2, and are just below and above 50% of the total number of tested drops (n).

The cumulative number N(T), of ice nuclei ml^{-1} active at a given temperature was calculated by an analogical variant of the equation of Vali [65] reported by Govindarajan and Lindow:[4]

$$N(T) = -\ln(f) \times \frac{10^D}{V} \quad (3)$$

where f = fraction of droplets unfrozen at temperature T, described as total number of droplets used divided by unfrozen droplets (N_0/ N_U), V = volume of each droplet used (10 μl), D = the number of 1:10serial dilutions of the original suspension. N(T) was normalized for the number of cells present in each suspension to obtain the nucleation frequency (NF) per cell by dividing ice nuclei $^{-ml}$ through cell density ($cell^{-ml}$).

Disclosure of potential conflicts of interest

No potential conflicts of interest were disclosed.

Acknowledgment

We thank Abbas Muhammad for fruitful discussions and reviewing of the manuscript.

Funding

This work was funded by BIRD-C.

References

[1] Gurian-Sherman D, Lindow SE. Bacterial ice nucleation: significance and molecular basis. Faseb J 1993; 7 (14):1338-43; PMID:8224607

[2] Warren G, Wolber P. Molecular aspects of microbial ice nucleation. Mol Microbiol 1991; 5(2):239-43; PMID:2041468

[3] Pandey R, Usui K, Livingstone RA, Fischer SA, Pfaendtner J, Backus EH, Nagata Y, Fröhlich-Nowoisky J, Schmüser L, Mauri S, et al. Ice-nucleating bacteria control the order and dynamics of interfacial water. Sci Adv 2016; 2(4):e1501630; PMID:27152346; http//dx.doi.org/10.1126/sciadv.1501630

[4] Govindarajan AG, Lindow SE. Size of bacterial ice-nucleation sites measured in situ by radiation inactivation analysis. Proc Natl Acad Sci U S A 1988; 85(5):1334-8; PMID:16593912; http//dx.doi.org/10.1073/pnas.85.5.1334

[5] Lindow SE, Lahue E, Govindarajan AG, Panopoulos NJ, Gies D. Localization of ice nucleation activity and the iceC gene product in Pseudomonas syringae and Escherichia coli. Mol Plant Microbe Interact 1989; 2(5):262-72; PMID:2520825

[6] Kozloff LM, Turner MA, Arellano F. Formation of bacterial membrane ice-nucleating lipoglycoprotein complexes. J Bacteriol 1991; 173(20):6528-36; PMID:1917877

[7] Phelps P, Giddings TH, Prochoda M, Fall R. Release of cell-free ice nuclei by Erwinia herbicola. J Bacteriol 1986; 167(2):496-502; PMID:3525514

[8] Muryoi N, Matsukawa K, Yamade K, Kawahara H, Obata H. Purification and properties of an ice-nucleating protein from an ice-nucleating bacterium, Pantoea ananatis KUIN-3. J Biosci Bioeng 2003; 95(2):157-63; PMID:16233385

[9] Lorv JS, Rose DR, Glick BR. Bacterial ice crystal controlling proteins. Scientifica (Cairo) 2014; 2014:976895; PMID:24579057; http//dx.doi.org/10.1155/2014/976895

[10] Maki LR, Galyan EL, Chang-Chien MM, Caldwell DR. Ice nucleation induced by pseudomonas syringae. Appl Microbiol 1974; 28(3):456-9; PMID:4371331; http//dx.doi.org/10.1111/1462-2920.12668

[11] Lindow SE, Arny DC, Upper CD. Bacterial ice nucleation: a factor in frost injury to plants. Plant Physiol 1982; 70(4):1084-9; PMID:16662618; http//dx.doi.org/10.1104/pp.70.4.1084

[12] Sun X, Griffith M, Pasternak JJ, Glick BR. Low temperature growth, freezing survival, and production of antifreeze protein by the plant growth promoting rhizobacterium Pseudomonas putida GR12-2. Can J Microbiol 1995; 41(9):776-84; PMID:7585354; http//dx.doi.org/10.1139/m95-107

[13] Lindow SE, Arny DC, Upper CD. Erwinia herbicola: A Bacterial Ice Nucleus Active in Increasing Frost Injury to

Corn. Phytopathology. 1978;68:523-7; http//dx.doi.org/10.1094/Phyto-68-523.

[14] Kawahara H. Cryoprotectants and Ice-Binding Proteins. In: Margesin R, Schinner F, Marx JC, Gerday C, editors. Psychrophiles: from Biodiversity to Biotechnology. Berlin, Heidelberg: Springer Berlin Heidelberg; 2008. p. 229-46

[15] Abe K, Watabe S, Emori Y, Watanabe M, Arai S. An ice nucleation active gene of Erwinia ananas. Sequence similarity to those of Pseudomonas species and regions required for ice nucleation activity. FEBS Lett 1989; 258 (2):297-300; PMID:2599095; http//dx.doi.org/10.1016/0014-5793(89)81678-3

[16] Zhao JL, Orser CS. Conserved repetition in the ice nucleation gene inaX from Xanthomonas campestris pv. translucens. Mol Gen Genet 1990; 223(1):163-6; PMID:2259339; http//dx.doi.org/10.1007/BF00315811

[17] Miller AM, Figueiredo JE, Linde GA, Colauto NB, Paccola-Meirelles LD. Characterization of the inaA gene and expression of ice nucleation phenotype in Pantoea ananatis isolates from Maize White Spot disease. Genet Mol Res 2016; 15(1):15017863; PMID:26985943; http//dx.doi.org/10.4238/gmr.15017863

[18] Lindow SE, Hirano SS, Barchet WR, Arny DC, Upper CD. Relationship between ice nucleation frequency of bacteria and frost injury. Plant Physiol 1982; 70 (4):1090-3; PMID:16662619; http//dx.doi.org/10.1104/pp.70.4.1090

[19] Christner BC, Morris CE, Foreman CM, Cai R, Sands DC. Ubiquity of biological ice nucleators in snowfall. Science 2008; 319(5867):1214; PMID:18309078; http//dx.doi.org/10.1126/science.1149757

[20] Huffman JA, Prenni AJ, DeMott PJ, Pöhlker C, Mason RH, Robinson NH, et al. High concentrations of biological aerosol particles and ice nuclei during and after rain. Atmos Chem Phys 2013; 13(13):6151-64; http//dx.doi.org/10.5194/acp-13-6151-2013

[21] Morris CE, Conen F, Alex Huffman J, Phillips V, Poschl U, Sands DC. Bioprecipitation: a feedback cycle linking earth history, ecosystem dynamics and land use through biological ice nucleators in the atmosphere. Glob Chang Biol 2014; 20(2):341-51; PMID:24399753; http//dx.doi.org/10.1111/gcb.12447

[22] Morris CE, Sands DC, Vinatzer BA, Glaux C, Guilbaud C, Buffiere A, Yan S, Dominguez H, Thompson BM. The life history of the plant pathogen Pseudomonas syringae is linked to the water cycle. ISME J 2008; 2(3):321-34; PMID:18185595; http//dx.doi.org/10.1038/ismej.2007.113

[23] Möhler O, DeMott PJ, Vali G, Levin Z. Microbiology and atmospheric processes: the role of biological particles in cloud physics. Biogeosciences 2007; 4(6):1059-71; http//dx.doi.org/10.5194/bg-4-1059-2007

[24] Möhler O, Georgakopoulos DG, Morris CE, Benz S, Ebert V, Hunsmann S, et al. Heterogeneous ice nucleation activity of bacteria: new laboratory experiments at simulated cloud conditions. Biogeosciences 2008; 5 (5):1425-35; http//dx.doi.org/10.5194/bg-5-1425-2008

[25] Orser C, Staskawicz BJ, Panopoulos NJ, Dahlbeck D, Lindow SE. Cloning and expression of bacterial ice nucleation genes in Escherichia coli. J Bacteriol 1985; 164 (1):359-66; PMID:3900043

[26] Baertlein DA, Lindow SE, Panopoulos NJ, Lee SP, Mindrinos MN, Chen TH. Expression of a bacterial ice nucleation gene in plants. Plant Physiol 1992; 100(4):1730-6; PMID:16653190; http//dx.doi.org/10.1104/pp.100.4.1730

[27] Lindgren PB, Frederick R, Govindarajan AG, Panopoulos NJ, Staskawicz BJ, Lindow SE. An ice nucleation reporter gene system: identification of inducible pathogenicity genes in Pseudomonas syringae pv. phaseolicola. EMBO J 1989; 8(5):1291-301; PMID:2548841

[28] van Bloois E, Winter RT, Kolmar H, Fraaije MW. Decorating microbes: surface display of proteins on Escherichia coli. Trends Biotechnol 2011; 29(2):79-86; PMID:21146237; http//dx.doi.org/10.1016/j.tibtech.2010.11.003

[29] Gao F, Ding H, Feng Z, Liu D, Zhao Y. Functional display of triphenylmethane reductase for dye removal on the surface of Escherichia coli using N-terminal domain of ice nucleation protein. Bioresour Technol 2014; 169:181-7; PMID:25058292; http//dx.doi.org/10.1016/j.biortech.2014.06.093

[30] Fan LH, Liu N, Yu MR, Yang ST, Chen HL. Cell surface display of carbonic anhydrase on Escherichia coli using ice nucleation protein for CO(2) sequestration. Biotechnol Bioeng 2011; 108(12):2853-64; PMID:21732326; http//dx.doi.org/10.1002/bit.23251

[31] Henrich B, Lubitz W, Plapp R. Lysis of Escherichia coli by induction of cloned phi X174 genes. Mol Gen Genet 1982; 185(3):493-7; PMID:6285147

[32] Schon P, Schrot G, Wanner G, Lubitz W, Witte A. Two-stage model for integration of the lysis protein E of phi X174 into the cell envelope of Escherichia coli. FEMS Microbiol Rev 1995; 17(1–2):207-12; PMID:7669347

[33] Witte A, Wanner G, Blasi U, Halfmann G, Szostak M, Lubitz W. Endogenous transmembrane tunnel formation mediated by phi X174 lysis protein E. J Bacteriol 1990; 172(7):4109-14; PMID:2141836

[34] Fu X, Himes BA, Ke D, Rice WJ, Ning J, Zhang P. Controlled bacterial lysis for electron tomography of native cell membranes. Structure 2014; 22(12):1875-82; PMID:25456413; http//dx.doi.org/10.1016/j.str.2014.09.017

[35] Witte A, Wanner G, Sulzner M, Lubitz W. Dynamics of PhiX174 protein E-mediated lysis of Escherichia coli. Arch Microbiol 1992; 157(4):381-8; PMID:1534215

[36] Witte A, Wanner G, Lubitz W, Holtje JV. Effect of phi X174 protein E-mediated lysis on murein composition of Escherichia coli. FEMS Microbiol Lett 1998; 164(1):149-57; PMID:9675861; http//dx.doi.org/10.1016/S0378-1097(98)00210-9

[37] Witte A, Lubitz W. Biochemical characterization of phi X174-protein-E-mediated lysis of Escherichia coli. Eur J Biochem 1989; 180(2):393-8; PMID:2522390; http//dx.doi.org/10.1111/j.1432-1033.1989.tb14661.x

[38] Witte A, Blasi U, Halfmann G, Szostak M, Wanner G, Lubitz W. Phi X174 protein E-mediated lysis of Escherichia coli. Biochimie 1990; 72(2–3):191-200; PMID:2143087; http//dx.doi.org/10.1016/0300-9084(90)90145-7

[39] Jechlinger W, Haller C, Resch S, Hofmann A, Szostak MP, Lubitz W. Comparative immunogenicity of the hepatitis B virus core 149 antigen displayed on the inner and outer membrane of bacterial ghosts. Vaccine 2005; 23 (27):3609-17; PMID:15855021; http//dx.doi.org/10.1016/j.vaccine.2004.11.078

[40] Jechlinger W, Szostak MP, Witte A, Lubitz W. Altered temperature induction sensitivity of the lambda pR/cI857 system for controlled gene E expression in Escherichia coli. FEMS Microbiol Lett 1999; 173:347-52; http//dx.doi.org/10.1111/j.1574-6968.1999.tb13524.x

[41] Haidinger W, Mayr UB, Szostak MP, Resch S, Lubitz W. Escherichia coli Ghost Production by Expression of Lysis Gene E and Staphylococcal Nuclease. Appl Environ Microbiol 2003; 69(10):6106-13; PMID:14532068; http//dx.doi.org/10.1128/AEM.69.10.6106-6113.2003

[42] Wagner S, Klepsch MM, Schlegel S, Appel A, Draheim R, Tarry M, Högbom M, van Wijk KJ, Slotboom DJ, Persson JO, et al. Tuning Escherichia coli for membrane protein overexpression. Proc Natl Acad Sci U S A 2008; 105 (38):14371-6; PMID:18796603; http//dx.doi.org/10.1073/pnas.0804090105

[43] Gurian-Sherman D, Lindow SE. Differential effects of growth temperature on ice nuclei active at different temperatures that are produced by cells of Pseudomonas syringae. Cryobiology 1995; 32(2):129-38; PMID:7743815; http//dx.doi.org/10.1006/cryo.1995.1012

[44] Langemann T, Mayr UB, Meitz A, Lubitz W, Herwig C. Multi-parameter flow cytometry as a process analytical technology (PAT) approach for the assessment of bacterial ghost production. Appl Microbiol Biotechnol 2016; 100(1):409-18; PMID:26521248; http//dx.doi.org/10.1007/s00253-015-7089-9

[45] Langemann T, Koller VJ, Muhammad A, Kudela P, Mayr UB, Lubitz W. The Bacterial Ghost platform system: production and applications. Bioeng Bugs 2010; 1(5):326-36; PMID:21326832; http//dx.doi.org/10.4161/bbug.1.5.12540

[46] Schmid D, Pridmore D, Capitani G, Battistutta R, Neeser J-R, Jann A. Molecular organisation of the ice nucleation protein InaV fromPseudomonas syringae. FEBS Letters 1997; 414(3):590-4; http//dx.doi.org/10.1016/s0014-5793(97)01079-x

[47] Turner MA, Arellano F, Kozloff LM. Three separate classes of bacterial ice nucleation structures. J Bacteriol 1990; 172(5):2521-6; PMID:2158972

[48] Ruggles JA, Nemecek-Marshall M, Fall R. Kinetics of appearance and disappearance of classes of bacterial ice nuclei support an aggregation model for ice nucleus assembly. J Bacteriol 1993; 175(22):7216-21; PMID:8226668

[49] Bi Y, Cabriolu R, Li T. Heterogeneous ice nucleation controlled by the coupling of surface crystallinity and surface hydrophilicity. J Phys Chem C 2016; 120(3):1507-14; http//dx.doi.org/10.1021/acs.jpcc.5b09740

[50] Turner MA, Arellano F, Kozloff LM. Components of ice nucleation structures of bacteria. J Bacteriol 1991; 173 (20):6515-27; PMID:1917876

[51] Lubitz W, Pugsley AP. Changes in host cell phospholipid composition of φX174 gene E product. FEMS Microbiol Lett 1985; 30(1–2):171-5; http//dx.doi.org/10.1111/j.1574-6968.1985.tb01006.x

[52] Hew CL, Yang DS. Protein interaction with ice. Eur J Biochem 1992; 203(1–2):33-42; PMID:1730239

[53] Bassi AS, Ding DN, Gloor GB, Margaritis A. Expression of single chain antibodies (ScFvs) for c-myc oncoprotein in recombinant Escherichia coli membranes by using the ice-nucleation protein of Pseudomonas syringae. Biotechnol Prog 2000; 16(4):557-63; PMID:10933828; http//dx.doi.org/10.1021/bp000053k

[54] Blasi U, Henrich B, Lubitz W. Lysis of Escherichia coli by cloned phi X174 gene E depends on its expression. J Gen Microbiol 1985; 131(5):1107-14; PMID:3160821; http//dx.doi.org/10.1099/00221287-131-5-1107

[55] Witte A, Brand E, Mayrhofer P, Narendja F, Lubitz W. Mutations in cell division proteins FtsZ and FtsA inhibit phiX174 protein-E-mediated lysis of Escherichia coli. Arch Microbiol 1998; 170(4):259-68; PMID:9732440

[56] Witte A, Lubitz W, Bakker EP. Proton-motive-force-dependent step in the pathway to lysis of Escherichia coli induced by bacteriophage phi X174 gene E product. J Bacteriol 1987; 169(4):1750-2; PMID:2951368

[57] Meitz A, Sagmeister P, Lubitz W, Herwig C, Langemann T. Fed-Batch Production of Bacterial Ghosts Using Dielectric Spectroscopy for Dynamic Process Control. Microorganisms 2016; 4(2):E18; PMID:27681912; http//dx.doi.org/10.3390/microorganisms4020018

[58] Jalava K, Hensel A, Szostak M, Resch S, Lubitz W. Bacterial ghosts as vaccine candidates for veterinary applications. J Control Release 2002; 85(1–3):17-25; PMID:12480307; http//dx.doi.org/10.1016/S0168-3659(02)00267-5

[59] Mayr UB, Walcher P, Azimpour C, Riedmann E, Haller C, Lubitz W. Bacterial ghosts as antigen delivery vehicles. Adv Drug Deliv Rev 2005; 57(9):1381-91; PMID:15878634; http//dx.doi.org/10.1016/j.addr.2005.01.027

[60] Sührer I, Langemann T, Lubitz W, Weuster-Botz D, Castiglione K. A novel one-step expression and immobilization method for the production of biocatalytic preparations. Microb Cell Fact 2015; 14:180; PMID:26577293; http//dx.doi.org/10.1186/s12934-015-0371-9

[61] Hoose C, Kristjánsson JE, Burrows SM. How important is biological ice nucleation in clouds on a global scale? Environ Res Lett 2010; 5(2):024009

[62] Kozloff LM, Turner MA, Arellano F, Lute M. Phosphatidylinositol, a phospholipid of ice-nucleating bacteria. J Bacteriol 1991; 173(6):2053-60; PMID:1848220

[63] Guzman LM, Belin D, Carson MJ, Beckwith J. Tight regulation, modulation, and high-level expression by vectors

containing the arabinose PBAD promoter. J Bacteriol 1995; 177(14):4121-30; PMID:7608087; http//dx.doi.org/0021-9193/95/$04.00+0

[64] Green RL, Warren GJ. Physical and functional repetition in a bacterial ice nucleation gene. Nature 1985; 317 (6038):645-8; http//dx.doi.org/10.1038/317645a0

[65] Vali G. Quantitative Evaluation of Experimental Results an the Heterogeneous Freezing Nucleation of Supercooled Liquids. J Atmospheric Sci 1971; 28(3):402-9; http//dx.doi.org/doi:10.1175/1520-0469(1971)028<0402:QEOERA>2.0.CO;2

[66] Kishimoto T, Yamazaki H, Saruwatari A, Murakawa H, Sekozawa Y, Kuchitsu K, Price WS, Ishikawa M. High ice nucleation activity located in blueberry stem bark is linked to primary freeze initiation and adaptive freezing behaviour of the bark. AoB Plants 2014; 6:plu044; PMID:25082142; http//dx.doi.org/10.1093/aobpla/plu044

2.3 Ice nucleation activity of ina$^+$ *E. coli* C41 overnight cultures

2.3.1 Introduction

Generally, when ice nucleation activity of ina$^+$ bacteria is determined, they are cultivated below 30°C to stationary phase [1-3]. Expression of recombinant INP has to be induced until late-log phase or stationary phase, respectively, to exhibit nearly identical ice nucleation activity compared to the INP originated bacteria [4-6]. As E-mediated lysis is restricted to mid-log phase, the expression time of recombinant proteins is limited too. Therefore, overnight *E. coli* C41 cultures, which were expressing InaZ for 15h, were tested for their ice nucleation activity.

2.3.2 Results

E. coli C41 (pBINP, pGLysivb) were grown in LBv (supplemented with 0.2 % L-arabinose) overnight at 23°C with constitutive induction of INP. INP expression was induced for 15h. The overnight (o/n) culture was washed with ROTISOLV® water as described in chapter 2 and adjusted to a concentration of 5x 10^8 cells ml^{-1} (determined by FCM). Afterwards, a series of ten-fold dilutions from the o/n suspension was prepared and the freezing spectrum of the dilution series was determined by a droplet-freezing assay (**Fig 1 A**). Out of the freezing spectrum cumulative ice nucleation spectra were calculated (**Fig 1 B**). Fifty to 100 (of 10 µl volume) droplets of each dilution were cooled from -2°C to -13°C at a constant rate of 0.5-1°C decrements. The number of frozen droplets was counted and specified as frozen droplets in percent (f_{ice} %).

An undiluted *E. coli* C41 (pBINP, pGLysivb) (C41-INP o/n) sample containing 5x 10^8 cells ml^{-1} grown o/n and expressing INP for 15 h exhibited first freezing activity at -2°C with a nucleation frequency (NF) of 3.1 x 10^{-8} (**Fig 1**). At this temperature 12.5 % of the droplets were frozen, at -5.5°C all tested droplets (100%) were frozen. Out of this freezing curve a T_{50} value of -3°C was calculated. The ten-fold diluted C41-INP o/n sample (5x 10^7 cells ml^{-1}) showed first ice-nucleation activity at a temperature of -2.5°C with 3.3 f_{ice} % and 100 f_{ice} % were detected at -7.5°C. First frozen droplets of the hundred-fold diluted C41-INP o/n sample (5 x 10^6 cells ml^{-1}) were also detected at -2.5 °C with 3.6 f_{ice} %, which is nearly identical to the 10^{-1} diluted sample. However, 100 % frozen droplets were detected at a much higher subzero temperature of -11.5 °C in comparison to the 10^{-1} diluted C41-INP o/n sample (-7.5°C), resulting in a flatter freezing curve.

C41-INP o/n sample with a dilution factor of 10^{-3} (5 x 10^5 cells ml^{-1}) exhibits reduced ice-nucleation active sites, as the first frozen droplets were detected at -7°C (21 f_{ice} %) and all droplets were frozen at -19.5°C. For typ I ice nuclei a NF value of 8 x 10^{-6} at -5°C was determined. By lowering the temperature down to -7°C (type II ice nuclei) a NF of 5.2 x 10^{-5} was achieved and increased to 1 x 10^{-9} at -9.5°C (type III ice nuclei) (**Fig 1 B**).

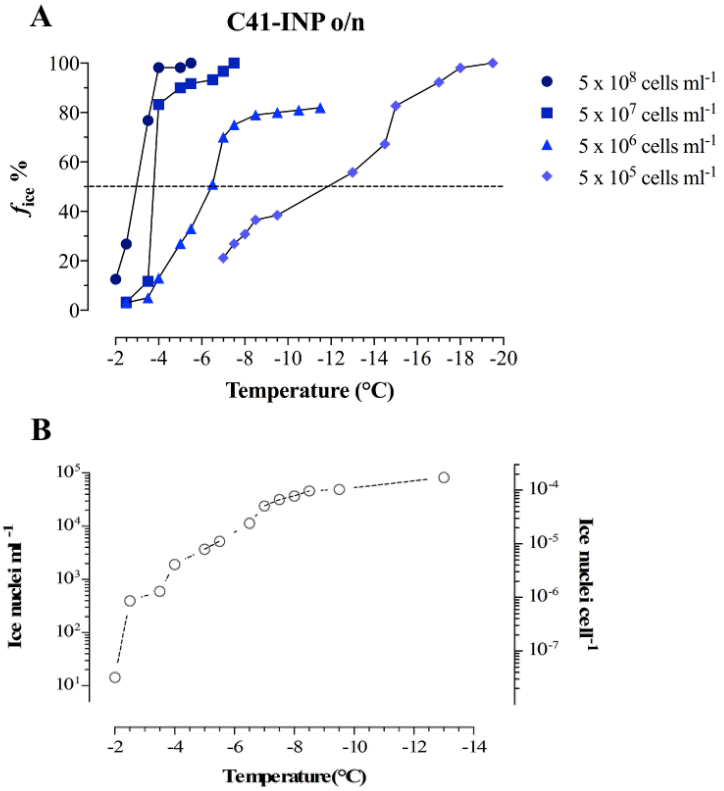

Figure 1. A. Freezing spectra of a dilution series of *E. coli* C41 (pBINP, pGLysivb) grown overnight at 23°C with constitutive induction of INP (C41-INP o/n). Ice nucleation curve is plotted as number fraction of frozen droplets in percent (f_{ice} %) at any temperature. From the undiluted sample (5 x 10^8 cells ml^{-1}) (●) 100 droplets were tested. 80 droplets were tested from the ten-fold dilution (5 x 10^7 cells ml^{-1}) (■). 80 droplets were tested from the 100-fold dilution (5 x 10^6 cells ml^{-1}) (▲), and 50 droplets were tested from the tone 1000-fold dilution (5 x 10^5 cells ml^{-1}) (◆). **B.** Cumulative concentration of ice nucleation activity of *E. coli* C41 (pBINP, pGLysivb) specified as number of ice nuclei ml^{-1} at a given temperature N(T) and Nucleation frequency (NF) expressed as ice nuclei $cell^{-1}$.

2.3.3 Discussion

Through extension of INP expression, it was demonstrated that few ina+ *E. coli* cells carrying INPs exhibit type I activity with highest nucleation temperatures at -2°C just like the INP originated *P. syringae.* Type I acting INPs are characterized as lipoglycoproteins as a result of post-translational modifications[7, 8]. Therefore, fed-batch procedures – which can prevent nutrient limitations to a certain amount resulting in extended log-phase – could be used to increase the cumulative concentration of nucleation frequency as well as the nucleation activity of ina^+ BGs acting as type I ice nuclei. Moreover, fed-batch fermentation procedures for the production of recombinant BGs have already been reported to enhance the yield of recombinant proteins[9].

2.4 References

1. **Lindow SE, Lahue E, Govindarajan AG, Panopoulos NJ, Gies D.** 1989. Localization of ice nucleation activity and the iceC gene product in Pseudomonas syringae and Escherichia coli. Mol Plant Microbe Interact **2:**262-272.
2. **Muryoi N, Matsukawa K, Yamade K, Kawahara H, Obata H.** 2003. Purification and properties of an ice-nucleating protein from an ice-nucleating bacterium, Pantoea ananatis KUIN-3. J Biosci Bioeng **95:**157-163.
3. **Gurian-Sherman D, Lindow SE.** 1995. Differential effects of growth temperature on ice nuclei active at different temperatures that are produced by cells of Pseudomonas syringae. Cryobiology **32:**129-138.
4. **Schmid D, Pridmore D, Capitani G, Battistutta R, Neeser J-R, Jann A.** 1997. Molecular organisation of the ice nucleation protein InaV fromPseudomonas syringae. FEBS Letters **414:**590-594.
5. **Orser C, Staskawicz BJ, Panopoulos NJ, Dahlbeck D, Lindow SE.** 1985. Cloning and expression of bacterial ice nucleation genes in Escherichia coli. J Bacteriol **164:**359-366.
6. **Nemecek-Marshall M, LaDuca R, Fall R.** 1993. High-level expression of ice nuclei in a Pseudomonas syringae strain is induced by nutrient limitation and low temperature. J Bacteriol **175:**4062-4070.
7. **Kozloff LM, Turner MA, Arellano F.** 1991. Formation of bacterial membrane ice-nucleating lipoglycoprotein complexes. J Bacteriol **173:**6528-6536.
8. **Turner MA, Arellano F, Kozloff LM.** 1990. Three separate classes of bacterial ice nucleation structures. J Bacteriol **172:**2521-2526.
9. **Suhrer I, Langemann T, Lubitz W, Weuster-Botz D, Castiglione K.** 2015. A novel one-step expression and immobilization method for the production of biocatalytic preparations. Microb Cell Fact **14:**180.

3 BGs carrying inner-membrane anchored INP

In order to anchor InaZ to the inner-membrane a N-terminal truncated form of InaZ was fused to different IM anchoring motifs resulting in three different fusion proteins which were expressed in *E. coli* C41 followed by E-mediated lysis. Full cells carrying IM anchored INP and free cytosolic INP, as well as their derived BG variants were tested for IN activity.

3.1 Manuscript I. Freezing from the inside. Ice nucleation in *Escherichia coli* and *Escherichia coli* ghosts by inner membrane bound ice nucleation protein InaZ.

Johannes Kassmannhuber[1,2], Mascha Rauscher[1]; Nadja Brait[3] Lea Schöner[1], Angela Witte[3] and Werner Lubitz[1]

Author details

[1]BIRD-C GmbH and CoKG; Vienna, Austria [2]Centre of Molecular Biology; University of Vienna; Vienna, Austria [3]Department of Microbiology, Immunobbiology and Genetics, Max F. Perutz Laboratories, University of Vienna, Vienna, Austria.

3.2 Contribution to manuscript I

The author of the thesis designed and performed all the experiments – except the FCM analysis – evaluated the data, created the figures & tables and contributed to writing the submitted manuscript.

Processing status:

Invited for submission, submitted for publishing in Bioengineered February, 21, 2017.

3.3 Manuscript I

For the sake of clarity and legibility the figures and tables were inserted near the respective text area.

Abstract

A N-terminal truncated form of the ice nucleation protein (INP) of *Pseudomonas syringae* lacking the transport sequence for the localization of InaZ in the outer membrane was fused to N- and C- terminal inner membrane (IM) anchors and expressed in *Escherichia coli* C41. The ice nucleation (IN) activity of the corresponding living recombinant *E. coli* catalyzing heterogeneous ice formation of supercooled water at high subzero temperatures were tested by droplet freezing assay. Median freezing temperature (T_{50}) of the parental living *E. coli* C41 cells without INP was detected at -20.1°C and with inner membrane anchored INPs at T_{50} value between -7°C and -9° demonstrating that IM anchored INPs facing the luminal IM site are able to induce IN from the inside of the bacterium almost similar to bacterial INPs located at the outer membrane. Bacterial Ghosts (BGs) derived from the different constructs showed first droplet freezing values between -6°C and -8°C whereas C41 BGs alone without carrying IM anchored INPs exhibit a T_{50} of -18.9°C. The more efficient IN of the INP-BGs compared to their living parental strains can be explained by the free access of the IM anchored INP constructs to the ultrapure water filling the inner space of the BGs. The cell killing rate of -NINP carrying *E. coli* at subzero temperatures is higher when compared to survival rates of the parental C41 strain.

Introduction

The conventional model for nucleation of water into embryo ice crystals by ice nucleation proteins (INPs) and further into ice describes stepwise aggregation of water molecules composed of a minimum of 275 water molecules[(1)] by electrostatic attraction of the polar parts of water by INPs until the critical size is exceeded[(2, 3)]. However, the mechanism of phase transition from water to ice is still not fully understood and of great scientific interest.

The mechanism of ice nucleation (IN) is generally divided into homogeneous and heterogeneous nucleation. Homogeneous IN occurs *without any foreign substance aiding the process of ice formation* [(4)] and homogeneous freezing of ultra-pure water occurs only at highest supercooled and supersaturated conditions, e.g. for atmospheric water at temperatures below -38°C.[(5)] Heterogeneous freezing is defined as IN *aided by the presence of a foreign substance such as bacteria or others so that nucleation takes place at a lesser supersaturation or supercooling than is required for homogeneous* IN[(4)]. *For homogeneous ice formation at -5°C, 45,000 water molecules are required in an embryo ice crystal though this number can drop to 600 or lower when ice nuclei are presen*t [(6)]. So-called ice nuclei trigger ice formation at temperatures between 0°C and -35°C[(7, 8)]. Heterogeneous IN is subdivided into four modes. (1) *Immersion freezing, where the ice nuclei is incorporated in a liquid*

body and initiates nucleation from inside the droplet[5]. (2) *Condensation freezing, where water droplets are formed by condensation around a cloud condensation nucleus (CCN), which acts simultaneously as ice nuclei*[9]. (3) Contact freezing is caused by an ice nuclei upon contact with a droplet surface[5, 10] and (4) deposition freezing where IN occurs directly from water vapor upon an ice nuclei surface[4, 5].

Bacterial IN proteins (INPs) bound to the outer membrane of some Gram-negative Bacteria can act as an ice nucleus *(e.g. Pseudomonas syringae, Pseudomonas putida, Erwinia herbicola, Erwinia ananas, or Xanthomonas campestris)*[11-18]. The well characterized plant pathogen *P. syringae* represents one of the most efficient bacterial ice nucleus known, initiating plant damaging ice formation at temperatures of -2°C[12, 19]. INPs have the property to catalyze heterogeneous ice formation of supercooled water by orienting water molecules into an ice-like structure [20, 21]. The biological function of INPs is thought to direct ice formation into the extracellular space at warm subzero temperatures to provide adaption time for the bacterium to freezing stress[22]. Furthermore, the resulting osmotic imbalance due to the extracellular ice formation results in an above-average water outflow from the cell to lower the intracellular IN temperature[23].

As described in this concept study freezing from the inside of the cytoplasmic space is artificial and evidently does not provide any advantage for the survival strategy of bacteria at low temperatures. Recombinant gene technology, however, provides tools for such an artificial system. It is of specific interest to investigate IN within *Escherichia coli* and derived Bacterial Ghosts (BGs) as it has been shown recently that BGs carrying INP on their outside are able to induce IN as effective as their living counterpart[24]. Here, in this investigation the expression of truncated forms of InaZ of *P. syringae* without its N-terminal transporter sequence for location in the outer membrane (OM) were anchored to the inner membrane (IM) or expressed in the cytoplasm of *E. coli*. IN and freezing properties of the live bacteria and their BG derivates were investigated and compared.

BGs in our hand are defined as empty cell envelops derived from a Gram-negative bacterium produced by controlled expression of cloned gene *E* of the bacteriophage PhiX174. E codes for a 91aa polypeptide which forms in an oligomeric conformation a transmembrane tunnel structure through the bacterial IM and OM[25]. Due to the osmotic pressure difference between cytoplasm and outside medium the cytoplasmic content of the bacterium is expelled[26, 27]. The size of the transmembrane tunnel is fluctuating between 40 - 200 nm and is located in areas of potential cell division sites predominantly in the middle of the cell or at polar sites[28, 29]. The BG internal lumen is free of nucleic acids, ribosomes or other constituents whereas the inner and outer membrane structures of the cell envelope are well preserved[30].

Bacterial INPs are composed of three characteristic protein domains, a highly repetitive central domain with several tandem consensus octapeptides (AGYGSTLT) and non-repetitive N- and C-terminal domains[31, 32]. The relatively hydrophobic N-terminal domain (approximately15% of the protein) is assumed to bind to phosphatidylinositol and polysaccharides and functions as membrane

anchor[22, 33-35]. The central domain is predicted to form ß-helical structures mimicking an ice like surface, which is able to bind water molecules and functions as template for orientating water into a lattice structure[36-39]. The function of the hydrophilic C-terminal domain is not completely understood, but is believed to have an important role in stabilizing the INP conformation[22, 34, 36]. Bacterial ice nuclei are classified according to their functional nucleation temperature into three different types; typ I acts at -5°C or warmer, type II from -5 to -7°C and type III below -7°C, where type III assemblies as a core protein, type II as a glycoprotein and type I as a lipoglycoprotein[33, 40, 41].

For biotechnological applications *P. syringaea* the most effective bacterial ice nuclei is used by the snowmaking industry. Cell surface display system based on INPs or its N-terminal domain alone exhibit fused proteins of interest in the OM[42-44]. Phage located reporter gene techniques using full length INPs have been developed[45] for diagnostic purposes to detect *Salmonella* food contaminations[46, 47].

In this study, a 162 amino acids (aa) truncated N-terminal form of InaZ (1200 aa)[31, 48] was anchored to the inner side of the *E. coli* C41 IM, using the membrane-targeting system reported by Szostak et al. (1990)[49]. The system is based on the hydrophobic membrane spanning domains of the truncated E (E´) and L (L´) proteins of the bacteriophages ΦX174 and MS2, respectively, that localize foreign proteins to the inner membrane of the cell envelope [49-51]. The protein of interest can be fused to the amino-terminal E´ sequence, the carboxy-terminal L´ sequence, or to both sequences. In this study *E. coli* cells carrying an IM anchored INP were used for ice nucleation studies of both, the living *E. coli* cells and of corresponding *E. coli* BGs.

To our knowledge intracellular INPs or anchored to the IM facing the cytoplasmic lumen or truncated forms of it have never been used as bacterial ice nuclei centers.

Results

E. coli and BGs carrying E´, L´ or E´-L´ anchored INP

For the production of living *E. coli* and BGs exposing INPs to the luminal site of the inner membrane (IM) directional targeting of InaZ lacking 162 aa of the 175 aa long N-terminal domain (-NINP) via N-terminal fusion (E´-NINP), C-terminal fusion (-NINP-L´), or by fusing -NINP with both anchor peptides (E´-NINP-L´) was used (schematic presentation **Fig. 1**). In order to express the three different forms of IM anchored -NINP fusion proteins, plasmids pBE-NINPH, pBH-NINPL and pBE-NINPHL (**Fig. 2**) were constructed. In these plasmids expression of the different INPs is under transcriptional control of the arabinose inducible P_{BAD} promoter of the cloning vector pBELK. For the production of BGs *E. coli* C41cells harboring either pBE-NINPH, pBH-NINPL, or pBE-NINPHL were co-transformed with the lysis plasmid pGLMivb. Growth and lysis of the bacteria was monitored by measuring the OD_{600}, flow cytometry, light microscopy and via colony forming units (cfu) analysis.

In lysis plasmid pGLMivb the expression of gene *E* is driven by the IPTG inducible P_{TAC} promoter. From the beginning of growth phase expression of the different -NINP constructs in *E. coli* C41 were induced by addition of 0.2 % arabinose to the growth medium.

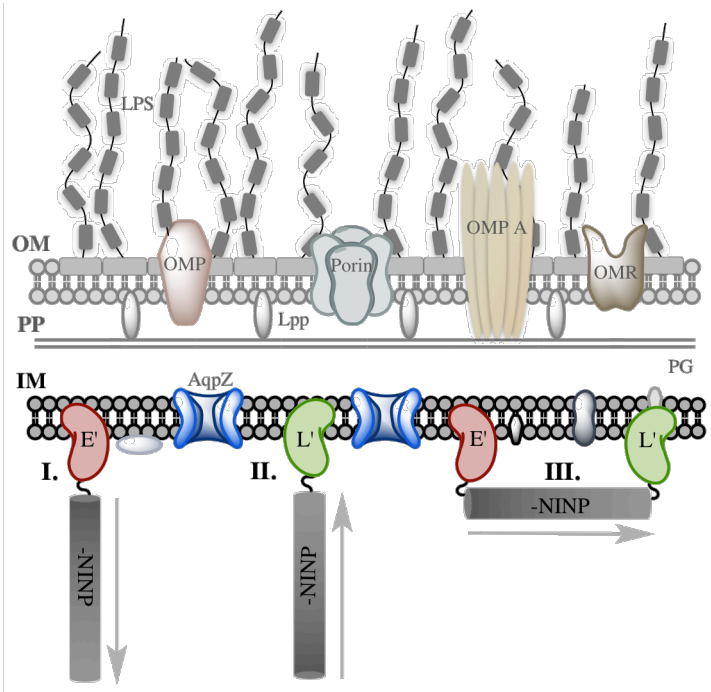

Figure. 1 Inner membrane targeting system anchoring N-terminal truncated INP (-NINP). Illustration of -NINP anchoring modes within the BG envelope, fused to the amino-terminal sequence of the IM spanning polypeptide E´ (I.), the carboxy-terminal sequence of the IM spanning polypeptide L´ (II.), or to both sequences (III.). OM: outer-membrane; PP: periplasm; IM: inner-membrane; LPS: lipopolysaccharide; OMP: outer-membrane protein; OMR: outer-membrane receptor; PG: peptidoglycan, Lpp: Braun's lipoprotein; AqpZ: aquaporin-Z; ↑,↓: orientation of truncated InaZ fused to E´, L´ and E´-L´ anchor sequences from N- to C-terminus.

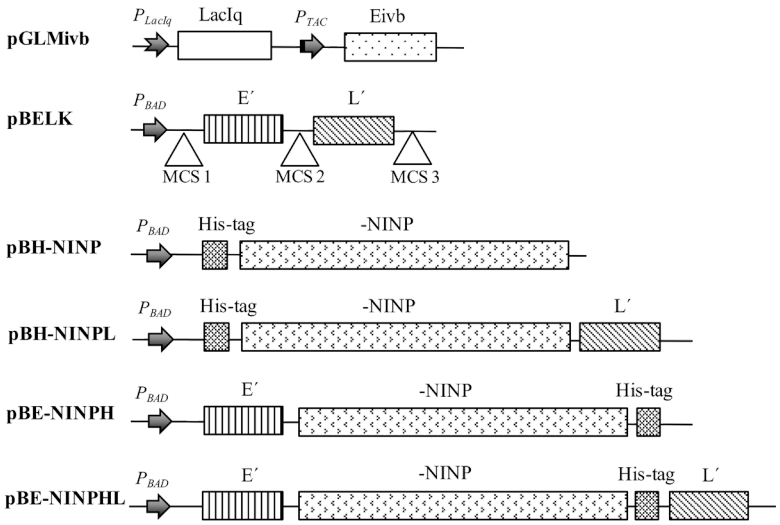

Figure 2. Partial map of plasmids used in this study for production of BGs carrying cytoplasmic membrane anchored -NINP. Eivb: C-terminal fusion of gene *E* to an in-vivo biotinylation sequence.

The culture was grown at 23°C since it was reported earlier that diminished IN activity was observed when ice nucleation active (ina$^+$) bacteria were grown above 25°C [52, 53]. At an optical density of 0.55-0.6 at 600 nm (OD_{600}) (mid-log phase after about 300 min of growth) the *E*-specific lysis was induced

in the recombinant bacteria by addition of 0.5 mM IPTG and is referred to time point 0 min in the growth curve (**Fig. 3**). The efficiency of E-lysis from time of lysis induction up to 120 min lysis time was determined by colony forming units (cfu) analysis (**Fig. 3**). Lysis efficiency (LE) for *E. coli* C41 carrying plasmids (pBE-NINPH and pGLMivb) amounts to 99.9 %, for *E. coli* C41 carrying plasmid (pBH-NINPL and pGLMivb) a LE of 99.8 % and for *E. coli* C41 harboring plasmids (pBE-NINPHL and pGLMivb) a LE of 99.7 % was achieved.

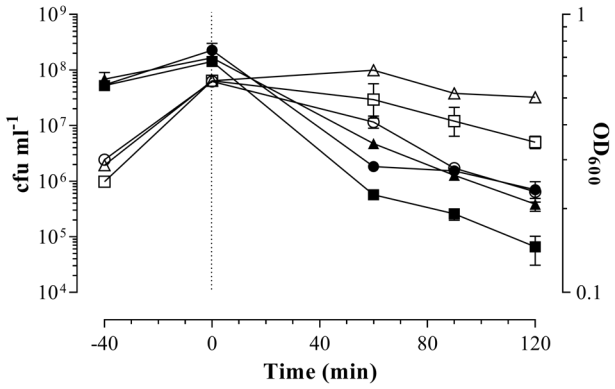

Figure. 3 Growth and E-lysis of *E. coli* C41 (pBE-NINPH, pGLMivb), (open square) C41(pBH-NINPL, pGLMivb) (open triangle) and C41 (pBE-NINPHL, pGLMivb) (open circle). The cultures were grown at 23°C in LBv complemented with 0.2 % arabinose to induce expression of the three distinct -NINP fusion proteins E´-NINP, -NINP-L` and, E´-NINP-L´. At time point zero (illustrated by vertical, sketched line) E-mediated lysis was induced by addition of 0.5 mM IPTG. Cfu of the corresponding cultures (closed symbols) were determined to calculate LE. After 120 min of E-lysis BG production was stopped by harvesting the cells. Data were obtained in three independent experiments. Error bars indicate standard errors.

The produced BGs showed slight elongation, that is specific to the used *E. coli* C41 (**Fig. 4**) but retained their morphological structure.

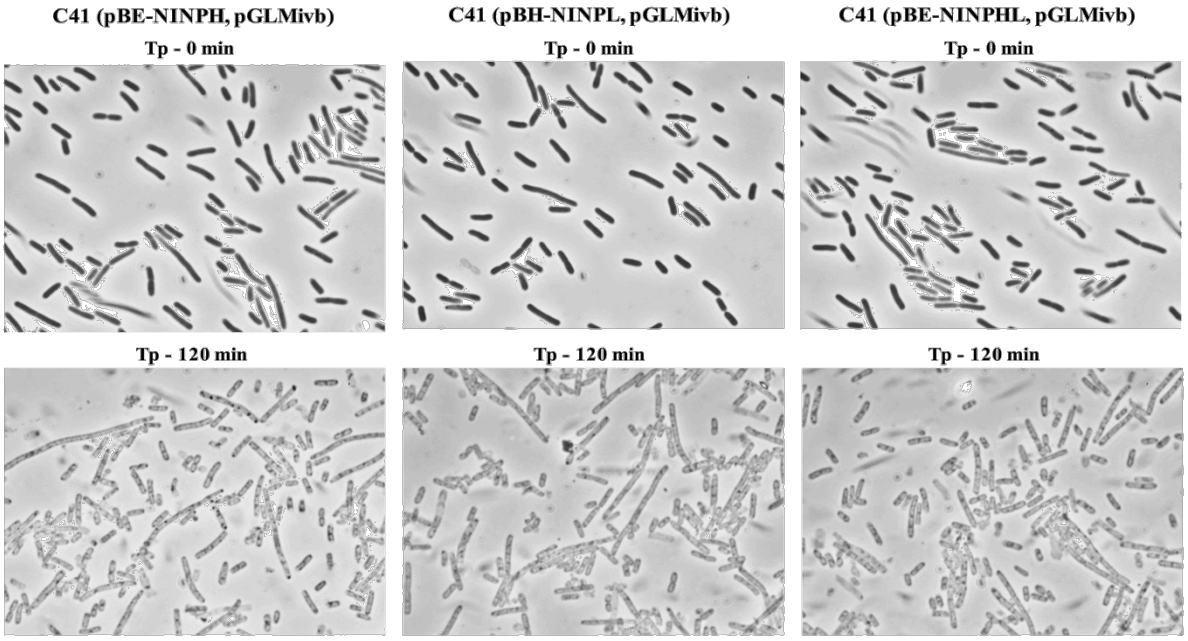

Figure. 4 Light microscopy pictures of the recombinant *E. coli* C41 strains carrying pBE-NINPH, pBH-NINPL and pBE-NINPHL, respectively at time point of lysis induction (Tp - 0 min) and endpoint of E-mediated lysis after 120 min.

E-lysis of the different *E. coli* clones were also monitored online via flow cytometry (FCM) (**Fig. 5**). The fluorescent dye RH414 staining phospholipid membranes enables discrimination of non-cellular background and DiBAC4(3) penetrating depolarized cell membranes binding to intracellular proteins or membrane compartments signaling changes in the membrane potential were used[54, 55]. A complete switch of DiBAC-negative cells with high scatter signal (G1), to DiBAC-positive cells with a diminished scatter signal (G2) marks the completion of protein E-mediated lysis process (**Fig. 5**).

In order to inactivate *E*-lysis escape mutants, the cultures were further incubated at 23°C and treated with 0.17 % (v/v) β-propiolactone for another 120 min. In the final preparation of *E. coli* BGs carrying either E´-NINP (E´-NINP-BG), -NINP-L´(-NINP-L´-BG) or E´-NINP-L´ (E´-NINP-L´-BG) no viable cells were detected.

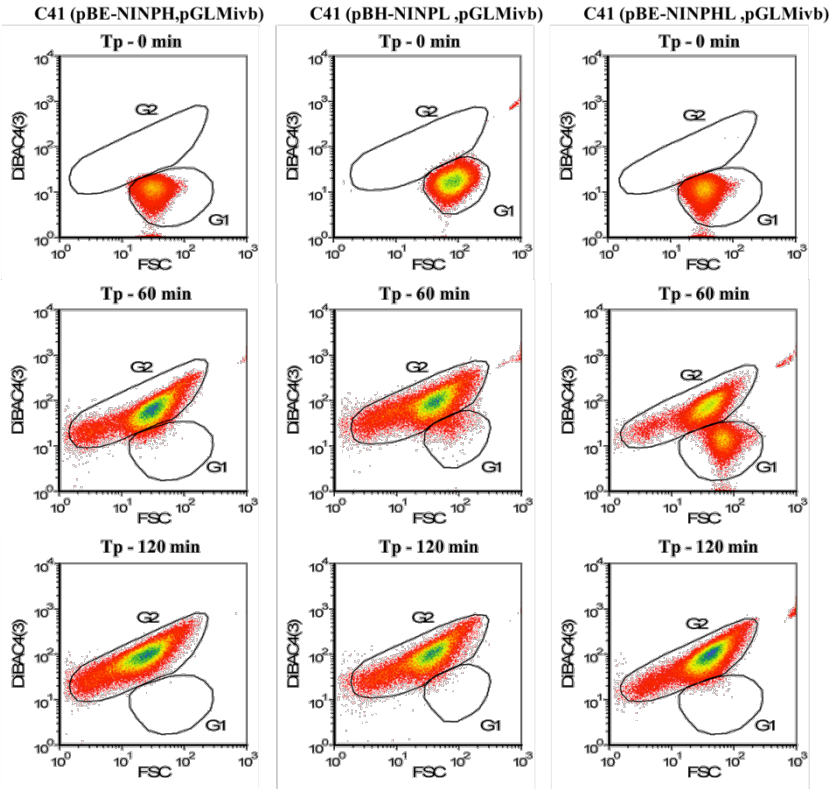

Figure. 5 Flow cytometry density dot plots during E-lysis process of *E. coli* C41 (pBE-NINPH, pGLMivb), C41 (pBH-NINPL, pGLMivb) and C41(pBE-NINPHL, pGLMivb) strains. Online monitoring of BG production, starting at time point of lysis induction (Tp - 0min), after 60min of lysis (Tp - 60min) and end of lysis phase (Tp-120min). Dot plots illustrate fluorescence intensity with $Dibac_4(3)$ versus – forward scatter (FSC); G1: living cells, G2: BGs.

Recombinant *E. coli* C41 bacteria from time point of E-lysis induction and corresponding BGs after β-propiolactone treatment were analyzed by Western blotting (**Fig. 6**) using a polyclonal antiserum against -NINP (α-H-NINP). The predicted molecular mass (M_r) of the fusion protein E´-NINP is 109.2 kDa, M_r of -NINP-L is 110.3 kDa and of E´-NINP-L´ 116.9 kDa.

The full length -NINP forms were detected around their specific M_r. Apart from the unspecific binding of the used polyclonal antibodies with proteins derived from *E. coli*, the lower migrated bands around 75 kDa most probably represent degradation products of the above mentioned INPs.

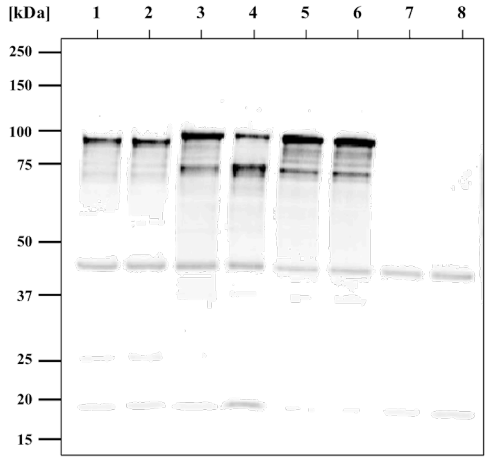

Figure. 6 Detection of -NINP fusion proteins in *E. coli* C41 and their derived BGs. Samples were taken before induction of E-mediated lysis (Tp-0min) (lane 1, 3, 5, 7) and after β-propiolactone treatment of BG samples (lane 2, 4, 6). Western blotting was performed with rabbit anti-H-NINP serum and anti-rabbit IgG horseradish peroxidase conjugated antibodies. Lane1: C41 (pBH-NINPL, pGLMivb), expressing -NINP-L; lane 2: -NINP-L-BG; lane 3: C41 (pBE-NINPH, pGLMivb), expressing E´-NINP; lane 4: E-NINP-BG; lane 5: C41(pBE-NINPHL, pGLMivb), expressing E´-NINP-L´; lane 6: E´-NINP-L´-BG; Lane 7: C41 control (pBAD24, pGLMivb) harvested before lysis induction (OD_{600} of 0.6); lane 8: BG form of C41(pBAD24, pGLMivb); Lines indicate molecular size marker proteins in kilodaltons (kDa).

Ice nucleation activity of IM anchored -NINP

Ice-nucleating activities of *E. coli* C41constructs and BG derived version carrying either E´-NINP, -NINP-L´, or E´-NINP-L´ were determined by a droplet-freezing assay. Additionally, full *E. coli* C41 cells carrying pBH-NINP encoding a cytoplasmic N-terminal His-tagged truncated INP lacking 162 aa of the N-terminal outer-membrane binding domain (C41-NINP) were tested for their ice-nucleating activity. For this purpose, all different -NINP constructs in *E. coli* C41 clones harboring the plasmids mentioned above were expressed by addition of 0.2 % arabinose to the growth medium at 23°C until the culture reached an OD_{600} of 0.6.

Forty-five drops (with a fixed volume of 10µl) from each culture suspension in ultra-pure water to be tested (containing 5 x 10^8 cells or BGs ml^{-1}) were cooled down and the number of frozen droplets at each temperature were counted. As the first frozen droplets of *E. coli* C41 cells (median freezing temperature, T_{50}, of -20.1°C) and *E. coli* C41 BGs (T_{50} of -18.9°C) were detected at -14°C [24] (**Fig. 7B**) the IN activity of recombinant *E. coli* C41 cells described here and their BGs were monitored up to a temperature decrease of -13°C. Out of the particular freezing temperatures of the tested droplets (**Fig. 7A**), the median freezing temperature, T_{50} (which is the temperature where 50% of all droplets are frozen) was calculated (**Fig. 7B**).

BG*s* carrying E´-NINP fusion protein (E´-NINP-BG) showed a T_{50} value at -7.7°C, T_{50} for BG carriers of -NINP-L´ (-NINP-L´-BG) was determined at -8.7°C and BGs with E´-NINP-L´ anchored (E´-NINP-L´-BG) a T_{50} at -9°C was recorded. Surprisingly, non- lysed *E. coli* C41 cells carrying E´-NINP (C41 E´-NINP), -NINP-L´ (C41-NINP-L´) and E´-NINP-L´(C41-E´-NINP-L´) (harvested before lysis induction) showed a bit higher subzero median freezing temperatures than their E-lysed forms (**Fig. 7, Table 1**).

The T_{50} value of C41-NINP carrying cytoplasmic N-terminal truncated INP was nearly identical to E´ and L´ anchored –NINP at -7.1°C. In contrast the T_{50} for *E. coli* C41 cells and *E. coli* C41 BGs were noted at -20.1°C and -18.9°C, respectively.[24]

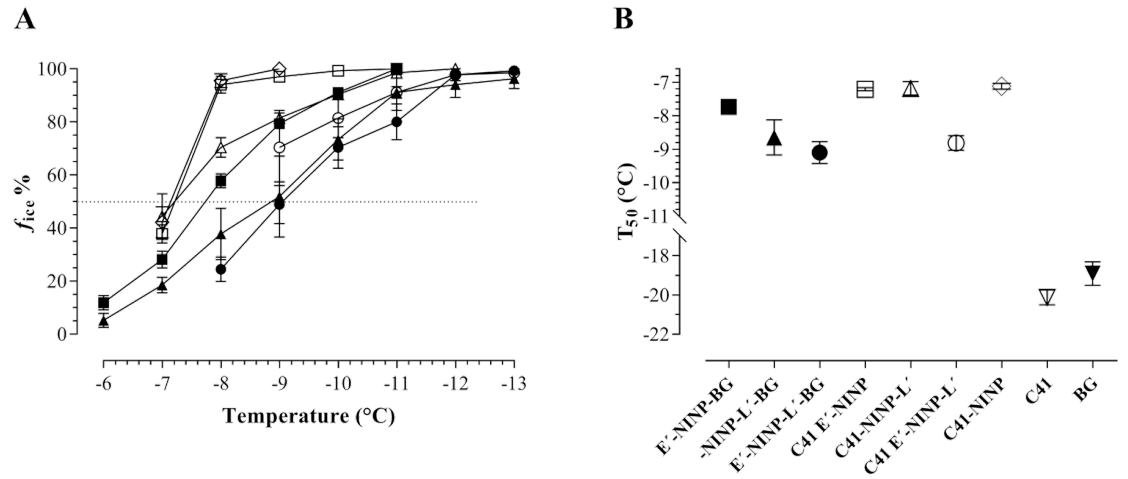

Figure 7. Freezing spectra (**A**) and median freezing temperatures (T_{50}) (**B**) of *E. coli* C41 (open symbols) and their BG derived version (full symbols): C41 E´-NINP, E´-NINP-BG (square); C41 -NINP-L´, -NINP-L´-BG (triangle); C41 E´-NINP-L´, E´-NINP-L´-BG (circle) C41-NINP(diamond). **A.** Nucleation curve plotted as number fraction of frozen droplets in percent (f_{ice} %) at any temperature. **B.** T_{50}, temperature where 50 % of all droplets are frozen. Forty-five 10 µl droplets of each suspension containing 5 x 10^8 cells or BGs ml^{-1} were tested by droplet freezing. T_{50} of living *E. coli* C41 (C41) is marked as star. Average numbers are obtained from three independent experiments. Error bars represent standard errors.

As the most active ice nuclei inside a droplet determines the temperature at which the droplet freezes [12, 56] a series of tenfold-dilutions from each suspension were tested to generate the cumulative IN spectra (**Fig. 8**).

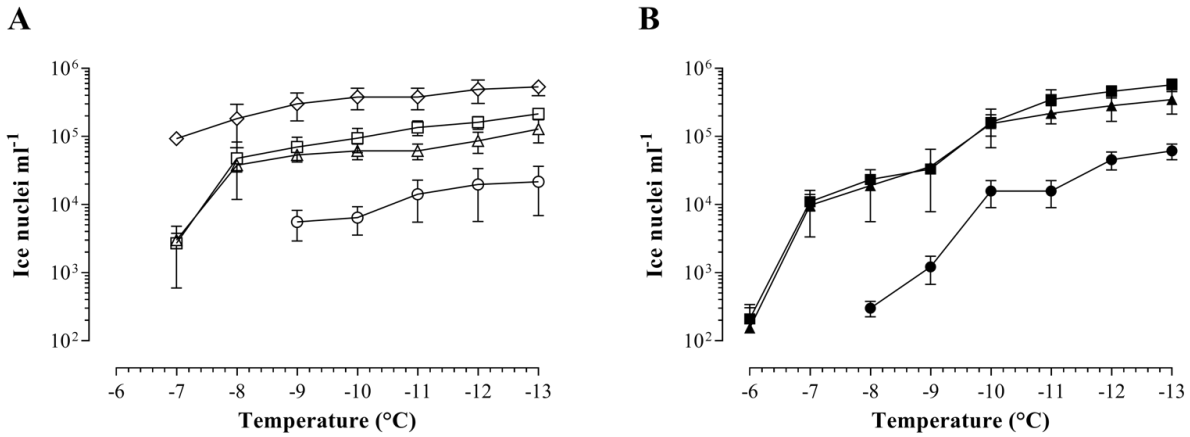

Figure 8. Cumulative spectrum of ice nucleation activity of recombinant *E. coli* C41 carrying three different anchored forms of -NINP and their BG derived form. **A** Living recombinant *E. coli* C41: C41 E´-NINP (□), C41 -NINP-L´ (△), C41 E´-NINP-L´ (○) and C41-NINP (◇); and **B** their E-lysis derived BG variant: E´-NINP-BG (■), -NINP-L´-BG (▲), E´-NINP-L´-BG (●). Average number of ice nuclei ml^{-1} at a given temperature; N(T). The spectrum of ice nucleation activity is representative of three replicate assays. Error bars represent the standard errors.

The nucleation frequency (NF), obtained by normalizing the number of ice nuclei ml^{-1} for the number of cells in the suspension, describes the fraction of cells in the suspension enfolding active IN sites at a

given temperature[57]. The average NF numbers of all tested IN active *E. coli* C41 and BGs at different temperatures are listed in **Table 1**. BGs carrying either an E´- or L´- inner-membrane anchored –NINP show a similar picture in IN spectrum with the lowest NF detected at -6°C. For E´-NINP-L´-BGs the first determinable NF was at -8°C, indicating a shift of class II INP activity ranging from -5°C to -7°C, when –NINP is fused to E´ and L´ cytoplasmic membrane anchors. The three different *E. coli* C41 variants carrying IM anchored -NINP exhibited first detectable NF at a 1°C lower temperature compared to their recombinant BG descendant form at -7°C and -9°C, respectively. C41 E´-NINP and C41-NINP-L´ with the lowest NF detected at -7°C function as type II ice nuclei, whereas C41-E´-NINP-L´ active from -9°C can be assigned to type III active ice nuclei. C41-NINP also showed first freezing activity at -7°C, however, the NF spectrum clearly contrasts with the others displaying significantly more nucleation sites at any temperature (**Table 1.**).

	T_{50} (°C)	**-6°C**	**-7°C**	**-8°C**	**-9°C**	**-10°C**	**-13°C**
ina$^+$ *E. coli*							
C41-NINP	-7.1	n.d.	1.9×10^{-4}	3.6×10^{-4}	6.0×10^{-4}	7.6×10^{-4}	1.1×10^{-3}
C41 E´-NINP	-7.2	n.d.	5.4×10^{-6}	9.5×10^{-5}	1.4×10^{-4}	1.9×10^{-4}	4.3×10^{-4}
C41 -NINP-L´	-7.2	n.d.	6.0×10^{-6}	7.6×10^{-5}	1.1×10^{-4}	1.2×10^{-4}	2.6×10^{-4}
C41 E´-NINP-L´	-8.8	n.d.	n.d.	n.d.	1.1×10^{-5}	1.3×10^{-5}	4.3×10^{-5}
ina$^+$ BGs							
E´-NINP-BG	-7.7	4.2×10^{-7}	2.2×10^{-5}	4.7×10^{-5}	6.7×10^{-5}	3.2×10^{-4}	1.2×10^{-3}
-NINP-L´-BG	-8.7	3.1×10^{-7}	2.0×10^{-5}	3.8×10^{-5}	7.3×10^{-5}	3.1×10^{-4}	7.0×10^{-4}
E´-NINP-L´-BG	-9.0	n.d.	n.d.	6.0×10^{-7}	2.4×10^{-6}	4.5×10^{-5}	1.2×10^{-4}

Table1. Median freezing temperature T_{50} (°C) and ice nucleation frequency (NF) at indicated temperature. Summary of the average ice nucleation frequencies at different temperatures. T_{50} (°C): temperature where 50 % of all droplets are frozen; NF: nucleation frequency expressed as ice nuclei cell^{-1}; n.d.: not determinable.

Discussion

In our investigation of heterogeneous immersion freezing live *E. coli* or BGs with INP bound to the IM were cooled down in ultra-pure water at subzero temperatures. Plain *E. coli* C41 or C41 BGs exhibit a T_{50} of -20.1°C and -18.9°C, respectively, whereas InaZ carrying versions performed for IN at a T_{50} around -8°C to -9°C. In contrast to the normal INP induced freezing starting from water surrounding the bacterial particles IM -NINP induced freezing has been initiated inside *E. coli* C41 or derived BGs. The inside growing ice crystal has to find its way to the surface of the cell envelope to initiate instantaneous freezing of the water droplets monitored for freezing. It was surprising that the Gram-negative cell envelope of *E. coli* C41 did not represent a real barrier suppressing or largely delaying ice formation. The T_{50} values were almost equal to IN seen in *E. coli* C41 and corresponding BGs where full length InaZ was expressed on the surface of the bacteria[24].

For BGs having a hole in their envelope connecting the inner aqueous lumen of the BG shell through the E-lysis tunnel with the surrounding water the enhanced IN and droplet freezing was not surprising. However, to explain the enhanced freezing for full bacteria there has to be postulated a water junction

facilitating ice crystal growth through the triple layered envelope of Gram-negative bacteria. The OM with its open porins is like a sieve and the periplasmic space with its peptidoglycan layer is an aqueous space, but not the IM as the ultimately permeability barrier of the cell regulating the passage of substances into and out of the cell. The normal osmotic pressure difference in *E. coli* of the cytoplasm and the surrounding medium is approximately 1-3 bar[58] and is compensated largely through the gel like structure of membrane derived polysaccharides in the periplasmic space (PPS). Osmotic changes in *E. coli* are highly regulated using in addition to free diffusion of water through the lipid barrier of the IM also aquaporin water channels embedded within the IM connecting the PPS with the cytoplasm. aquaporines have a role in both short- and long-term osmoregulatory responses and are required by rapidly growing bacteria[59]. Hence, it is proposed that the INP expressed in the cytoplasmic lumen induce the formation of ice crystal growth from the inside of the cell to the outside shell through a connection of the cytoplasmic lumen via water channels to the outside environment.

BGs carrying E´and L´ anchored -NINP were ice nucleation active at -6°C (1 cell of 2.4 x 10^6 cells and 3.2 x 10^6 cells, respectively) and showed a quite similar IN spectrum. This indicates that the N- or C- terminal orientation of the IM anchored -NINP is not significant and does not affect its nucleation activity. However, in contrast to live *E. coli* C41 where NF over the temperature range of -7°C to -13°C is almost similar with T_{50} of -7.2°C, the same constructs in BGs differ by 0.6 and 1.5°C °C, respectively in their $T_{50.}$ -NINP anchored at both terminal ends to the IM of *E. coli* C41 showed IN activity at lower temperatures when compared to E´ and L´ anchored -NINP. It seems very likely that E´-NINP-L´ anchoring could impair the mobility of the construct in the IM. Self-assembly of InaZ molecules is necessary for efficient IN bringing together the flat threonine and serine rich ice binding surface sites for mimicking the basal plane of ice [60]. The aggregation size of INP monomers cause the different threshold temperatures[56] where one INP monomer is functional at -12°C, a minimum of three co-operative INP monomers are needed for ice nuclei active at -8°C and at least 50 INP monomers for activity at -2°C to -3°C.[60, 61] As in the E´-NINP-L´ construct IN occurs at -9°C it is strongly felt that the latter assumption seems to be probable.

The free-movement of cytoplasmic -NINP facilitates its aggregation potential leading to significant higher NF numbers of C41-NINP compared to the membrane bound ina^+ versions.

It is surprising that even in an osmotic high concentrated cytoplasm ice nuclei/cell were more frequent in living *E. coli* C41 than in the BGs constructs with membrane anchored -NINP. The fact that components with larger volumes nucleate first[62, 63] and that IM -NINP BGs are connected to the water space through the E-tunnel structure it is obvious that first freezing events of such BGs can be detected earlier (-6°C for E´-NINP-BGs and -NINP-L´-BGs compared to -7°C and -8°C for E´-NINP-L´-BG compared to -9°C) than in intact *E.coli* cells. Our findings also indicate that according to T_{50} of IM anchored INPs full *E.coli* cells promote the assembling of cytosolic water molecules (water content of the cell estimated to be 70%)[64] into ice lattice structures somewhat better than in the BG derivatives.

In our investigation of intact bacteria carrying IM bound or free INP ice crystal formation starts in the

cytoplasma and is proceeding to the outside of the cell by crossing the cellular membrane. Water surrounding the cells gets in contact with the cytoplasmic originated ice crystals that promote further ice crystal growth. The killing rate by ice formation in living C41-NINP and C41-E´-NINP, C41-NINP-L´and C41-E´-NINP-L´ at -20°C is accelerated injuring 100% of all recombinants at 15 minutes residence time in the deep freezer versus approximately 80% of the controls. It is obvious that freezing from the outside and not from the inside increases the survival chances of bacteria and has therefore been favored by nature[22].

Material and Methods

Strains, plasmids and plasmids construction

All bacterial strains, plasmids and primers utilized in this study are listed in **Table 2**.

The *E. coli* strain K-12 5-α has been used for routine cloning and *E. coli* C41 (DE3) (Lucigen) for BG production. Plasmid pBAD24[65], *E*-lysis plasmid pGLMivb and plasmid pBELK were obtained from BIRD-C plasmid collection. Plasmid pBELK contains a E´- L´- anchoring cassette derived from pKSEL5-2[66] under control of P_{BAD} promoter. Plasmid pEX-A2INP (Eurofins Genomics) harbors a chemically synthesized 3603 bp *inaZ* gene encoding INP of *Pseudomonas syringae* S203[31]. In Lysis plasmid pGLMivb expression of the lysis gene *E* is under control of P_{TAC} promoter and translational fused to an in vivo biotinylation sequence. Expression vector pBH-NINP, coding for a N-terminal His-tagged truncated INP lacking 486 bp of the 525 bp long N-terminal domain (H-NINP) has been described previously[24].

In order to construct a fusion between INP and the E´-anchor first a truncated INP lacking N-terminal domain (-NINP) (lacking first 485 nt) was generated. A 3171 bp fragment absent of INP N-domain sequence was produced by PCR amplification using plasmid pEX-A2INP as template and primers P1 and P2 to introduce *XbaI*- and *PstI*- restriction sites at the termini and a 6x-His tag coding sequence at 3´-end with a terminal coding sequence. The amplified PCR-product coding for -NINP-His was cloned into the corresponding sites of pBELK resulting in plasmid pBE-NINPHSLK. The 3338 bp translational fused *E´-NINP-His* PCR-fragment was amplified using pBE-NINPHSLK as template and primers P3 and P4 containing *EcoRI* and *HindIII* at terminal restriction sites. The fragment was cloned into the equivalent sites of pBAD24 to construct the E´-NINP-His anchor fusion protein expression-vector pBE-NINPH under transcriptional control of the arabinose-inducible expression system.

Using pEX-A2INP as template a 3171 bp PCR-fragment, encoding the His-NINP protein without termination codon, was obtained by PCR amplification. Primers P5 and P6 were used to introduce a 6x-His tag coding sequence at 5´-end and *EcoRI- PstI-* restriction sites at the terminal ends. In frame fusion of the L´- anchor and His-NINP sequence was generated by cloning the fragment into the equivalent sites of pBELK resulting in pBH-NINPLK. By PCR using pBH-NINPLK as template and primers P7 and P8 to introduce restriction sites *EcoRI* and *XbaI* at the termini a 3366 bp PCR-fragment was obtained encoding the anchor fusion protein His-NINP-L´. The fragment was cloned

into the corresponding sites of pBAD24 resulting in pBH-NINPL.

A 3165 bp PCR-fragment was generated by using P1 and P9 primers and pEX-A2INP as template to obtain the -NINP-His gene without a terminal coding sequence and 5´*XbaI* and 3´*PstI* restriction sites. The fragment was cloned into the *XbaI/PstI* sites of pBELK resulting in pBE-NINPHLK carrying the *E´- NINPH - L´* fusion gene, which translational fuses the -NINP-His sequence to the amino-terminal E´ sequence and the carboxy-terminal L´ sequence. The *E´ -NINP - L´* gene was amplified by using primers P3 and P10 to introduce *EcoRI* and *NcoI* restriction sites at the termini. The 3528 bp fragment was cloned into the corresponding sites of pBAD24 resulting in pBE-NINPHL. Figure 1 illustrates the plasmids used and constructed in this study for production of BGs carrying cytoplasmic anchored INPs facing the BG luminal site.

Growth, E-lysis conditions and inactivation of bacteria

Bacterial cultures were grown in animal protein-free, vegetable variant of Luria-Bertani (LBv: 10.0 g/l soy peptone (Car Roth) 5.0 g/l yeast extract (Carl Roth) and 5.0 g/l NaCl) and supplemented with appropriate antibiotics, ampicillin (100µg / ml), gentamycin (20µg / ml) and kanamycin (50µg / ml) at 37° or 23°C. To induce expression of the anchor fusion gene which is under the control of P_{BAD} promoter the *E. coli* C41 cells carrying plasmid (pBE-NINPH, pBH-NINPL, or pBE-NINPHL) were grown in LBv supplemented with 0.2 % L-arabinose at 23°C. In plasmid pGLMivb the expression of lysis gene *E* is under the control of synthetic P_{TAC} promotor. The bacterial lysis was induced with 0.5 mM isopropyl-D-1-thiogalactopyranoside (IPTG). Gene *E*-mediated lysis of bacteria was induced when cells reached an optical density at 600 nm (OD_{600}) of 0.6, and was extended for duration of 120min. At the end of the E-lysis procedure the BGs were harvested and washed four times with 1x Vol. of sterile de-ionized water (dH_2O) by centrifugation and finally resuspended in 1x Vol. of sterile dH_2O. For inactivation of any surviving E-lysis escape mutants from BG production representing a minor fraction of about 0.1 % - 0.3 % the washed BGs harvest was treated with 0.17 % (v/v) of the DNA-alkylating agent β-propiolactone (BPL, 98.5 %, Ferak) and kept for 120min at 23°C with slow agitation. After inactivation process, the fully inactivated cell broth consisting of BGs and inactivated surviving cells were washed twice with 1x Vol. of sterile dH_2O and once with ROTISOLV® water (Carl Roth) and resuspended in 1/10x Vol. ROTISOLV® water. The suspensions of *E. coli* C41 cells and BGs carrying cytoplasmic membrane anchored ice nucleation protein were adjusted to a concentration of 5 x 10^8 cells ml^{-1} determined by flow cytometry (FCM) in ROTISOLV® water.

Determination of colony forming units (cfu)

For cfu determination appropriate dilutions of samples (0.85 % (w/v) NaCl Solution) were plated on Plate Count Agar (PCA) (Carl Roth) using a WASP spiral plater (Don Whitley Scientific). 50 µl samples were plated on PCA plates as triplicates. The plates were incubated at 35°C over night and the next day the cfu was analyzed by a ProtoCOL SR 92000 colony counter (Synoptics Ltd).

Lysis efficiency (LE) is defined as ratio of BGs to total cell counts and can be calculated as following equation:

$$LE = \left(1 - \frac{cfu_{(t)}}{cfu_{(t_0)}}\right) \times 100\% \quad (1)$$

where t_0 is the time point of lysis induction (LI) and t any time after LI.

E-lysis monitoring

The BG production was monitored by light-microscopy (Leica DM R microscope, Leica Microsystems), by measuring the optical density at 600 nm (OD_{600}) and fluorescence-based flow cytometry (FCM) as reported earlier. [24] Briefly, flow cytometry was performed using a CyFlow® SL flow cytometer (Partec) and the membrane potential-sensitive dye DiBAC4(3) was well as the phospholipid membranes staining RH414 (both from AnaSpec) were used for fluorescent labeling . dye RH414 was used for discriminating non-cellular background and DiBAC for the evaluation of cell-viability. Data were analyzed using FloMax V 2.52 (CyFlow SL; Quantum Analysis) illustrating forward scatter (FSC) against DiBAC fluorescence signal (FL1, DiBAC) and presented as 2D density dot plots.

Western blot analyses

Pellets of 5 x 10^{-8} cells or BGs, respectively per ml were boiled in 1x SDS gel-loading buffer for 5min and separated on Bolt™ 4-12 % Bis-Tris Plus gel by using XCell SureLock™ Mini-Cell electrophoresis system (Thermo Fisher Scientific). By using XCell II™ Blot Module (Thermo Fisher Scientific) the electrophoretically separated proteins were then transferred to nitrocellulose membrane (GE Healthcare) with transfer buffer (25 mM Tris, 192mM glycine, 20 % methanol). The membrane was placed in TBST (20 mM Tris-HCl, pH7.5, 100 mM NaCl, 0.05 % Tween-20) with 5 % milk powder (Carl Roth) overnight at 4°C. Polyclonal α-H-NINP serum from rabbit was used to detect recombinant INP. Production of the antiserum has been described [24]. Immunodetection was performed using α-H-NINP serum followed by α-rabbit IgG-HRP (GE Healthcare). Detection was performed using Amersham ECL Western blot detection kit (GE Healthcare) and developed with ChemiDoc™ XRS (Bio-Rad).

Measurement of ice nucleation activity

The ice nucleation activity was measured by droplet freezing assay using a modified device based on a method of Vali. [67] Out of each suspension to be tested, forty-five 10 µl droplets of each tenfold dilutions series (ranging from 5 x 10^8 cells ml^{-1} to 5 x 10^4 cells ml^{-1}) were tested for active ice nuclei inside the droplet at a given temperature. The experimental setup has already been used and described in detail in a former study. [24] Here, only a short description is given. The droplets were distributed on a sterile aluminum plate coated with a hydrophobic film and surrounded by styrofoam and covered by a plexiglas plate for isolation. The temperature of the working plate was decreased by two in series

circuited two-stage Peltier elements of the type TEC2-127-63-04. The surface temperature of the plate was measured by a small precision temperature sensor TS□NTC□103A (B+B Thermo-Technik). Ice nucleation activity was tested from -2 to -13°C at a constant rate of 1°C decrements. After a 30 sec dwell time at each temperature the Plexiglas plate was removed and the number of frozen droplets was recorded.

Determination of ice nucleation activity

Forty-five (of 10 µl volume) drops containing a known number of BGs or bacterial cell suspension was allowed to cool to a fixed temperature as mentioned above and the number of frozen droplets were counted. This measurement was repeated for each and every series of 10-fold dilutions to obtain statistically significant values The different samples were compared by their median freezing temperature (T_{50}), which represents the temperature where 50 % of all droplets are frozen. The T_{50} was calculated with the equation reported by Kishimoto et al. [68],

$$T_{50} = \frac{T_1 + (T_2 - T_1)(2^{-1}n - F_1)}{(F_2 - F_1)} \quad (2)$$

where, F1 and F2 are the number of frozen droplets at temperature T1 and adjacent temperature T2, and are just below and above 50 % of the total number of tested drops (n).

The cumulative number N(T), of ice nuclei ml^{-1} active at a given temperature was calculated by an analogical variant of the equation of Vali [67] reported by Govindarajan and Lindow[56].

$$N(T) = -\ln(f) \times \frac{10^D}{V} \quad (3)$$

Where, f = fraction of unfrozen droplets at temperature T, V = volume of each droplet used (10 µl), D = the number of 1:10 serial dilutions of the original suspension. N(T) was normalized for the number of cells present in each suspension to obtain the nucleation frequency (NF) per cell by dividing ice nuclei $^{-ml}$ through cell density ($cell^{-ml}$).

Strains, plasmids and primers	Description	Source or Reference
Bacterial Strain		
E. coli C41 (DE3)	F – ompT hsdSB (rB- mB-) gal dcm (DE3).	Lucigen
E. coli K-12 5-α	F´ *proA*$^{+}$*B*$^{+}$ *lacI*^{q} Δ*(lacZ)*M15 *zzf::Tn10* (Tet^{R}) / *fhuA2*Δ*(argF-lacZ)U169 phoA glnV44 Φ80Δ(lacZ)*M15 *gyrA96 recA1 relA1 endA1 thi-1 hsdR17.*	NEB
Plasmids		
pBAD24	Bacterial expression vector containing the arabinose P_{BAD} promotor system; restriction enzyme cloning; AmpR; ColE1 ori.	BIRD-C
pGLMivb	LacIq-P_{TAC}-*Eivb; Gent*^{R}.	(24)
pEX-A2INP	P_{LAC}-*inaZ,* coding for InaZ, PUC Origin; Amp^{R}.	Eurofins Genomics
pBELK	P_{BAD}-*E´-L´*-cassette for inner-membrane anchoring of proteins, Kan^{R}.	BIRD-C
pBH-NINP	P_{BAD}-*H-NINP*; Amp^{R}. Coding for InaZ lacking N-terminal domain sequence with N-terminal His-tagged fusion.	(24)
pBE-NINPHSLK	P_{BAD}-*E´-NINP-His*; Kan^{R}. Coding for E´ -NINP-His fusion protein.	This study
pBE-NINPH	P_{BAD}-*E´-NINP-His*; Amp^{R}. Coding for E´ -NINP-His fusion protein.	This study
pBH-NINPLK	P_{BAD}-*His-NINP-L´*;Kan^{R}. Coding for His -NINP-L´ fusion protein.	This study
pBH-NINPL	P_{BAD}-*His-NINP-L´*;Amp^{R}. Coding for His -NINP-L´ fusion protein.	This study
pBE-NINPHLK	P_{BAD}-*E´-NINPhis-L´*;Kan^{R}. Coding for E`-NINPHis-L´ fusion gene.	This study
pBE-NINPHLK	P_{BAD}-*E´-NINPhis-L´*;Amp^{R}. Coding for E`-NINPHis-L´ fusion gene.	This study
Primers	*Sequence (5´→ 3´)*	*Restriction site*
P1: -N_INP-fwd	GTACGCTCTAGAAGTAAACACCCTGCCGGT	*XbaI*
P2: INP-His-rev	AAAAAACTGCAGTTATTA*ATGGTGATGGTGATGGTG*AGAGCCGG ATCCCTTTACCTCTATCCAGTCATC	*PstI*
P3: E`-fwd	GTACCGGAATTCTTTATGGTACGCTGGACT	*EcoRI*
P4: His-tag-rev	GACCCAAGCTTGCAGTTATTAATGGTGATGG	*HindIII*
P5: His-NINP-fwd	GTACCGGAATTCACTACTC*ATGCACCATCACCATCACCAT*GGATC CGGCTCTGTAAACACCCTGCCGGT	*EcoRI*
P6: INP-rev	AAAAAACTGCAGACTTTACCTCTATCCAGTCATC	*PstI*
P7: His-tag-fwd	GTACCGGAATTCCATGCACCATCACCATC	*EcoRI*
P8: L´-rev	GTACGCTCTAGACTTTGTGAGCAATTCGTC	*XbaI*
P9:INP-His1-rev	AAAAAACTGCAGA*ATGGTGATGGTGATGGTG*AGAGCCGGATCCC TTTACCTCTATCCAGTCATC	*PstI*
P10: L´1-rev	AACATGCCATGGCTTTGTGAGCAATTCGTC	*NcoI*

The primer restriction sites are underlined and 6x His-tag sequence is highlighted in italic.

Table 2. Bacterial strains, plasmids and primers used for construction of recombinant plasmids.

References

1. **Pradzynski CC, Forck RM, Zeuch T, Slavicek P, Buck U.** 2012. A fully size-resolved perspective on the crystallization of water clusters. Science **337:**1529-1532.
2. **Franks F.** 2003. Nucleation of ice and its management in ecosystems. Philosophical Transactions of the Royal Society of London Series A: Mathematical, Physical and Engineering Sciences **361:**557-574.
3. **Zachariassen KE, Kristiansen E.** 2000. Ice Nucleation and Antinucleation in Nature. Cryobiology **41:**257-279.
4. **Vali G, DeMott PJ, Möhler O, Whale TF.** 2015. Technical Note: A proposal for ice nucleation terminology. Atmos Chem Phys **15:**10263-10270.
5. **Cziczo DJ, Froyd KD.** 2014. Sampling the composition of cirrus ice residuals. Atmospheric Research **142:**15-31.
6. **McCorkle AM.** 2009. Natural Ice-Nucleating Bacteria Increase the Freezing Tolerance of the Intertidal Bivalve Geukensia demissa. DigitalCommons@Connecticut College, Biology Honors Papers.
7. **Lundheim R.** 2002. Physiological and ecological significance of biological ice nucleators. Philos Trans R Soc Lond B Biol Sci **357:**937-943.
8. **Möhler O, Georgakopoulos DG, Morris CE, Benz S, Ebert V, Hunsmann S, Saathoff H, Schnaiter M, Wagner R.** 2008. Heterogeneous ice nucleation activity of bacteria: new laboratory experiments at simulated cloud conditions. Biogeosciences **5:**1425-1435.
9. **Fukuta N, Schaller RC.** 1982. Ice Nucleation by Aerosol Particles. Theory of Condensation-Freezing Nucleation. Journal of the Atmospheric Sciences **39:**648-655.
10. **Li T, Donadio D, Ghiringhelli LM, Galli G.** 2009. Surface-induced crystallization in supercooled tetrahedral liquids. Nat Mater **8:**726-730.
11. **Maki LR, Galyan EL, Chang-Chien MM, Caldwell DR.** 1974. Ice nucleation induced by pseudomonas syringae. Appl Microbiol **28:**456-459.
12. **Lindow SE, Arny DC, Upper CD.** 1982. Bacterial ice nucleation: a factor in frost injury to plants. Plant Physiol **70:**1084-1089.
13. **Sun X, Griffith M, Pasternak JJ, Glick BR.** 1995. Low temperature growth, freezing survival, and production of antifreeze protein by the plant growth promoting rhizobacterium Pseudomonas putida GR12-2. Can J Microbiol **41:**776-784.
14. **Lindow SE, Arny DC, Upper CD.** 1978. Erwinia herbicola: A Bacterial Ice Nucleus Active in Increasing Frost Injury to Corn. Phytopathology **68:**523-527.
15. **Phelps P, Giddings TH, Prochoda M, Fall R.** 1986. Release of cell-free ice nuclei by Erwinia herbicola. J Bacteriol **167:**496-502.
16. **Kawahara H.** 2008. Cryoprotectants and Ice-Binding Proteins, p 229-246. *In* Margesin R, Schinner F, Marx J-C, Gerday C (ed), Psychrophiles: from Biodiversity to Biotechnology doi:10.1007/978-3-540-74335-4_14. Springer Berlin Heidelberg, Berlin, Heidelberg.
17. **Abe K, Watabe S, Emori Y, Watanabe M, Arai S.** 1989. An ice nucleation active gene of Erwinia ananas. Sequence similarity to those of Pseudomonas species and regions required for ice nucleation activity. FEBS Lett **258:**297-300.
18. **Zhao JL, Orser CS.** 1990. Conserved repetition in the ice nucleation gene inaX from Xanthomonas campestris pv. translucens. Mol Gen Genet **223:**163-166.
19. **Lindow SE, Hirano SS, Barchet WR, Arny DC, Upper CD.** 1982. Relationship between Ice Nucleation Frequency of Bacteria and Frost Injury. Plant Physiol **70:**1090-1093.
20. **Gurian-Sherman D, Lindow SE.** 1993. Bacterial ice nucleation: significance and molecular basis. Faseb j **7:**1338-1343.
21. **Warren G, Wolber P.** 1991. Molecular aspects of microbial ice nucleation. Mol Microbiol **5:**239-243.
22. **Lorv JS, Rose DR, Glick BR.** 2014. Bacterial ice crystal controlling proteins. Scientifica (Cairo) **2014:**976895.

23. **Oude Vrielink AS, Aloi A, Olijve LL, Voets IK.** 2016. Interaction of ice binding proteins with ice, water and ions. Biointerphases **11:**018906.
24. **Kassmannhuber J, Rauscher M, Schöner L, Witte A, Lubitz W.** 2017. Functional Display of Ice Nucleation Protein InaZ on the Surface of Bacterial Ghosts. Bioengineered doi:10.1080/21655979.2017.12847120-0.
25. **Blasi U, Linke RP, Lubitz W.** 1989. Evidence for membrane-bound oligomerization of bacteriophage phi X174 lysis protein-E. J Biol Chem **264:**4552-4558.
26. **Witte A, Wanner G, Blasi U, Halfmann G, Szostak M, Lubitz W.** 1990. Endogenous transmembrane tunnel formation mediated by phi X174 lysis protein E. J Bacteriol **172:**4109-4114.
27. **Witte A, Blasi U, Halfmann G, Szostak M, Wanner G, Lubitz W.** 1990. Phi X174 protein E-mediated lysis of Escherichia coli. Biochimie **72:**191-200.
28. **Witte A, Wanner G, Sulzner M, Lubitz W.** 1992. Dynamics of PhiX174 protein E-mediated lysis of Escherichia coli. Arch Microbiol **157:**381-388.
29. **Fu X, Himes BA, Ke D, Rice WJ, Ning J, Zhang P.** 2014. Controlled bacterial lysis for electron tomography of native cell membranes. Structure **22:**1875-1882.
30. **Witte A, Brand E, Schrot G, Lubitz W.** 1993. Pathway of PHIX174 Protein E Mediated Lysis of Escherichia coli, p 277-283. *In* de Pedro MA, Höltje JV, Löffelhardt W (ed), Bacterial Growth and Lysis: Metabolism and Structure of the Bacterial Sacculus doi:10.1007/978-1-4757-9359-8_33. Springer US, Boston, MA.
31. **Green RL, Warren GJ.** 1985. Physical and functional repetition in a bacterial ice nucleation gene. Nature **317:**645-648.
32. **Kawahara H.** 2002. The structures and functions of ice crystal-controlling proteins from bacteria. J Biosci Bioeng **94:**492-496.
33. **Kozloff LM, Turner MA, Arellano F.** 1991. Formation of bacterial membrane ice-nucleating lipoglycoprotein complexes. J Bacteriol **173:**6528-6536.
34. **Kawahara H.** 2013. Characterizations of Functions of Biological Materials Having Controlling-Ability Against Ice Crystal Growth, in Advanced Topics on Crystal Growth, Dr. Sukarno Ferreira (Ed.). INTECH doi:10.5772/54535
35. **Li Q, Yan Q, Chen J, He Y, Wang J, Zhang H, Yu Z, Li L.** 2012. Molecular characterization of an ice nucleation protein variant (inaQ) from Pseudomonas syringae and the analysis of its transmembrane transport activity in Escherichia coli. Int J Biol Sci **8:**1097-1108.
36. **Kajava AV, Lindow SE.** 1993. A model of the three-dimensional structure of ice nucleation proteins. J Mol Biol **232:**709-717.
37. **Graether SP, Jia Z.** 2001. Modeling Pseudomonas syringae ice-nucleation protein as a beta-helical protein. Biophys J **80:**1169-1173.
38. **Wolber P, Warren G.** 1989. Bacterial ice-nucleation proteins. Trends Biochem Sci **14:**179-182.
39. **Pandey R, Usui K, Livingstone RA, Fischer SA, Pfaendtner J, Backus EH, Nagata Y, Frohlich-Nowoisky J, Schmuser L, Mauri S, Scheel JF, Knopf DA, Poschl U, Bonn M, Weidner T.** 2016. Ice-nucleating bacteria control the order and dynamics of interfacial water. Sci Adv **2:**e1501630.
40. **Turner MA, Arellano F, Kozloff LM.** 1990. Three separate classes of bacterial ice nucleation structures. J Bacteriol **172:**2521-2526.
41. **Ruggles JA, Nemecek-Marshall M, Fall R.** 1993. Kinetics of appearance and disappearance of classes of bacterial ice nuclei support an aggregation model for ice nucleus assembly. J Bacteriol **175:**7216-7221.
42. **van Bloois E, Winter RT, Kolmar H, Fraaije MW.** 2011. Decorating microbes: surface display of proteins on Escherichia coli. Trends Biotechnol **29:**79-86.
43. **Fan LH, Liu N, Yu MR, Yang ST, Chen HL.** 2011. Cell surface display of carbonic anhydrase on Escherichia coli using ice nucleation protein for CO(2) sequestration. Biotechnol Bioeng **108:**2853-2864.
44. **Kwak YD, Yoo SK, Kim EJ.** 1999. Cell surface display of human immunodeficiency virus type 1 gp120 on Escherichia coli by using ice nucleation protein. Clin Diagn Lab Immunol **6:**499-503.

45. **Lindgren PB, Frederick R, Govindarajan AG, Panopoulos NJ, Staskawicz BJ, Lindow SE.** 1989. An ice nucleation reporter gene system: identification of inducible pathogenicity genes in Pseudomonas syringae pv. phaseolicola. Embo j **8:**1291-1301.
46. **Wolber PK, Green RL.** 1990. Detection of bacteria by transduction of ice nucleation genes. Trends Biotechnol **8:**276-279.
47. **Pattnaik PB, V. K.; Sunita Grover; Niyaz Ahmed.** 1997. Bacterial ice nucleation: prospects and perspectives. Current Science **72:**316-320.
48. **Wolber PK, Deininger CA, Southworth MW, Vandekerckhove J, van Montagu M, Warren GJ.** 1986. Identification and purification of a bacterial ice-nucleation protein. Proc Natl Acad Sci U S A **83:**7256-7260.
49. **Szostak M, Wanner G, Lubitz W.** 1990. Recombinant bacterial ghosts as vaccines. Res Microbiol **141:**1005-1007.
50. **Szostak MP, Mader H, Truppe M, Kamal M, Eko FO, Huter V, Marchart J, Jechlinger W, Haidinger W, Brand E, Denner E, Resch S, Dehlin E, Katinger A, Kuen B, Haslberger A, Hensel A, Lubitz W.** 1997. Bacterial ghosts as multifunctional vaccine particles. Behring Inst Mitt 191-196.
51. **Witte A, Reisinger GR, Sackl W, Wanner G, Lubitz W.** 1998. Characterization of Escherichia coli lysis using a family of chimeric E-L genes. FEMS Microbiol Lett **164:**159-167.
52. **Chen M-L, Chiou T-K, Jiang S-T.** 2002. Isolation of ice-nucleating active bacterium from mackerel and its properties. Fisheries science **68:**934-941.
53. **Obata H, Takinami K, Tanishita J-i, Hasegawa Y, Kawate S, Tokuyama T, Ueno T.** 1990. Identification of a New Ice-nucleating Bacterium and Its Ice Nucleation Properties. Agricultural and Biological Chemistry **54:**725-730.
54. **Langemann T, Koller VJ, Muhammad A, Kudela P, Mayr UB, Lubitz W.** 2010. The Bacterial Ghost platform system: production and applications. Bioeng Bugs **1:**326-336.
55. **Langemann T, Mayr UB, Meitz A, Lubitz W, Herwig C.** 2016. Multi-parameter flow cytometry as a process analytical technology (PAT) approach for the assessment of bacterial ghost production. Appl Microbiol Biotechnol **100:**409-418.
56. **Govindarajan AG, Lindow SE.** 1988. Size of bacterial ice-nucleation sites measured in situ by radiation inactivation analysis. Proc Natl Acad Sci U S A **85:**1334-1338.
57. **Orser C, Staskawicz BJ, Panopoulos NJ, Dahlbeck D, Lindow SE.** 1985. Cloning and expression of bacterial ice nucleation genes in Escherichia coli. J Bacteriol **164:**359-366.
58. **Rojas E, Theriot JA, Huang KC.** 2014. Response of Escherichia coli growth rate to osmotic shock. Proc Natl Acad Sci U S A **111:**7807-7812.
59. **Calamita G.** 2000. The Escherichia coli aquaporin-Z water channel. Mol Microbiol **37:**254-262.
60. **Garnham CP, Campbell RL, Walker VK, Davies PL.** 2011. Novel dimeric beta-helical model of an ice nucleation protein with bridged active sites. BMC Struct Biol **11:**36.
61. **Hew CL, Yang DS.** 1992. Protein interaction with ice. Eur J Biochem **203:**33-42.
62. **Dumont F, Marechal PA, Gervais P.** 2003. Influence of cooling rate on Saccharomyces cerevisiae destruction during freezing: unexpected viability at ultra-rapid cooling rates. Cryobiology **46:**33-42.
63. **Dumont F, Marechal PA, Gervais P.** 2004. Cell size and water permeability as determining factors for cell viability after freezing at different cooling rates. Appl Environ Microbiol **70:**268-272.
64. **Milo R.** 2013. What is the total number of protein molecules per cell volume? A call to rethink some published values. Bioessays **35:**1050-1055.
65. **Guzman LM, Belin D, Carson MJ, Beckwith J.** 1995. Tight regulation, modulation, and high-level expression by vectors containing the arabinose PBAD promoter. J Bacteriol **177:**4121-4130.
66. **Szostak M. AT, Lubitz W.** 1993. Immune response against recombinant bacterial ghosts carrying HIV-1 reverse transcriptase. In: Brown F, RM, Ginsberg HS, Lerner RA, editors. Vaccines

67. **Vali G.** 1971. Quantitative Evaluation of Experimental Results an the Heterogeneous Freezing Nucleation of Supercooled Liquids. Journal of the Atmospheric Sciences **28:**402-409.
68. **Kishimoto T, Yamazaki H, Saruwatari A, Murakawa H, Sekozawa Y, Kuchitsu K, Price WS, Ishikawa M.** 2014. High ice nucleation activity located in blueberry stem bark is linked to primary freeze initiation and adaptive freezing behaviour of the bark. AoB Plants **6:**

4 BGs carrying truncated forms of InaZ

4.1 BGs carrying INP288

4.1.1 Introduction

The repetitive central domain of the INP InaZ consists of 122 imperfect octapeptide repeats[1], in which the largest repeat element consists of 48 residues (twenty 48-residues) [2, 3]. Bacterial INPs and AFPs share a similar mechanism but with opposite effect. [4, 5] Like INPs, AFPs also possess a central repeating domain responsible for ice binding, but on a much smaller scale. [4, 5] Kobashigawa *et al.* (2005) demonstrated that a truncated form of InaZ composed of 2 x 48 repeats (INP96) produce moderate levels of antifreeze activity. [6] Moreover INP96 exhibits quite high sequence similarity with a beetle AFP from *Tenebrio molitor* (*Tm*AFP) [6, 7]. The following aim was to generate a fragment containing the N-terminal sequence (nt 1 - 525) and the sequence coding for 6 x 48 repeats (*inp288*) of *inaZ* (nt 526 – 1390) for recombinant expression in *E. coli* C41. Out of the recombinant *E. coli* C41 the BG form was produced and tested for antifreeze activity by a droplet freezing assay. All methods used in this chapter are described in section "Materials and Methods".

4.1.2 Construction of plasmid pBinp288

To generate the *inp288* fragment out of *inaZ* consisting of the N-terminal sequence and 6 x 48 repeats, a PCR was performed using plasmid pBINP as template and primers inaZ-fw (5´ GTACCGGAATTC AATGAATCTCGACAAGGC´3) and inp288-rv (5`GACCCAAGCTTTTATTACTGCGTGCTGCC ATAT `3) to introduce terminal restriction sites (*EcoRI* and *HindIII*) and two stop codons (**Fig 1**).

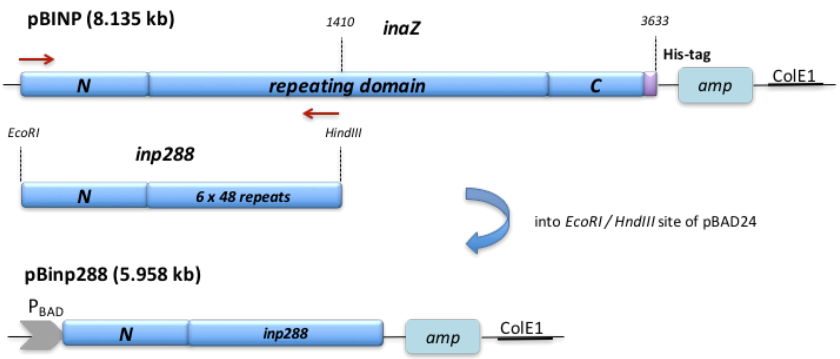

Figure 1. Cloning procedure of pBinp288. Sequence of *inp288* was amplified by PCR using primers inaZ-fw and inp288-rv. The obtained PCR product was cloned into *EcoRI* and *HindIII* restriction sites of plasmid pBAD24 to generate pBinp288.

The 1423 bp fragment was then cloned into the corresponding restriction sites of pBAD24 generating pBinp288.

4.1.3 E-lysis studies and droplet-freezing assay

In order to produce BGs displaying INP288 on the outer membrane surface (INP288-BG) expression vector pBinp288 (coding for INP288) and lysis plasmid pGLysivb were co-transformed into *E. coli* C41 [*E. coli* C41(pGLysivb, pBinp288)]. Induction of INP288 was constitutive for the overnight culture of *E. coli* C41(pGLysivb, pBinp288) (C41-INP288 o/n) clones used for E-lysis studies which were grown at 23°C. C41-INP288 o/n were inoculated in fresh LBv with appropriate antibiotics, expression of INP288 was induced by the addition of 0.2 % arabinose and the culture was grown at 23°C until OD_{600} reached approximately 0.6. At this time point, called as 'time point 0 min' (**Fig. 2**), the E-specific lysis was induced by a temperature up-shift of the culture from 23 to 42°C. Growth and lysis of the bacteria were monitored by measuring the OD_{600} and lysis efficiency was determined by cfu analysis (**Fig. 2**).

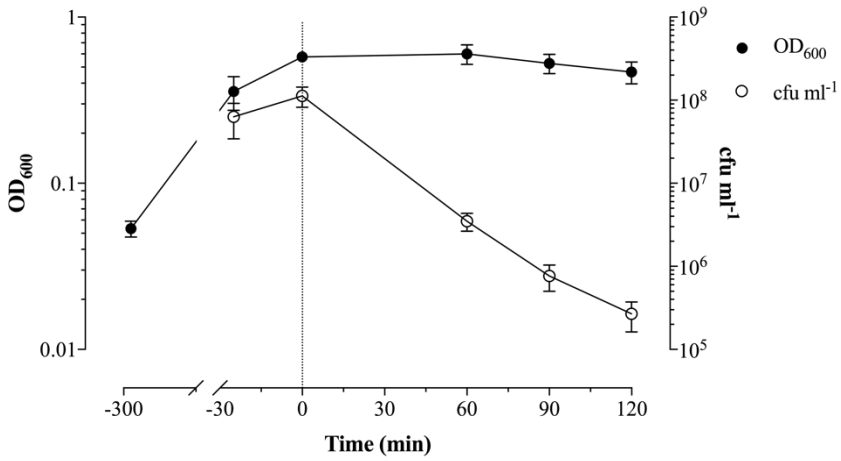

Figure 2. Growth and E-lysis of *E. coli* C41 for expression of INP and ghost production. *E. coli* C41(pGLysivb, pBinp288). The culture was grown in LBv supplemented with 0.2 % arabinose to induce INP288 expression at 23°C. At time point zero (illustrated by vertical sketched line) E-mediated lysis was induced by a temperature up-shift from 23°C to 42°C. Open symbols indicate OD_{600} values of growth and lysis phase. During E-lysis cfu (closed symbols) was determined to calculate lysis efficiency. Data were obtained out of three independent experiments. Error bars indicate standard errors.

The average lysis efficiency out of three independent experiments was 99.76% at 120 min after lysis induction (LI) (**Fig. 2**). To inactivate E-lysis escape mutants and non-lysed bacteria at time of harvest (after 120 min of lysis induction), the cultures were further incubated for 2h at 23°C with 0.17 % β-propiolactone.

Freezing spectra of INP288-BG, C41-INP288 (representing living *E. coli* C41 carrying INP288, which were harvested at time-point of LI) and C41-INP288 o/n were determined by droplet-freezing assay (**Fig.3**).

Sixty to ninety 10 µl droplets of each suspension containing 5x 10^8 cells ml^{-1} were tested. First frozen droplets of C41-INP288 were detected at -10°C which represents 1.3 % of all tested droplets (N_0). For C41-INP288 o/n first freezing activity was obtained at -11°C, representing 2.5 % of N_0. At -14°C first frozen droplets of INP288-BGs which detected what corresponds to 1.4 % of N_0. The T_{50} value for INP288-BGs was calculated to be at -18.3°C, for C41-INP288 at -19.4°C and for C41-INP288 o/n at -17.3°C.

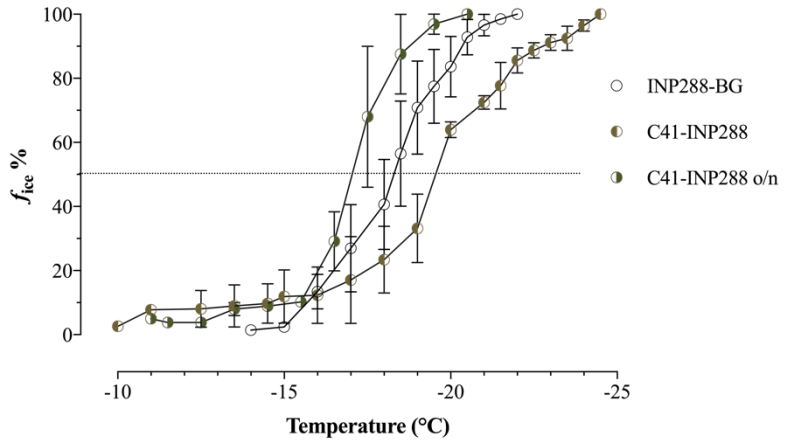

Figure 3. Average number of freezing spectra of INP288-BGs living C41-INP288 and C41-INP288 o/n. Ice nucleation curve plotted as number fraction of frozen droplets in percent (f_{ice} %) at any temperature. *E.coli* C41 (pGLysivb, pBinp288) BGs (INP288-BGs) (○); *E.coli* C41 (pGLysivb, pBinp288) (C41-INP288), harvested at time point of lysis induction (□); *E.coli* C41 (pGLysivb, pBinp288) expressing INP288 over-night (C41-INP288 o/n) (□). Horizontal sketched line indicates T_{50} value, temperature where 50 % of all droplets are frozen. Sixty to ninety 10 µl droplets of each suspension containing 5x 10^8 cells ml^{-1} were tested by droplet freezing. Average numbers are obtained from three independent experiments. Error bars represent the standard errors.

The T_{50} values for the tested INP288 samples do not differ significantly compared to *E. coli* C41 living bacteria (C41-24-pLy) and its BG derived form, which were noted to be at -20.1°C and -18.9°C, respectively.

4.2 BGs carrying INP96 on the outer membrane

4.2.1 Introduction

Beside the moderate antifreeze activity of the INP96 Kobashigawa *et al.* (2005) demonstrated ice-binding ability of INP96 [6]. INP96 represents a 96-residue polypeptide corresponding to a segment of InaZ (Tyr^{176}-Gly^{273}) from *P. syringae* [6] (**Fig. 1**). In addition, it was reported that minimum two to three 48-residue repetitive blocks are necessary to maintain the intrinsic tertiary INP structure which is necessary for its ice-binding ability [6, 8]. Aim of this study was to display INP96 on the outer membrane (OM) of *E. coli* C41 by fusing INP96 to the N-terminal domain of InaZ, which links the polypeptide via a glycosylphosphatidylinositol anchor to the OM [9] (**Fig. 2**). All methods used in this chapter are described in section "Materials and Methods".

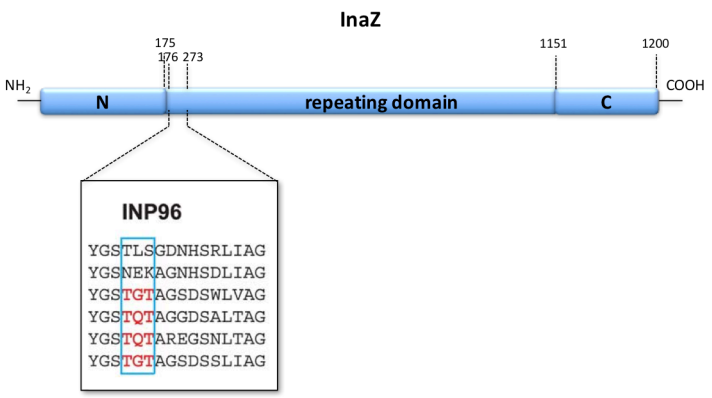

Figure 1. Illustration of the amino acid sequence of INP96 and its location within InaZ from *P. syringae*. Graphical single letter code of INP96 amino acid sequence was adapted from Kobashigawa *et al.* (2005) [6].

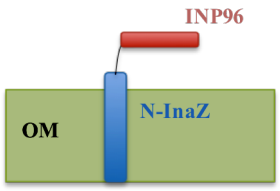

Figure 2. Chart of the N-INP96 fusion protein localization within the bacterial cell surface. Blue bar represents the N-terminal domain of InaZ (N-InaZ), red bar INP96, they are connected by a spacer sequence. Abbreviations: OM, outer membrane.

4.2.2 Construction of plasmid pBNinaZ_inp96/his

The N-terminal sequence of InaZ was amplified by PCR using plasmid pNInaZScFv-bsaAI [10] (obtained from Addgene, Cambridge, USA) carrying the 3600 bp *inaZ* gene, which harbors a 795 bp *αc-myc ScFv* gene at the C-terminal coding domain. Primers NinaZ-fw (5´- GTCGAGCTCATGAAT CTCGACAAGGC-`3) and NinaZ-rv (5´- GTCTCTAGATA CGGCAGCACGTTGAG-`3) were used to introduce a *SacI* restriction-site at the 5´-end and a *XbaI* restriction-site at the 3´-end. The PCR-fragment (537 bp) was cloned into the corresponding sites of pUC19, resulting in pUCN-inaZ. Plasmid pEX-A2INP (Eurofins Genomics, Ebersberg, Germany) harbors a chemically synthesized 288 bp *inp96* gene encoding INP96 and was used as template for PCR amplification of INP96. Primer inp96-fw (5´- GTCTCTAGATACGGCAGCACGTTGAG-`3) was used to introduce a *XbaI*

restriction-site at the 5´-end and primer inp96-2st-rev (5´- GTACGCAAGCTTTAATAAACCGGC GATCAGCGAAC-`3) to tag two terminal stop codon sequences and a 3´-end *HindIII* restriction site. Additionally, primer Inp96-his-2st-rev (5´- GTACGCAAGCTTTAATAATTAATGGTGATGGTGA TGGTGAGAGCCGGATCC ACCGGCGATCAGCGAAC `3) was used to introduce a C-terminal His-tag sequence with two stop codon sequences and a *HindIII* restriction site. The two amplicons were introduced into the appropriate restriction sites of pUCN-inaZ to generate the plasmids pUCNinaZ_inp96 and pUCNinaZ_inp96his, respectively, expressing a fusion protein of the InaZ N-terminal domain and INP96 (N-INP96), respectively a His-tagged version (N-INP96H). In order to express N-INP96 and N-INP96H under control of P_{BAD} promoter the fusion proteins were PCR amplified using following primer pairs: NinaZ-fw and inp96-2st-rev to amplify N-INP96; NinaZ-fw and His-tag-rv (5´- GACCCAAGCTTGCAGTTATTAATGGTGATGG `3). Each primer pair introduces a *XbaI*/*HindIII* restriction site at the terminal ends. The PCR-amplicons were cloned into the corresponding sites of the expression vector pBAD24, resulting in pBNinaZ_inp96 and pBNinaZ_inp96his, respectively (**Fig. 3**).

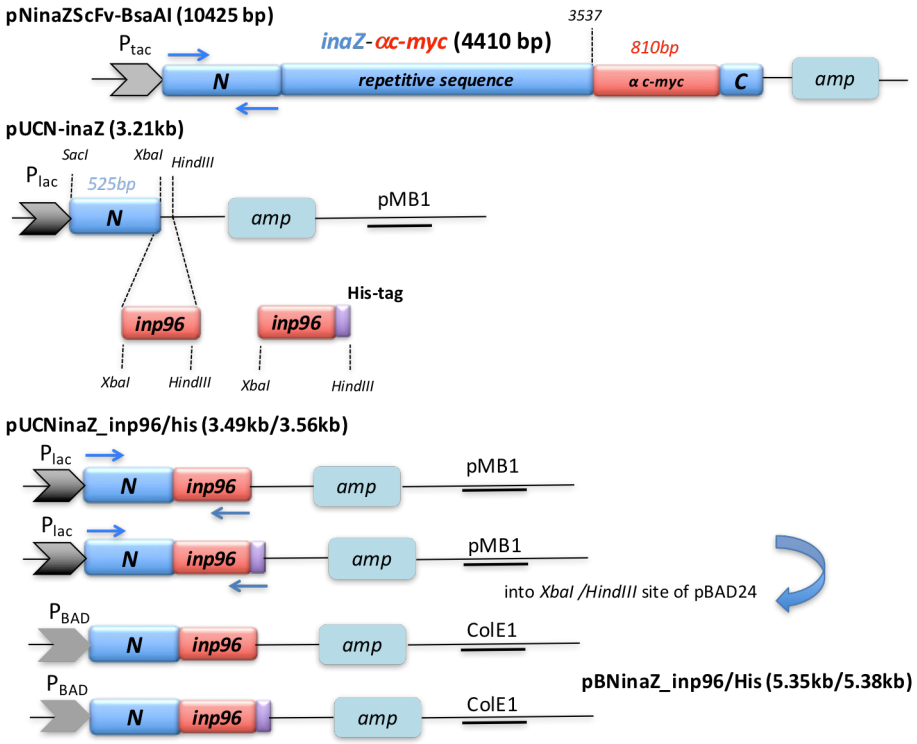

Figure 3. Graphical illustration of the cloning procedure of pUCN-inaZ, pBNinaZ_inp96 and pBNinaZ_inp96his.

4.2.3 Expression and E-lysis studies

For the production of BGs displaying N-INP96H on the outer membrane facing the cell surrounding site *E. coli* C41 cells harboring pBNinaZ_inp96his were co-transformed with the heat inducible lysis plasmid pGlysivb resulting in the bacterial strain *E. coli* C41 (pGlysivb, pBNinaZ_inp96his). From the beginning of growth phase of *E. coli* C41 (pGlysivb, pBNinaZ_inp96his) expression of N-INP96H was induced by the addition of 0.2 % arabinose and the culture was grown at 30°C. At an optical density (OD) of 0.55-0.6 at 600 nm (after 135 min of growth) the expression of gene *E* in lysis plasmid pGLysivb was induced by a temperature up-shift meaning the growing culture was transferred from 30°C to 42°C (**Fig. 4B**). The growth- and lysis-phase of the bacteria was monitored by measuring the optical density at 600nm (OD_{600}), and by microscopy. The efficiency of protein E-mediated lysis from time of lysis induction (LI) up to end of the lysis process (after 120 min) was determined by cfu-analysis (**Fig. 4B**). The average lysis efficiency (LE) from two independent experiments for *E. coli* C41 carrying plasmids (pGlysivb and pBNinaZ_inp96his) was 99.7 %. In addition, Western blot analysis was performed from samples taken at time point of lysis induction (0 min) after 60 min, 90 min and 120 min of LI with anti-His antibodies. (**Fig. 4A**). N-INP96H with a molecular weight of 29 kDa was detected in all tested samples from time point of lysis induction until end of lysis at suitable molecular size. For E-lysed *E. coli* C41 carrying lysis plasmid pGlysivb and expression vector pBAD24 (backbone of pBNinaZ_inp96his), serving as negative control (-ctrl) no signal was detected at 29 kDa. The detected N-INP96H band intensity remains quite stable during lysis process. Hence, it can be supposed that the fusion protein N-INP96H is successfully located at the outer membrane.

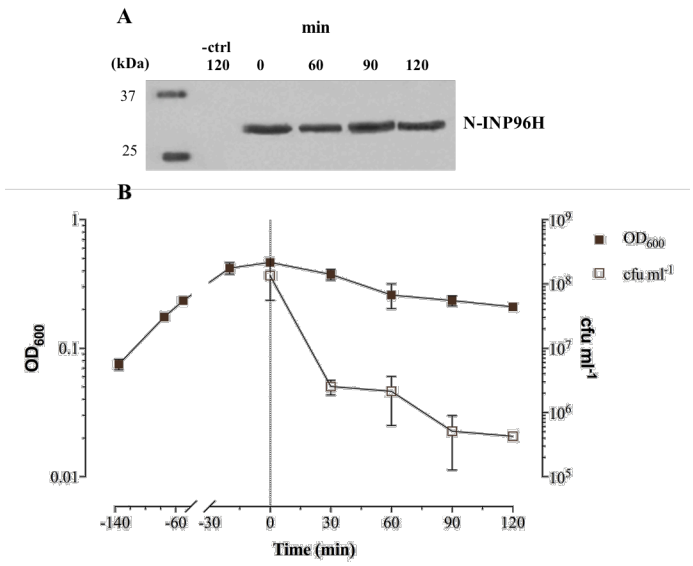

Figure 4. Western blot analysis (**A**), growth and E-lysis curve (**B**) of *E. coli* C41 (pGlysivb, pBNinaZ_inp96his) expressing C-terminal His-tagged N-INP96 (N-INP96H) and lysis gene *E*. **A.** *E. coli* C41 (pGlysivb, pBNinaZ_inp96his) samples from time point of lysis induction and 60 min, 90 min and 120 min after LI were separated on a 4-12 % Bolt™ 8 % Bis-Tris Plus gel and transferred onto nitrocellulose membranes. Anti-His antibodies were used to detect N-INP96H with a molecular weight of 29 kDa. *E. coli* C41 harboring lysis plasmid pGlysivb and expression vector pBAD24 were E-lysed for 120 min and served as negative control (-ctrl). Only the relevant sections of the immunoblots showing N-INP96H are presented. **B.** Monitoring of growth and E-lysis of *E. coli* C41 (pGlysivb, pBNinaZ_inp96his) by measuring OD_{600} (■) and determination of cfu (□). Bacterial samples were grown in LBv supplemented with 0.2 % arabinose to induce expression of N-INP96H at 30°C. At time point zero (illustrated by vertical sketched line) E-mediated lysis was induced by a temperature shift from 30°C to 42°C and prolonged for 120 min. Data were obtained from three independent experiments. Error bars indicate standard errors.

4.3 BGs displaying OmpA-INP96 fusion protein

4.3.1 Introduction

An OmpA surface display system reported by Hobom *et al.* (1995) [11] was used to localize INP96 on the outer membrane of *E. coli*. The OmpA-INP96 in frame sandwich fusion was generated by an insertion of INP96 in the second surface exposed region (**Fig. 1**). All methods used in this chapter are described in section "Materials and Methods".

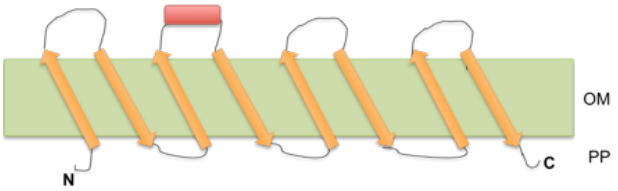

Figure 1. Arrangement of the OmpA-INP96 insertional fusion protein within the outer membrane (OM). INP96 is inserted into the second outer vertices of OmpA. The antiparallel transmembrane β-sheets of OmpA are shown as arrows. Abbreviations: PP, periplasm.

4.3.2 Construction of plasmid pHS64inp96/his

For expression of the OmpA-INP96 fusion protein the plasmids pHS64inp96 and pHS64inp96his were constructed as follows (**Fig. 2**).

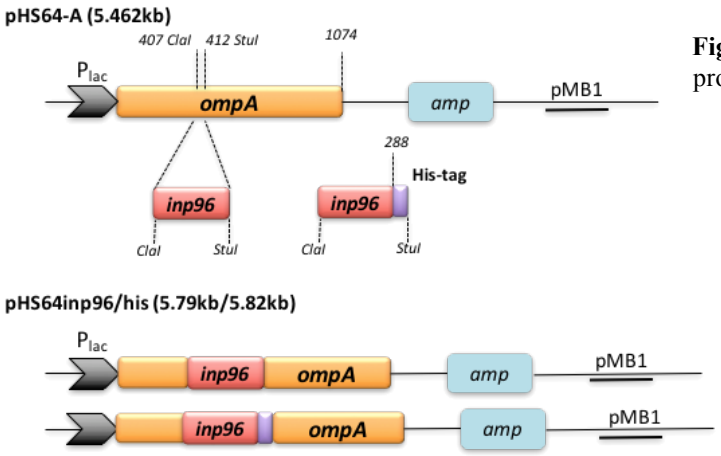

Figure 2. Graphical illustration of the cloning procedure of pHS64inp96 and pHS64inp96his.

The sequence of *inp96* was amplified by PCR using pEX-A2-inp96 as template. With primers inp96-claI-fw (5´GCCATCGATCTACGGCAGCACGTTGAG ´3) and inp96-StuI-rev (5´ GAAGGCCTCT ACCGGCGATCAGCGAAC´3) *ClaI* /*StuI* restriction sites were added at the fragment 5´- and 3´- end. Additionally, reverse primer inp96his-StuI-rev (5´GAAGGCCTTTAATGGTGATGGTGATGGTG AGAGCCGGATCCCTACCGGCGATCAGCGAAC´3) was used to introduce a C-terminal His-tag. The inp96 and inp96his fragments were cloned into the corresponding restriction sites of plasmid pHS-64 [11] (obtained from BIRD-C plasmid collection), to obtain the plasmids pHS64inp96 and pHS64inp96his, where inp96 and inp96his is under transcriptional control of the *lac* operon.

4.3.3 E-lysis of *E. coli* C2988J (pGLysivb, pHS64inp96his)

E. coli C2988J cells harboring either plasmid pHS64inp96 or pHS64inp96his expressing OmpA-INP96 and OmpA-INP96His, respectively were co-transformed with E-lysis plasmid pGLysivb to produce BGs carrying OmpA-INP96His (OmpA-INP96His-BG). *E. coli* C41 (pGLysivb, pHS64inp96his) was inoculated in LBv supplemented with appropriate antibiotics and grown at 23°C. When the culture reached an OD_{600} of 0.2, expression of OmpA-INP96His was induced by the addition of IPTG. E-mediated lysis was induced when the culture reached an OD_{600} of approximately 0.6 by shifting the culture from 23°C to 42°C referred to as time point 0' (**Fig. 3**). The lysis process was monitored by measuring OD_{600} and microscopy. E-lysis efficiency from time of lysis induction up to completed lysis after 120 min was determined by cfu analysis (**Fig. 3**).

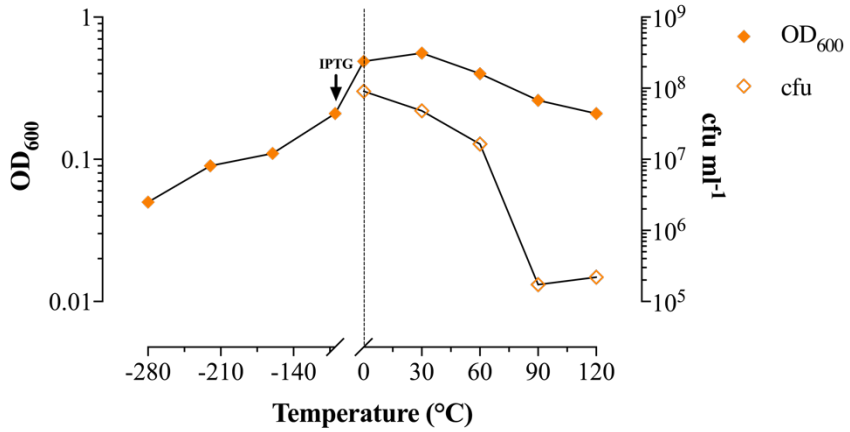

Figure 3. Growth- and E-lysis-curve of *E. coli* C2988J (pGLysivb, pHS64inp96his). *E. coli* C2988J (pGLysivb, pHS64inp96his) was grown in LBv at 30°C, at OD_{600} of 0.2 expression of OmpA-INP96His was induced by the addition of 0.5 mM IPTG. Growth and lysis was monitored by measuring OD_{600} (◆). Cfu analysis (◇) was performed from time point of lysis induction (time point 0 min, indicated by a sketched vertical line) when the culture was shifted from 30°C to 42°C at an OD_{600} of 0.6 until completion of lysis (120 min).

E. coli C2988J (pGLysivb, pHS64inp96his) culture reached a lysis efficiency of 99.8 % at 120 min. Western Blot analysis of *E. coli* C2988J (pGLysivb, pHS64inp96his) samples taken at time point of LI, 60 min and 120 min after LI was performed using anti-His antibodies. Detection of the OmpA-INP96His was not successful, as most probably the His-tag conformation within the fusion protein is not accessible for the used anti-His antibodies.

4.4 BGs carrying cytoplasmic located INP96 integrated into S-layers SbsA and SbsB

4.4.1 Introduction

Expression of the surface layer (S-layer) proteins SbsA and SbsB in *E. coli* lead to self-assembly of the protein monomers forming sheet-like structures, which remain within the cytoplasmic space after E-mediated lysis [12-14]. According to the feature of immobilization, S-layers can be used as carriers of foreign proteins located in the cytoplasmic lumen of BGs. Therefore, a fusion protein of SbsA and SbsB, respectively with INP96 was constructed. The INP96 sequence was incorporated into the C-terminal sequence of SbsB domain I (domain I: residues 32-201) at amino acid residue 161. Domain I of SbsB is responsible for the cell-wall attachment and is not integrated into the disk-like φ-shaped quaternary structure (organized by doman II-VII) [15]. Therefore, in SbsB domain I integrated INP96 is not being embedded in the two-dimensional oblique (p2) lattice structure of SbsB. Additionally, INP96 sequence is incorporated into SbsA at amino acid residue 296 and is thought – when expressed recombinantly – to be embedded into the crystallization region of SbsA that naturally assembles in a hexagonal (p6) two-dimensional lattice. All methods used in this chapter are described in section "Materials and Methods".

4.4.2 Construction of plasmid pUCsbsAinp96/his and pAKinp96/his

To generate a fusion protein of SbsA and INP96, *inp96* was PCR amplified by using plasmid pEX-A2-inp96 as template and primers inp96-apaI-fw (5´GGCGGGCCCTGTACGGCAGCACGTTGAG ´3), inp96-apaI-rev (5´GGCGGGCCCGACCGGCGATCAGCGAAC´3) to introduce an *ApaI* restriction site at the terminal ends. Primer inp96his-apaI-rev (5´GGCGGGCCCTTAATGGTGATGGTGATGG TGAGAGCCGGATCCGACCGGCGATCAGCGAAC ´3), was used to introduce a C-terminal His-tag. The 294 bp and 334 bp fragment, respectively were cloned into the corresponding *ApaI* site of plasmid pSL878 [13] (obtained from BIRD-C plasmid collection) resulting in pSL878inp96 and pSL878inp96his (**Fig. 1**). Subsequent, the fusion genes (*sbsAinp96* and *sbsAinp96his)* were amplified to introduce *SacI*/*XbaI* terminal restriction sites using primers sbsA-fw (5´ GTCATGGAGCTCAT GGATAGGAAAAAAGCTG´3) and sbsA-rv (5´ GTACGCTCTAGAGATACAGATTTGAGCAA ´3). The two fragments were cloned into the appropriate restriction sites of the expression vector pUC18 resulting in pUCsbsAinp96 and pUCsbsAinp96his (**Fig. 1**).

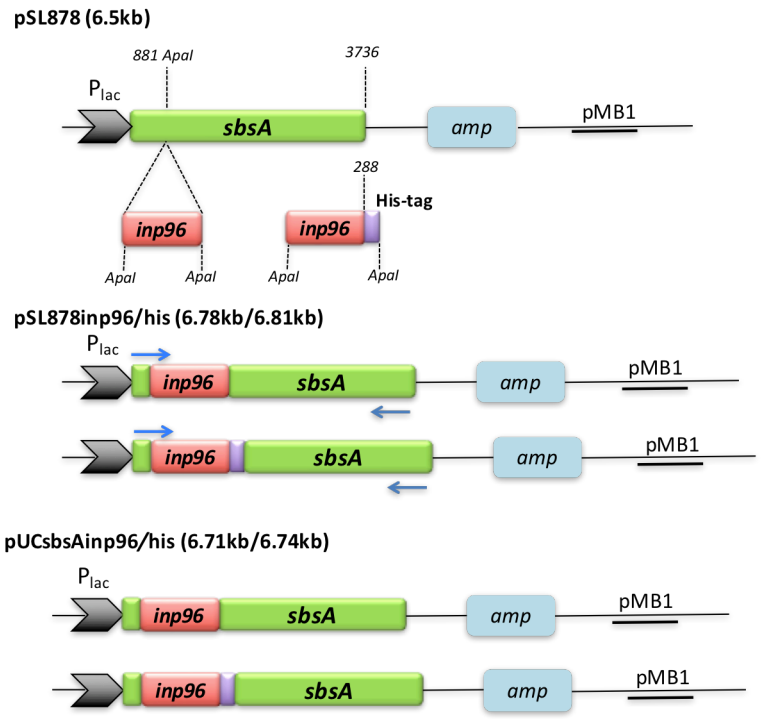

Figure 1. Illustration of the cloning procedure of pUCsbsAinp96 and pUCsbsAinp96his.

To generate a fusion protein of SbsB and INP96 (**Fig. 2**), *inp96* was PCR amplified by using plasmid pEX-A2-inp96 as template and primers inp96-snabI-fw (5´ GGCTACGTATACGGCAGCACGT TGAG ´3) and inp96-snabI-rv (5´ GGCTACGTAACCGGCGATCAGCGAAC ´3) to introduce a *SnaBI* restriction site at the 5´- and 3´- ends. Primer inp96his-snabI-rv (5´ GGCTACGTATTAATGGT GATGGTGATGGTGAGAGCCGGATCCACCGGCGATCAGCGAAC ´3) was used to introduce a C-terminal His-tag.

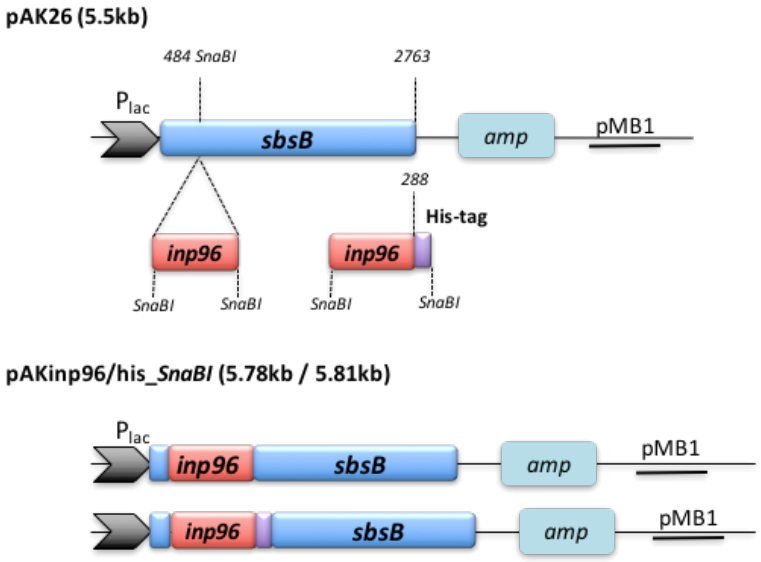

Figure 2. Illustration of the cloning procedure of pAKsbsBinp96 and pAKsbsBinp96his.

The fragments (*inp96* and *inp96his*) were blunt-end cloned into the corresponding restriction site of pAK26 [12] (obtained from BIRD-C plasmid collection), resulting in pAKinp96 and pAKinp96his (**Fig. 2**).

4.4.3 E-lysis

E. coli C2988J harboring E-lysis plasmid pGLysivb was co-transformed with plasmid pUCsbsAinp96his and pAKsbsBinp96his, respectively, to produce BGs carrying either cytoplasm located SbsA-INP96H (SbsA-INP96H-BGs) or SbsB-INP96H (SbsB-INP96-BGs) (**Fig. 3**).

For E-mediated lysis of *E. coli* C2988J (pGlysivb, pUCsbsAinp96his) and *E. coli* C2988J (pGlysivb, pAKsbsBinp96his), bacteria were grown in LBv at 30°C and expression of S-layer fusion proteins was induced when the culture reached an OD_{600} of 0.2 by adding 0.5 mM IPTG to the culture (**Fig. 4**). At an OD_{600} of 0.5 E-lysis from plasmid pGLysivb was induced by shifting the cultures from 30°C to 42°C (**Fig. 4**). After 120 min of lysis induction *E. coli* C2988J (pGlysivb, pUCsbsAinp96his) and *E. coli* C2988J (pGlysivb, pAKsbsBinp96his) reached a LE of 99.8 % and 99.9 %, respectively, determined by cfu analysis.

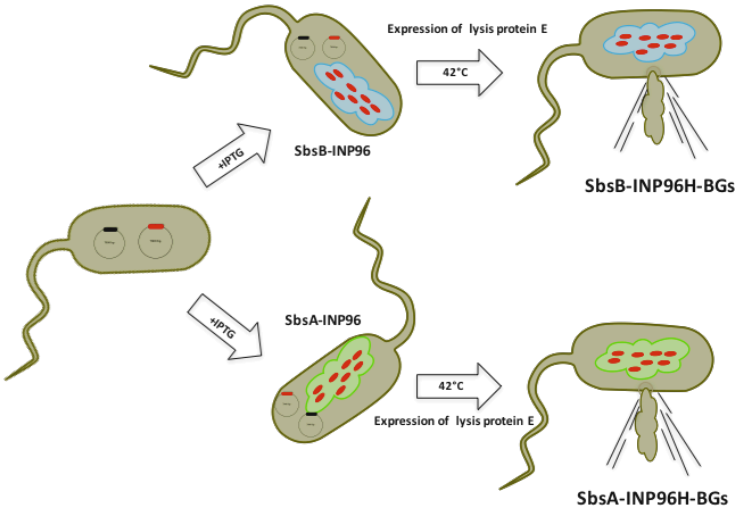

Figure 3. Graphic representation of SbsA-INP96H-BGs and SbsB-INP96H-BGs, respectively. In *E. coli* C2988J cells harboring plasmid pAKsbsB-inp96his or pUCsbsA-inp96his and lysis plasmid pGLysivb expression of S-layer fusion proteins (SbsA-INP96H or SbsB-INP96H) is induced by addition of IPTG to the culture medium and E-mediated lysis is induced by shifting the culture from their growth temperature to 42°C.

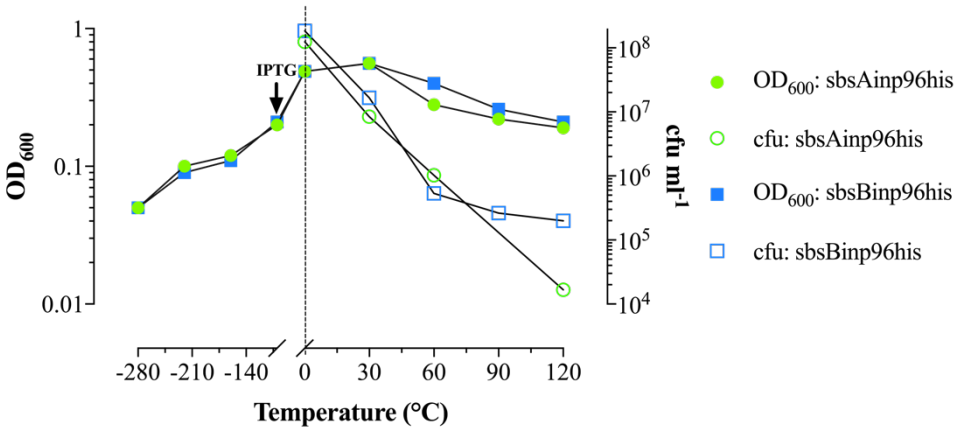

Figure 4. Growth and E-lysis of *E. coli* C41carrying plasmids for expression of SbsA-INP96His, SbsB-INP96His and BG production. *E. coli* C41 (pGLysivb, pUCsbsAinp96his) (green circle) and *E. coli* C41 (pGlysivb , pAKsbsBinp96his) (blue square) cultures were grown in LBv at 30°C and supplemented at an OD_{600} of 0.2 with 0.5 mM IPTG to induce expressions of S-layer fusion proteins. At an OD_{600} of 0.5 (referred as time point 0) the cultures were shifted to 42°C

4.5 Discussion

Despite the similar characteristics of AFP and INP they exhibit opposite effects. INPs are supposed to be larger forms of AFPs. Therefore, the C-terminal truncated InaZ variant INP288 (chapter 4.1) composed of the membrane anchoring N-terminal domain and a ~3 fold shortened repetitive domain was expressed in *E. coli* C41 followed by E-mediated lysis to produce INP288-BG with a LE of 99.76%

By droplet freezing assays the potential of AF activity could not be detected, as no freezing inhibition of ultra-pure water, compared to *E. coli* C41 and *E. coli* BGs could be monitored. Bacterial AFPs are characterized by their ability to inhibit ice crystal growth through TH activity (which is generally low compared to other AFPs, below 2°C) and/or inhibition of ice recrystallization [16, 17]. Therefore, nanoliter osmometer measurements for TH determination – which monitor the released latent heat during ice crystal growth to determine the freezing point depression[6] – combined with microscopic ice crystal analysis to determine ice recrystallization inhibition may be the method of choice to determine the possible AF activity of INP288. Furthermore, BGs as carriers of AFPs should be further investigated as there is a broad application spectrum, like agricultural or aquacultural frost damage, improvement of frozen food texturing, or deicing of surfaces.

In chapter 4.2 recombinant N-INP96H-BGs displaying INP96H on the BGs surface via fused N-terminal domain of InaZ were produced with a LE of 99.7%. Western blot analysis showed maintained N-INP96H signal detection during the whole lysis process. These data represent a successful BG surface display system using N-terminal domain of InaZ. Additionally, compared to the display system of insertional fused OmpA, the N-domain INP (NINP) anchoring system can be expressed at high levels without negatively influencing cell viability and enzymatic functionality[9, 18]. Therefore, the NINP display system could be widely used for the functional display of a broad spectrum of biocatalysts on the envelope surface of BGs. The OmpA outer-membrane targeting system has also been used to display INP96H on the surface of *E. coli* C41 BGs. However, using anti-His antibodies the recombinant OmpA could not be detected.

Plasmids (pUCsbsAinp96 and pAKsbsBinp96, see chapter 4.4) expressing INP96 integrated SbsA and SbsB have been constructed. BGs carrying SbsA-INP96 and SbsB-INP96 could be produced with a LE of 99.8 % and 99.9 %, respectively. However, the AFP AfpA of *P. putidia* G12-2 was reported to exhibit similarities to the amino acid sequence of S-layer proteins, and their Ca^{2+}-binding and N-glycosylation motifs [19]. Within the recombinant S-layer matrix – where INP96 is multiple embedded in the assembled two-dimensional lattice structure – INP96 is thought to function as ice-binding protein enhancing the ordering of water molecules for ice crystal growth.

4.6 References

1. **Green RL, Warren GJ.** 1985. Physical and functional repetition in a bacterial ice nucleation gene. Nature **317:**645-648.
2. **Graether SP, Jia Z.** 2001. Modeling Pseudomonas syringae ice-nucleation protein as a beta-helical protein. Biophys J **80:**1169-1173.
3. **Schmid D, Pridmore D, Capitani G, Battistutta R, Neeser J-R, Jann A.** 1997. Molecular organisation of the ice nucleation protein InaV fromPseudomonas syringae. FEBS Letters **414:**590-594.
4. **Davies PL.** 2014. Ice-binding proteins: a remarkable diversity of structures for stopping and starting ice growth. Trends Biochem Sci **39:**548-555.
5. **Garnham CP, Campbell RL, Walker VK, Davies PL.** 2011. Novel dimeric beta-helical model of an ice nucleation protein with bridged active sites. BMC Struct Biol **11:**36.
6. **Kobashigawa Y, Nishimiya Y, Miura K, Ohgiya S, Miura A, Tsuda S.** 2005. A part of ice nucleation protein exhibits the ice-binding ability. FEBS Lett **579:**1493-1497.
7. **Marshall CB, Daley ME, Graham LA, Sykes BD, Davies PL.** 2002. Identification of the ice-binding face of antifreeze protein from Tenebrio molitor. FEBS Lett **529:**261-267.
8. **Tsuda S, Ito A, Matsushima N.** 1997. A hairpin-loop conformation in tandem repeat sequence of the ice nucleation protein revealed by NMR spectroscopy. FEBS Lett **409:**227-231.
9. **van Bloois E, Winter RT, Kolmar H, Fraaije MW.** 2011. Decorating microbes: surface display of proteins on Escherichia coli. Trends Biotechnol **29:**79-86.
10. **Bassi AS, Ding DN, Gloor GB, Margaritis A.** 2000. Expression of single chain antibodies (ScFvs) for c-myc oncoprotein in recombinant Escherichia coli membranes by using the ice-nucleation protein of Pseudomonas syringae. Biotechnol Prog **16:**557-563.
11. **Hobom G, Arnold N, Ruppert A.** 1995. OmpA fusion proteins for presentation of foreign antigens on the bacterial outer membrane. Dev Biol Stand **84:**255-262.
12. **Kuen B, Koch A, Asenbauer E, Sara M, Lubitz W.** 1997. Molecular characterization of the Bacillus stearothermophilus PV72 S-layer gene sbsB induced by oxidative stress. J Bacteriol **179:**1664-1670.
13. **Kuen B, Sara M, Lubitz W.** 1996. Heterologous expression and self-assembly of the S-layer protein SbsA of Bacillus stearothermophilus in Escherichia coli. Mol Microbiol **19:**495-503.
14. **Kuen B, Sleytr UB, Lubitz W.** 1994. Sequence analysis of the sbsA gene encoding the 130-kDa surface-layer protein of Bacillus stearothermophilus strain PV72. Gene **145:**115-120.
15. **Baranova E, Fronzes R, Garcia-Pino A, Van Gerven N, Papapostolou D, Pehau-Arnaudet G, Pardon E, Steyaert J, Howorka S, Remaut H.** 2012. SbsB structure and lattice reconstruction unveil Ca2+ triggered S-layer assembly. Nature **487:**119-122.
16. **Scotter AJ, Marshall CB, Graham LA, Gilbert JA, Garnham CP, Davies PL.** 2006. The basis for hyperactivity of antifreeze proteins. Cryobiology **53:**229-239.
17. **Raymond JA, DeVries AL.** 1977. Adsorption inhibition as a mechanism of freezing resistance in polar fishes. Proc Natl Acad Sci U S A **74:**2589-2593.
18. **van Bloois E, Winter RT, Janssen DB, Fraaije MW.** 2009. Export of functional Streptomyces coelicolor alditol oxidase to the periplasm or cell surface of Escherichia coli and its application in whole-cell biocatalysis. Appl Microbiol Biotechnol **83:**679-687.
19. **Muryoi N, Sato M, Kaneko S, Kawahara H, Obata H, Yaish MW, Griffith M, Glick BR.** 2004. Cloning and expression of afpA, a gene encoding an antifreeze protein from the arctic plant growth-promoting rhizobacterium Pseudomonas putida GR12-2. J Bacteriol **186:**5661-5671.

5 Ethyleneimine (EI) inactivation of BG preparations

In most cases β-propriolactone (BPL) is used for inactivation of surviving E-lysis escape mutants from BG production[1]. In this study E-lysis escape mutants from BG preparations of *Bordetella bronchiseptica* (*Bb*) were investigated for inactivation using ethyleneimine (EI). The quality of EI inactivated BGs as vaccine candidate for kennel cough in dogs had to be immunogenetically compared to a commercial vaccine also inactivated with EI. Furthermore, inactivation of E-lysis escape mutants from INP carrying *E. coli* used for INP-BG production with EI had to be compared by their ability to catalyze ice nucleation (IN). As IN is dependent on structural integrity of INP this test more reflects changes induced by the inactivation agents EI or BPL itself and/or the procedure used.
All methods used in this chapter are described in section "Materials and Methods".

5.1 EI inactivation studies of *Bordetella bronchiseptica* BGs

Bordetella bronchiseptica BGs were produced and different concentrations of EI were tested for inactivation efficiency of surviving E-lysis escape mutants during BG production.

5.1.1 Results

Mid-scale fermentation in a working volume of 4l was performed to investigate growth and E-lysis performance of *B. bronchiseptica* 110H-EL carrying lysis plasmid pGlysivb in TPv supplemented with gentamycine (20 mg L^{-1}). Fermentation parameters were set at 35°C with a pH of 7.5 and a dissolved oxygen (dO_2) saturation level above 20% guaranteeing optimal conditions for exponential growth.
At an OD_{600} of ~0.5 (indicated at time-point 0 min) E-lysis of the *Bb* culture was induced by temperature up-shift from 35°C to 44°C (**Fig. 1**). The E-lysis phase continued for 360 min where the dO_2 level reached a value of > 75% (**Fig. 1**).
The growth and lysis of bacteria were monitored by measuring the OD_{600}, phase contrast microscopy and by determination of colony forming units (cfu) analysis (**Fig. 2 and Fig. 3**). The efficiency of E-lysis from time of lysis induction up to 360 min lysis time was determined by cfu analysis (**Fig. 2**) and amounts to 98.8 %. Phase contrast microscopy of *Bb* BGs at end of lysis showed a typical empty cell appearance as seen in most BG preparations (**Fig. 3**).

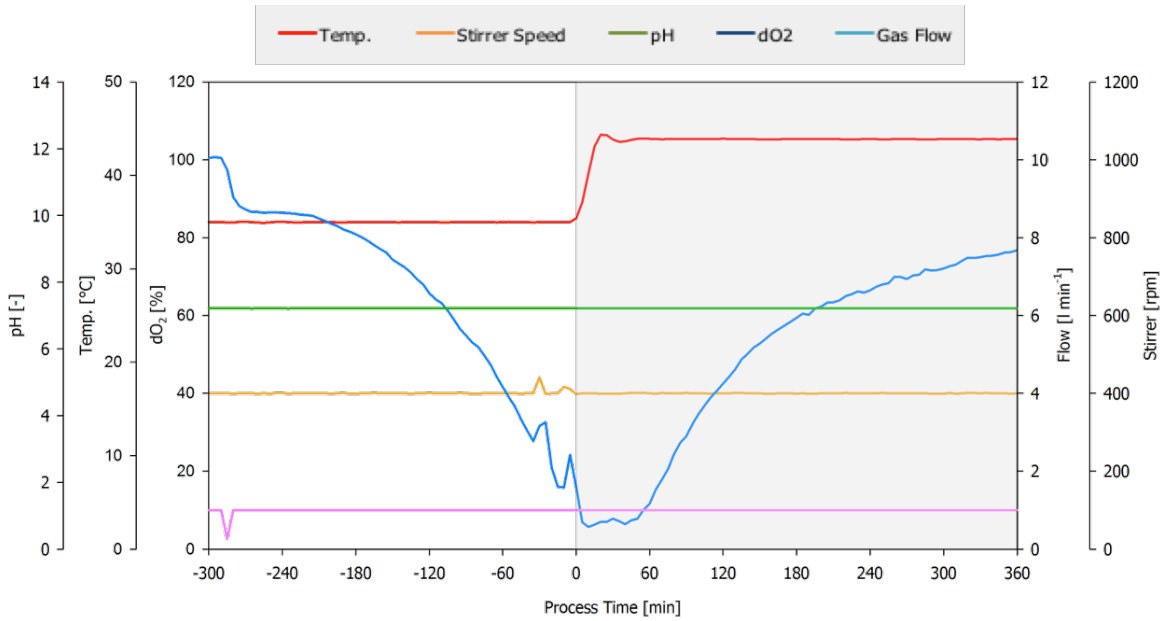

Figure 1. Fermentation protocol for BG production of *B. bronchiseptica* 110H-EL carrying lysis plasmid pGlysivb. All relevant process parameters are monitored during growth- and E-lysis-phase. Temperature: red line; stirrer speed: orange line, pH: green line; dO_2: blue line; gas flow: turquoise line. E-mediated lysis is induced by a temperature up-shift from 35°C to 44°C indicated as time-point 0 min.

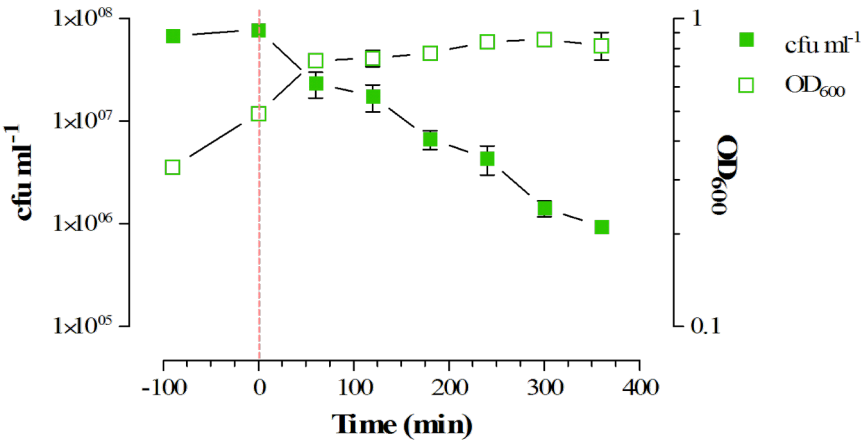

Figure 2. Growth and E-lysis performance of *B. bronchiseptica* 110H-EL (pGlysivb) during BG production. At time point zero (illustrated by vertical sketched line) E-mediated lysis was induced from pGLysivb by temperature shift from 35°C to 44°C. Open symbols indicate OD_{600} values of growth and lysis phase. During E-lysis colony forming units (closed symbols) were determined to calculate lysis efficiency. After 360 min BG production was completed. Data were obtained from three independent experiments. Error bars indicate standard errors.

After a lysis-phase of 360 min the cells were washed with 4 liters of dH_2O using Tangential Flow Filtration (TFF), concentrated to a final volume of ~400 mL and harvested. The amount of E-lysis escape mutants of the harvest was determined by cfu analysis.

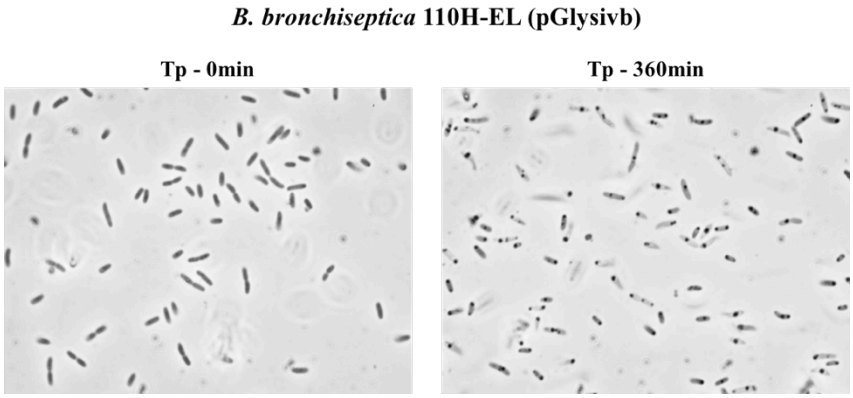

Figure 3. Light microscopy pictures of *B. bronchiseptica* 110H-EL (pGlysivb) at time point of E-lysis induction (Tp - 0min) and endpoint of E-mediated lysis after 360 min.

For evaluation of EI inactivation efficiency (IE) the *B. bronchiseptica* 110H-harvest was aliquoted á 50 ml into 250 ml Erlenmeyer-flasks and treated with different concentrations of EI (1mM, 2mM, 3mM, 4mM, 6mM, 8mM, 10mM) and incubated for six hours at 35°C with agitation. Every hour EI treated bacteria were checked for viability by plating serial 10-fold dilutions of the bacteria on TPv agar plates in duplicate. Already after an hour inactivation using EI concentrations of 10mM to 6mM no viable *B. bronchiseptica* 110H (pGLysivb) E-lysis escape mutant could be detected (**Table 1.**). With concentrations of 4mM and 3mM EI two hours of inactivation time were needed for full inactivation (**Table 1.**). Whereas for bacteria treated with 2mM EI it took three hours, respectively five hours for bacteria treated with 1mM EI for complete inactivation (**Table 1.**).

	Inactivation efficiency (IE) in cfu/ml ± SD						
EI concentration:	10mM	8mM	6mM	4mM	3mM	2mM	1mM
living E-lysis escape mutants (cfu/ml):	8.8E+06	8.8E+06	8.8E+06	3.2E+06	3.2E+06	3E+06	3E+06
inactivation time (h)							
1	0	0	0	2.5E+00 ± 1.9E+00	2.5E+00 ± 1.9E+00	2.5E+00 ± 1.9E+00	n.d.
2	0	0	0	0	2.5E+00 ± 1.9E+00	2.5E+00 ± 1.9E+00	n.d.
3	0	0	0	0	0	0	9.1E+02 ± 1.6E+02
4	0	0	0	0	0	0	3.8E+02 ± 2.0E+02
5	0	0	0	0	0	0	0
6	0	0	0	0	0	0	0

Table 1. Average numbers of EI inactivation efficiency (IE) of *B. bronchiseptica* 110H-EL (pGlysivb) BGs after TFF washing and concentration using different concentrations of EI. Data were obtained from three independent experiments. SD: standard deviation; n.d.: not determinable.

5.2 Ice nucleation activity of EI treated BGs carrying ice nucleation protein InaZ

In chapter 2.3 the effect of the two different inducible E-lysis plasmids (pGLMivb and pGLysivb) – used for production of IN active *E. coli* BGs – were tested for the effectiveness of ice nucleation. Here the impact of ethyleneimine (EI) in its binary form – used for inactivation of any surviving E-lysis escape mutants during BG production – on *E. coli* INP-BGs nucleation activity is compared to the ice nucleation spectrum of BPL treated INP-BGs described in chapter 2.3. EI acts in the same mode of action as BPL by alkylating nucleic acids by modification of purines resulting in replication arrest and is widely used in virus vaccine production and has been reported not to harm proteins [(2-5)]. Moreover, EI has been demonstrated to fully inactivate *Shigella flexneri* without limiting the antigenic and immunogenic quality of their outer membrane vesicles [(6)].

5.2.1 Results

The half volume of the E-lysed *E. coli* C41 (pBINP, pGLMivb) and *E. coli* C41 (pBINP, pGLysivb) culture – produced for ice nucleation activity measurements of BPL treated INP-BGs– was used to inactivate any surviving E-lysis escape mutants from INP-BG production (INP-BG-pLM and INP-BG-pLy) with EI. After washing of E-lysed *E. coli* C41 (pBINP, pGLMivb) and *E. coli* C41 (pBINP, pGLysivb) EI (6 mM final conc.) was added to the washed harvest and kept for 120 min at 35°C. Afterwards EI was inactivated by addition of 1 M sodium thiosulfate at 10% of initial volume of EI used and kept for 30 min at 35°C, followed by another washing step with 3 x Vol of Rotisolve H_2O. Western blot analysis was performed to detect the presence of expressed INP after treatment with EI (**Fig.1**).

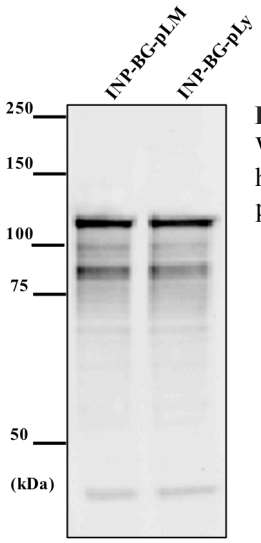

Figure 1 Western blot analysis of EI-treated INP-BG-pLM and INP-BG-pLy samples. Western blotting was performed with rabbit anti-H-NINP serum and anti-rabbit IgG horseradish peroxidase conjugated antibodies. Positions of molecular size marker proteins are indicated in kilodalton (kDa).

The detected protein pattern and signal intensity of the crucial detected bands showed no deviation compared to Western blot analysis performed with BPL-treated ina$^+$ BGs in chapter 2. Full length INP

was visible at 120 kDa as well as the additional minor band at 87 kDa representing most probably a degradation product of INP.

Out of the EI treated INP-BG-pLM and INP-BG-pLy samples ice-nucleating activity was determined by a droplet-freezing assay. Both ina$^+$ BG samples were adjusted to a concentration of 5 x 10^8 cells/ml and freezing temperatures of the tested droplets plotted against the temperature was used to determine the median freezing temperature T_{50} (**Fig. 2A** and **Fig. 2B**). INP-BG-pLM showed first freezing events starting at -6°C (**Fig. 2A**) and the T_{50} value was calculated to be at -6.6°C (**Fig. 2A** and **Fig. 2B**). For the tested droplets containing INP-BG-pLy first freezing event (one droplet out of 45 droplets) was detected at -8°C (**Fig. 2A**) and a T_{50} value of -9.7°C was calculated (**Fig. 2A** and **Fig. 2B**).

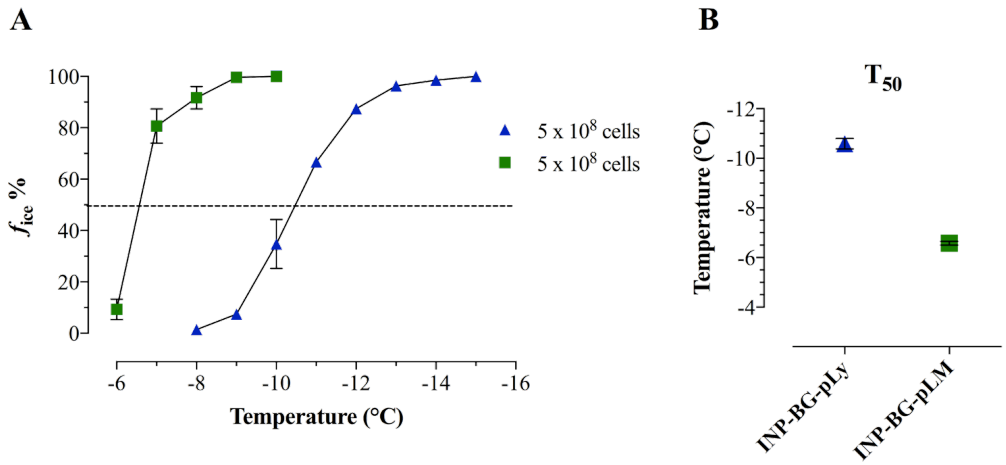

Figure 2. Average number of freezing spectra (**A**) and median freezing temperatures (T_{50}) (**B**) of INP-BG-pLM (■) and INP-BG-pLy (▲)**A.** Ice nucleation curve plotted as number fraction of frozen droplets in percent (f_{ice} %) at any temperature. **B.** T_{50}, temperature where 50 % of all droplets are frozen. Forty-five 10 µl droplets of each suspension containing 5x 10^8 cells ml^{-1} were tested by droplet freezing. Average numbers are obtained from three independent experiments. Error bars represent the standard errors.

Cumulative ice nucleation spectra (**Fig. 3A** and **Fig. 3B**) of the IN active BG samples were obtained by determining the freezing spectra of a series of tenfold dilutions from each suspension. The nucleation spectra are described as cumulative number N(T) of ice nuclei ml^{-1} active at a given temperature (**Fig. 3A**) and normalized N(T) (with the number of cells in the original suspension) resulting in the nucleation frequency (NF) (**Fig. 3B**). The lowest NF for INP-BG-pLM detected at -6°C was 3.7 x 10^{-8} and raised up to 3.2 x 10^{-6} at -7°C. With further temperature decrease the NF for INP-BG-pLM increased from 5.1 x 10^{-6} at -8°C to 1.4 x 10^{-4} at -13°C. On the other hand, for INP-BG-pLy samples the lowest determinable NF (2.3 x 10^{-9}) was detected at -8°C and increased to 2.5 x 10^{-5} at -9°C. With further decrease in temperature down to -13°C, NF of INP-BG-pLy increased a little up to 1.7 x 10^{-4}, where the NF of both ina$^+$ BGs was nearly identical.

Nucleation frequencies of INP-BG-pLM and INP-BG-pLy treated with BPL and EI at several temperature points are summarized in **Table 1**.

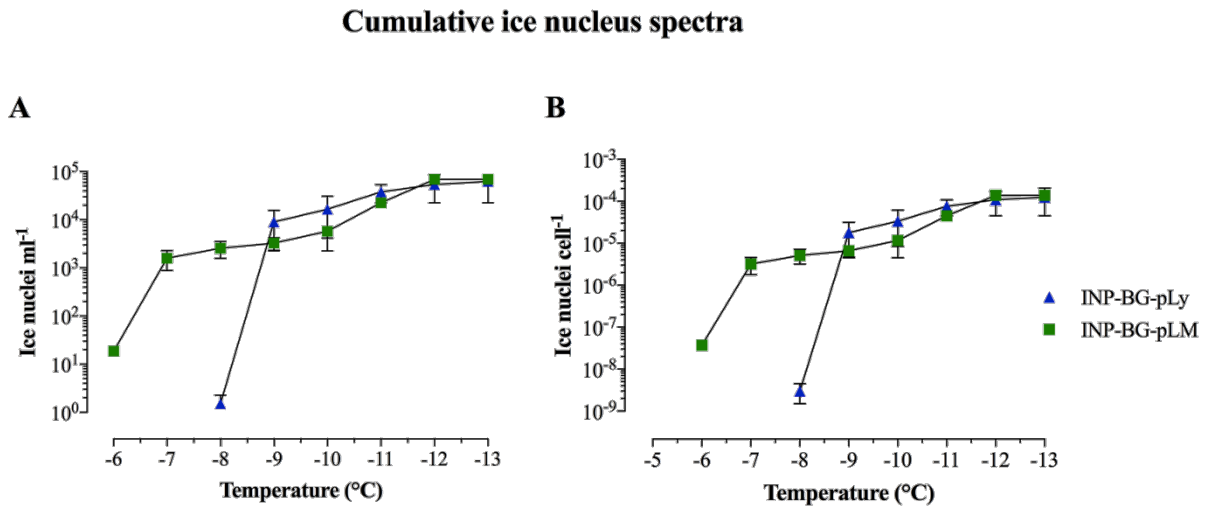

Figure 3. Cumulative ice nucleation activity for EI- treated INP-BG-pLM (■) and INP-BG-pLy (▲). **A.** Average Number of ice nuclei ml^{-1} at a given temperature N(T). **B.** Average of Nucleation frequency (NF) expressed as ice nuclei $cell^{-1}$. Data obtained from three independent experiments. Error bars represent the standard errors.

Both BPL treated INP-BG samples (INP-BG-pLM and INP-BG-pLy) showed a very close T_{50} value of -6.9°C and -6.7°C respectively, with first freezing events starting at -6.0°C with a nucleation frequency of 3 x 10^{-8} for INP-BG-pLM and 1.9 x 10^{-7} for INP-BG-pLy. As the temperature decreased from -6°C to -8°C, the total number of ice nucleation active sites per cell at -8°C for BPL treated INP-BG-pLM and INP-BG-pLy reached 1.2 x 10^{-4} and 3.8 x 10^{-5}, respectively. At a temperature of -10°C both types of BPL treated INP-BGs exhibit closer NF activity values of 1.6 x 10^{-4} for INP-BG-pLy and 3 x 10^{-4} for INP-BG-pLM. With further decrease in temperature down to -13°C, NF of INP-BG-pLM and INP-BG-pLy was 6.3 x 10^{-4} and 6.4 x 10^{-4}.

		-6°C		-7°C		-8°C		-10°C		-13°C	
	T_{50} (°C)	N(T)	NF	N(T)	NF	N(T)	NF	N(T)	NF	N(T)	NF
BPL-treated ina$^+$ BGs											
INP-BG-pLM	-6.9	1.5 x 10^1	3.0 x 10^{-8}	2.5 x 10^4	5.0 x 10^{-5}	6.2 x 10^4	1.2 x 10^{-4}	1.5 x 10^5	3.0 x 10^{-4}	3.1 x 10^5	6.3 x 10^{-4}
INP-BG-pLy	-6.7	9.5 x 10^1	1.9 x 10^{-7}	3.2 x 10^3	3.3 x 10^{-6}	1.9 x 10^4	3.8 x 10^{-5}	7.8 x 10^4	1.6 x 10^{-4}	3.2 x 10^5	6.4 x 10^{-4}
EI-treated ina$^+$ BGs											
INP-BG-pLM	-6.6	1.9 x 10^1	3.7 x 10^{-8}	1.6 x 10^3	3.2 x 10^{-6}	2.6 x 10^3	5.1 x 10^{-6}	5.8 x 10^3	1.2 x 10^{-5}	6.9 x 10^4	1.4 x 10^{-4}
INP-BG-pLy	-9.7	n.d.	n.d.	n.d.	n.d.	1.1	2.3 x 10^{-9}	2.4 x 10^4	4.8 x 10^{-5}	8.3 x 10^4	1.7 x 10^{-4}

Table 1. Summary of the average ice nucleation frequencies at different temperatures of BPL- and EI-treated ina$^+$ BGs from chapter 2.3 and 5.2. T_{50} (°C): temperature where 50 % of all droplets are frozen; N(T): the cumulative number of ice nuclei ml^{-1}active at a given temperature; NF: nucleation frequency expressed as ice nuclei $cell^{-1}$; n.d.: not determinable.

5.3 Discussion

For the first time BGs were successfully produced from the animal pathogen *B. bronchiseptica* (*Bb*)with an E-mediated lysis efficiency of 98.8 %. Also for the first time ethyleneimine (EI) was used to inactivate E-lysis escape mutants from a BG production. Inactivation efficiency of different EI concentrations was tested and the obtained data agrees with already published results *Shigella flexneri* and *Pasteurella haemolytica* that low concentrations of EI are sufficient for full inactivation of bacteria [6, 7].

The ice-nucleation spectra of EI treated *E. coli* C41 INP-BG-pLM and *E. coli* C41 INP-BG-pLy were determined and the data were compared with the ice-nucleation spectrum of BPL-treated *E. coli* C41 INP-BG-pLM and *E. coli* C41 INP-BG-pLy. The freezing spectra of BPL- and EI-treated INP-BG-pLM exhibit no significant differences in their freezing spectra as both showed first freezing activity at -6°C and 100 % of frozen droplets were detected at -10°C, resulting in a T_{50} value of -6.9°C and -6.6°C for BPL- and EI-treated INP-BG-pLM, respectively. However, the cumulative concentration of ice nucleation active type II IN active BGs – which are ice active down to -7°C – compared to the BPL-treated INP-BG-pLM obtained a ~16-fold reduction when BG samples were treated with EI. This reduction indicates a significant impact of EI treatment on ice nucleation sites. The same observations are valid for typ III ina^+ INP-BG-pLM, which are ice nucleation active below -7°C. A ~28-fold reduction in NF at -10°C of EI-treated INP-BG-pLM was detected compared to the BPL-treated samples.

Even a higher discrepancy in nucleation activity was observed between BPL- and EI-treated *E. coli* C41 INP-BG-pLy. The EI-treated samples fully lost their typ II activity resulting in a T_{50} value of -9.7°C. The nucleation frequencies of typ III acting *E. coli* C41 INP-BG-pLy treated with EI were reduced ~3-fold compared to BPL- treated *E. coli* C41 INP-BG-pLy.

Although the INP protein could be detected via Western blot analysis in both EI- treated *E. coli* C41 INP-BG versions without any differences regarding signal intensity or migration behavior, the treatment with EI for inactivation of E-lysis escape mutants during BG production led to a considerable reduction in nucleation frequency compared to their BPL-treated samples.

EI has been shown to alkylate viral glycoproteins when used at high concentrations [8]. As ice nucleation active type II INP of *P. syringae* is defined as a glycoprotein [9, 10], alkylation of ina^+ BGs INP might cause the decreased nucleation activity compared to BPL-treated ina^+ BGs.

5.4 References

1. **Langemann T, Koller VJ, Muhammad A, Kudela P, Mayr UB, Lubitz W.** 2010. The Bacterial Ghost platform system: production and applications. Bioeng Bugs **1:**326-336.
2. **Aarthi D, Ananda Rao K, Robinson R, Srinivasan VA.** 2004. Validation of binary ethyleneimine (BEI) used as an inactivant for foot and mouth disease tissue culture vaccine. Biologicals **32:**153-156.
3. **Bahnemann HG.** 1976. Inactivation of viruses in serum with binary ethyleneimine. J Clin Microbiol **3:**209-210.
4. **Bahnemann HG.** 1990. Inactivation of viral antigens for vaccine preparation with particular reference to the application of binary ethylenimine. Vaccine **8:**299-303.
5. **Brown F.** 2001. Inactivation of viruses by aziridines. Vaccine **20:**322-327.
6. **Camacho AI, Souza-Reboucas J, Irache JM, Gamazo C.** 2013. Towards a non-living vaccine against Shigella flexneri: from the inactivation procedure to protection studies. Methods **60:**264-268.
7. **Bauer K, Wittmann G, Mussgay M, Irion E, Geilhausen H.** 1977. Ethyleneimine inactivated microorganisms. US patent 4036952.
8. **Broo K, Wei J, Marshall D, Brown F, Smith TJ, Johnson JE, Schneemann A, Siuzdak G.** 2001. Viral capsid mobility: a dynamic conduit for inactivation. Proc Natl Acad Sci U S A **98:**2274-2277.
9. **Kozloff LM, Turner MA, Arellano F.** 1991. Formation of bacterial membrane ice-nucleating lipoglycoprotein complexes. J Bacteriol **173:**6528-6536.
10. **Turner MA, Arellano F, Kozloff LM.** 1991. Components of ice nucleation structures of bacteria. J Bacteriol **173:**6515-6527.

5.5 Manuscript II. *Bordetella bronchiseptica* Bacterial Ghost vaccine for canines

Abbas MUHAMMAD [1], Johannes KASSMANNHUBER [1], Alaric A. FALCON [2], Marek SRAMKO[1], David W. WHEELER [2], Alan A. ZHANG [2], Petra LUBITZ [1], Werner LUBITZ [1]

[1] BIRD-C GmbH & Co KG, Dr. Bohrgasse 2-8/14/1, A-1030 Vienna, Austria
[2] ELANCO Animal Health, 2500 Innovation Way Greenfield, IN - 46140, United States of America

Abbreviations

Ag, antigen; APCs, antigen-presenting cells; BB, bacterial backbone; *Bb*, *Bordetella bronchiseptica*; *Bb*BG*, Bordetella bronchiseptica* bacterial ghosts; BGA, Bordet Gengou agar; BGs, Bacterial Ghosts*; Bp*, *Bordetella pertussis*; *Bpp*, *Bordetella parapertussis*; CIRD, chronic inflammatory respiratory disease; EI, ethyleneimine; IM, intra muscular; IN, intra nasal; MAT, Micro Agglutination Test; pO_2, saturated oxygen; SC, subcutaneous; TFF, tangential flow filtration; TLR, Toll-Like receptors; TP, Tryptose phosphate; TPv, Tryptose phosphate vegetable source.

5.5.1 Contribution to Manuscript II

Abbas Muhamad (AM) and Johannes Kassmannhuebr (JK) the first two authors of the manuscript contributed equally to the work performed. AM was in charge of the genetic constructions and JK for the *Bordetella bronchiseptica* fermentation procedure for BG production. All other authors were involved in conceptual work and organization of the animal studies.

5.5.2 Manuscript II (style *Vaccine* to be submitted)

For the sake of clarity and legibility the figures and tables were inserted near the respective text area. In order to maintain a uniform bibliography in the thesis, the references are given here in *ASM Journals* style.

Abstract

Objective: This study was designed to evaluate the safety and efficacy of experimental parenteral *Bordetella bronchiseptica* Bacterial Ghost vaccines (*Bb*BG) in dogs.

Animals: Thirty-two *B. bronchiseptica* seronegative dogs divided into 4 equal treatment groups

Study Design and Procedure: Dogs were randomly assigned to one of the four treatment groups; T01-T04 (un-vaccinated control, vaccinated control Bronchicine CAe, *Bb*BG – 7 and *Bb*BG – 5) respectively. Dogs were vaccinated subcutaneously SC on day 0, and 21. Systemic and injection site reactions were monitored after both vaccination doses. Nasal swabs were collected from each dog prior to challenge and on every second day after challenge on study days 41 and 44 through 54. These swabs were used to determine *Bordetella bronchiseptica* (*Bb*) sheading. Serum samples for serological studies were collected prior to first vaccination, prior to second vaccination, prior to challenge and on the last day of the study (Day54). The animals were challenged (by aerosol) with virulent *Bb* strain on study day 42. Following challenge, clinical observations (coughing, nasal and conjunctival discharges) were made daily over period of 12 days.

Results: Dogs vaccinated with positive control (Bronchicine CAe) or newly developed *Bb*BG – 7 vaccine demonstrated significant protection from spontaneous coughing, duration of coughing, and induced coughing scores when compared to placebo treated dogs.

Conclusions: The *Bb*BG – 7 vaccine conferred significant protection in the face of a severe bacterial challenge. The *Bb*BG – 7 vaccine was equivalent to the positive control vaccine in terms of safety and efficacy. The new *Bb*BGs were stable in liquid formulation for several months.

Introduction

A gram-negative aerobic coccobacilli, *Bordetella bronchiseptica (Bb)* is widely known for causing canine infectious respiratory disease (CIRD) [(1)]. *Bb* is capable to cause clinical condition in several mammals like dogs (kennel cough), rabbits, guinea-pigs (pneumonia) and swine (atrophic rhinitis) [(2-10)]. It is reported in various papers that *Bb* along with *Bordetella pertussis (Bp)* and *Bordetella parapertussis (Bpp)* may cause whooping cough in immune compromised humans. Several cases of *Bb* infection in humans are reported in individuals with history of close contact with infected dogs or recently vaccinated with live attenuated *Bb vaccine* [(9-13)]. *Bb* colonizes the ciliated respiratory epithelium of dogs and cats and is not found in other body tissues [(14)]. Due to its colonization the canine respiratory cilia's loses their beating motion so quickly that within 3 hours of phase I or

intermediate phase *Bb* infection almost 100% of ciliary activity is lost [15]. Due to this ciliostasis the respiratory epithelia of dogs are more prone to secondary viral and bacterial infections [1, 14, 15]. *Bb* infection is endemic in many non-human mammalian populations [16] and therefore several whole cell bacteria [17], recombinant purified protein [18] and combination intranasal (IN) modified-live vaccines [19] have been tested in dogs successfully.

Bacterial Ghost (BG) system is an advanced approach for production of safe and potent vaccines for prevention and control of a wide range of infectious diseases [20-22]. BGs are produced by expression of cloned gene *E* of bacteriophage ΦX174 under tight regulation [21-25]. Protein *E* expression initiates the formation of a trans-membrane tunnel structure spanning the whole cell envelope, through which the entire cytoplasmic content is expelled. This expulsion of cytoplasmic content is due to the change in osmotic pressures between the cell interior and the culture medium [26]. These resulting empty bacterial cells have wide range of use, as a vaccine or a delivery vehicle for delivering other immunogens or biological active substances [27, 28]. BGs have advantage over other inactivated non-living vaccines in terms of efficacy as all of the surface structural components of the BG envelope are non-denatured and remain intact [29]. The process of producing BGs is lenient and does not harm the essential structural components of the bacteria giving raise to immunologically active particles that are capable to stimulate the host immune system and deliver specific antigens (Ag) to professional antigen presenting cells (APCs) through pattern-recognition receptors, making them ideal for parenteral and mucosal administration [30-33]. Production of BGs is an efficient, stable and safe process resulting in freeze dried vaccine preparations which are stable at ambient temperatures for many months [34].

Material and Methods

Bacterial Ghost Vaccine production

Bacterial strain plasmids and growth conditions

Bordetella bronchiseptica strain 110H was provided by Elanco Animal Health, Eli Lilly, Indianapolis U.S.A. The bacteria were grown on Tryptose Phosphate Agar (TPA) (Difco Laboratories, US) and or on Bordet Gengou Agar plates (BGA) (Difco Laboratories US) supplemented with 15% defibrinated sheep blood (VWR international – ROCKR111-0050) and incubated at 36°C for 24 – 36 hrs. For transformation lysis plasmid pGLysivb [34] was used in which the expression of lysis gene *E* is driven by the λPR_{mut} – c*I*857 promoter-repressor system to regulate the lysis gene *E* expression by temperature up-shift from 36°C to 42°C. Plasmid pBBR1MCS-5 [35] is a broad host range cloning vector and was used for construction of lysis plasmid pGLysivb. Plasmid pBBR1MCS-5 lacking the lysis gene *E* was used for control experiments. For bacterial selection, gentamycin was used at final concentration of 20 µg / mL. Both of the above mentioned plasmid DNA were isolated from *E. coli* C2988J using Pure Yield Plasmid Midiprep system (Promega) using the manufacturers protocol. The identity of the obtained plasmid DNA was confirmed by restriction enzyme analysis using FastDigest® restriction enzymes (Fermentas). The purity and quantity of plasmid DNA was evaluated using NanoDrop ND-2000 (PeqLab).

Electro competent cell preparation and transformation procedure

The electroporation experiments were performed as described by Miller [36] with slight modifications. For production of competent cells, *Bordetella bronchiseptica* 110H was grown on BGA plates (supplemented with 15% sheep blood) for ~16 hrs at 36°C after which the cells were harvested in ice cold GlySuc buffer (15% Glycerol and 272 mM Sucrose solution) and pelleted at 5000 x g for 10 min at 0°C. The cells were gently resuspended and washed in half volume of GlySuc buffer (same conditions as above) followed by wash with ¼ volume of GlySuc buffer. Cells were resuspended gently in 300 – 500 µL of GlySuc buffer (depending on the size of pellet) and aliquoted in ~100 µL to be used immediately for electroporation or store at -80°C for later use. 1 – 3 µg of isolated plasmid DNA (pGLysivb or pBBR1MCS-5) was added to the 100 µL aliquot of competent cells and the mixture was incubated on ice for 45 – 60 min. High voltage pulses were delivered to the ice cold

samples that are shifted to 1 mm gap cuvettes (PeqLab). Genepulser® II, Electroporation system (Bio-Rad) was used with following settings: 2.5 Kv, 25 F, 400 Ω with time constraint ranging from 3.5 – 7 ms. Following the electroporation the cells were regenerated by addition of 800 µL of Tryptose Phosphate (TP) broth (Difco Laboratories) and incubated at 34°C for 90 min. The regenerated cells were then platted on TP-agar plates (Difco Laboratories), supplemented with 20 µg / mL of gentamycin. Screening of positive recombinant strains were performed via restriction enzyme digestion (Fermentas).

Growth Media.

Cells were grown in Tryptose Phosphate broth – vegetable source (TPv) (Difco Laboratories), supplemented with 0.004 g / L nicotinic acid, 0.02 g / L $FeSO_4 7.H_2O$ and 0.02 g / L ascorbic acid.

Bordetella bronchiseptica Bacterial Ghost production

The medium scale fermentation of *B. bronchiseptica* 110H were performed in Labfors 3 fermenter (Infors Ag, Bottmingen, Switzerland) with working volume of 4 liters. Medium scale fermentation was performed in TPv supplemented with gentamycin at 20 mg / liter. Five mL of 30 hours culture of *B. bronchiseptica* 110H (carrying lysis plasmid pGLysivb) was used to prepare 200 mL pre-culture (35°C for 12 – 14 hours). This pre-culture with the OD_{600nm} of 1.15 was used to inoculate the fermenter containing 3.8 litters of TPv to get starting OD_{600nm} of 0.052. The cells were grown to OD_{600} of ~0.5 at 35°C and the lysis was induced by temperature upshift to 44°C. The lysis was complete after 420 min after which the lysed cells were washed to get rid of the cytoplasmic contents using 4 liters of sterile dH_2O using Tangential Flow Filtration (TFF) module (0.2µm cut-off, GE healthcare) for 60 min. This was accomplished by matching the flow of media out of the TFF module with the same amount of dH_2O pumped into the fermenter. During the course of fermentation following parameters were documented: temperature, flow, stirrer, pH, pO_2, foaming and pumps for acid and base. Antifoam-A (Sigma) was added via sterile septum when needed. After the completion of washing, the broth was concentrated to approximately 200 mL in TFF module (0.2 µm cut, GE, healthcare) and flushed from the module with ~200 mL sterile dH_2O into the "inactivation bottle" to get a final volume of ~400 mL (conc. I).

Final Inactivation and vaccine storage

Due to regulatory requirements for veterinary vaccines by United States Department of Agriculture (USDA) and European Medicines Agency (EMA), the remaining un-lysed cells or escape mutants are inactivated / killed by one of the prescribed chemical procedures [37]. To fulfil the above requirement, ethyleneimine (EI) was used. A final concentration of 20 mM EI (FERAK, Berlin) was added to conc. I and incubated for 3 hrs with slight agitation at 35°C (2 mM, if calculated for initial volume of 4 liters before concentration). Samples for *cfu* count and microscopy were drawn hourly and the inactivation activity was halted by addition of 1 M sodium thiosulfate, at 10% of initial volume of EI used and kept for another 30 min at 35°C, while shaking. The inactivated sample was washed with 4 liters of sterile dH_2O using a fresh TFF module (sterile 0.2 µm cut-off, GE, healthcare). This was accomplished by matching the flow of media out of the TFF module, with the same amount of dH_2O pumped into the inactivation bottle. Later the broth was concentrated to ~200 mL, before being flushed out of the module with ~200 mL sterile dH_2O to bring the volume to ~400 mL (conc. II). This sample was stored at -20°C for approx. 15 days, and were later thawed, and resuspended in dH_2O for final dose defining and shipped in liquid form at +4°C, for animal experiments. The animals were vaccinated with *Bb*BG vaccine approximately after three months of liquid formulation which was shipped and stored at +4°C upon arrival.

Animals and animal housing

Thirty-two *Bb* seronegative dogs (beagles 7 wk old) were selected and housed in the research facility at Ridglan farms for the vaccination phase (8 wk old) and later at BSL-2 facility of the University of Wisconsin for the challenge phase (14 wk old). Blood samples from all animals were collected prior to inclusion in the study. Serum was separated from the blood and used to determine antibody titers against *Bordetella bronchiseptica.* A dog was considered sero-negative with a titer of < 4 by Micro Agglutination Test (MAT). The test was run by the University of Wisconsin according to their prescribed standards. The study animals were randomly assigned to one of the treatment groups - T01 – T04 with (n=8) animals per treatment group. The randomization was performed by the study statistician. Animals in each group were assigned unique identification codes and ear tattooed for easy record. The puppies in different treatment groups were three-housed in stainless steel caging at

Ridglan farms during vaccination phase and gang housed during the challenge phase at (bio safety level-2) BSL-2 facility of University of Wisconsin as prescribed in "*Guide for Care and Use of Laboratory Animals*" by the regulatory bodies [38]. Animals were fed with high density canine diet 5L18 PMI nutrition international LLC or similar quality diet and had access to water *ad libitum* in both facilities. Since *Bordetella bronchiseptica* is infectious bacteria, strict isolation procedures were used during the challenge phase at University of Wisconsin in BSL-2 facility.

Study design and study vaccine

The dogs were moved to the vaccination facility at Ridglan farms on study day -7, study animals were observed daily to determine general health status by qualified veterinarian to ensure that the subjects are free of any kind of respiratory diseases. Observations were made at approximately the same time each day and were documented on the HOR. Animal health observations consisted of cage side visual assessments of animals for indicators of animal health. Since the shedding of *Bordetella* is of epidemiological interest in this disease, nasal swabs were collected at day -1 and 20 from all dogs before 1st and 2nd vaccinations occurred and on day 41 through 44, 46, 48, 52 and 54. Two swabs were collected from each dog, one from each nostril. The swab samples were used for quantitative PCR and *Bb* culturing. Similarly, serum samples were used to monitor *Bb* titers. Blood samples were collected from Jugular / cephalic vein in 4 mL serum separation tube (SST) before each vaccination; day -1 and 20, before challenge; day 41 and at the end of study; day 54.

Dogs were randomly assigned to four (04) treatment groups - T01 to T04. Group –T01 dogs were used as negative control (PBS). Group –T02 dogs were used as positive control and vaccinated with commercially available vaccine - Bronchicine CAe. Group –T03 dogs were vaccinated with 1 x 10^7 *Bordetella bronchiseptica* Bacterial Ghosts (*BbBG – 7*) and Group –T04 dogs were vaccinated with 1 x 10^5 *Bordetella bronchiseptica* Bacterial Ghosts (*BbBG – 5*) (**Table 1.**).

Table 1. Study design and groups

Treatment group	Experimental biological product and (estimated dose)	No. of animals	Route of administration	Challenge
T01	PBS (Negative Control)	8	s/c	*B. bronchiseptica*
T02	Bronchicine CAe (Positive Control)	8	s/c	*B. bronchiseptica*
T03	*Bb*BG – 7 (~1 x 10^7 BG particles)	8	s/c	*B. bronchiseptica*
T04	*Bb*BG – 5 (~1 x 10^5 BG particles)	8	s/c	*B. bronchiseptica*

All animals in different treatment groups were injected with 1 mL of respective test material. Vaccines were administered on day 0 and again on day 21. All vaccines were administered subcutaneously in the interscapular region (between the shoulder blades at the base of neck). First vaccination was on the right side, and the second vaccination was given on the left side. A patch of hair was clipped prior to vaccination at the injection site so that it was easier to examine the dogs for injection site reactions. Latex examination gloves were worn by all personnel during the vaccination. Gloves were changed regularly after handling each dog to avoid chances of cross contamination. Dogs were monitored for systemic and or local injection site reactions after each vaccination. Examinations occurred at ~4, ~24, ~48, ~72 hours post vaccination. Monitoring consisted of mainly temperature, general attitude / behavior and for injection site reactions in dogs. For reactions present at the 3 day post-vaccination examination, monitoring was continued daily until the reaction was resolved.

Challenge and clinical observations

The challenge was conducted by study investigators and technicians under the supervision of investigator. Four dogs were challenged at a time. All vaccinated dogs including the unvaccinated control (T01) were exposed to the challenge (aerosolized *Bordetella)* for 20 min in an isolator cag. The challenge dose was ~10mL at target conversation of 1 x 10^8 CFU/m^3. Nebulizer was used for ~15 - 20 min in 1m^3 isolator cage. Baseline challenge clinical observations were made on study day 42, prior to challenge. The study animals were observed daily after challenge beginning of study day 43 and continuing through study day 54. Clinical observations were made approximately the same time each day. These observations consisted of 20 minutes in-room visual assessments of animals for

clinical signs of *B. bronchiseptica*. Clinical signs included, but were not limited to, the following: coughing, retching, +/- labored breathing.

At the conclusion of the 20 min observation period, each dog was observed for nasal and conjunctival discharge. Labored breathing was noted if present. After which animals were administered mild laryngeal palpation for induced coughing signs. This consisted of placing a thumb and forefinger on either side of the larynx was sufficient to move the skin up and down with the palpation, without causing undue pressure.

Bacteriologic culture

To quantitate growth of *B. bronchiseptica* in swab samples, selective culture methods [(39)] and standard semi quantitative techniques were used [(40)]. Briefly, swab specimens from the nasal cavity were inoculated onto 1 quadrant of Mc-Conkey and peptone agar plates. A sterile bacteriologic loop was then used to sequentially streak the 4 quadrants of each plate without flaming the loop until all quadrants were streaked. Plates were incubated at 37°C and checked at 24 and 48 hours for growth of microorganisms. Suspicious colonies (i.e., organisms that grew as non-lactose fermenters on Mc-Conkey's agar and as blue colonies on peptone agar) were quantitated as follows: no growth, 0; growth on the first quadrant, 1+; growth in first and second quadrants, 2+; growth in first 3 quadrants, 3+; growth in all quadrants,4+ Data derived from peptone agar (plate counts) were analyzed statistically. To confirm that quantitated colonies were *Bb*, typical colonies were sub-cultured on blood agar and tested by use of conventional methods of identification. Tests on identification strips o used for gram-negative organisms as positive confirmation of *Bb* TSI (alkaline), urease (+), citrate (+), and arginine (–).

Statistical analysis

The individual animal was evaluated as the experimental unit. The primary variable was spontaneous coughing. Secondary variables included the other clinical signs of Bordetella infection. Differences were evaluated using two-sided tests at alpha = 0.1. For each dog, the severity of coughing (maximum coughing score post-challenge), the duration of coughing (number of days with coughing scores of 1 or 2), and the summed spontaneous coughing scores during the post-challenge were evaluated as the primary outcome variables. The maximum score for coughing and the summed coughing scores were

evaluated as a categorical variable. The probability that an observation from a vaccination group was different from an observation from the control group (or that there was a shift in distribution between the groups) was tested using Wilcoxon's Rank Sum Test (the NPAR1WAY procedure in SAS, SAS Institute, Cary NC, SAS/STAT 13.1). Maximum scores and summed scores were analyzed using mitigated fraction (MF) and a 95% confidence interval calculated (CI; the FREQ procedure in SAS). The influence of vaccination on the duration of coughing was evaluated using Wilcoxon's Rank Sum Test (the FREQ procedure in SAS). The placebo control and positive control were compared to each of the remaining groups. Experimental biological products were also compared to each other.

Least squares means and standard errors by treatment group (over time where appropriate) are used to summarize the results. Counts and frequencies are used as appropriate. Arithmetic means and standard deviations by treatment group over time are also provided. Clinical scores for coughing, ocular discharge, nasal discharge, and laryngeal palpation were analyzed individually and as a composite score. They were statistically analyzed as ordinal data using Wilcoxon's Rank Sum Test (the NPAR1WAY procedure in SAS). Results from each day were analyzed independently. If within day treatment effects were significant, the placebo control and positive control were compared to each of the remaining groups; differences between groups were evaluated using an unadjusted alpha = 0.1. Median scores by day are used to summarize the results.

Special test criteria

The study was to be considered valid if all animals were sero-negative for *B. bronchiseptica* prior to entry into the study. Dogs were also to remain seronegative prior to vaccination, and the negative controls must be seronegative prior to challenge. These criteria's were met for the study. Further the test was to be considered invalid if more than 2 of the control dogs showed no typical signs of *Bordetella* infection after challenge. This was a valid test with all control dogs showing signs of infection.

Results

Bacterial Ghost vaccine production

Lysis plasmid pGLysivb [34] was used to transform the *Bordetella bronchiseptica strain* 110H. The plasmid pGLysivb allowed the induction of gene *E* by a temperature upshift of 36°C to 44°C. Transformed *Bb* 110H was grown with aeration in a total volume of 4 litres, and the OD and live cell counts were monitored during the growth and lysis phase. The lysis was continued to 420 min after which the cells were washed with 4 litres of dH_2O using Tangential Flow Filtration (TFF) and harvested. The CFU count showed a lysis efficiency of 98% and the phase contrast microscopy showed a typical empty cell appearance as seen in most BG preparations (**Fig. 1**). The remaining survivors were killed by incubating the culture harvest with 20mM of Ethyleneimine solution at 35°C for 3 hours and cells were once again washed with 4 litres dH_2O and concentrated to 400mL using TFF. No single bacterial colony was detected on the plates with EI treated samples incubated at 36°C for up to 7 days.

Fig. 1: Microscopic picture of *B. bronchiseptica* Bacterial Ghosts (*Bb*BG)

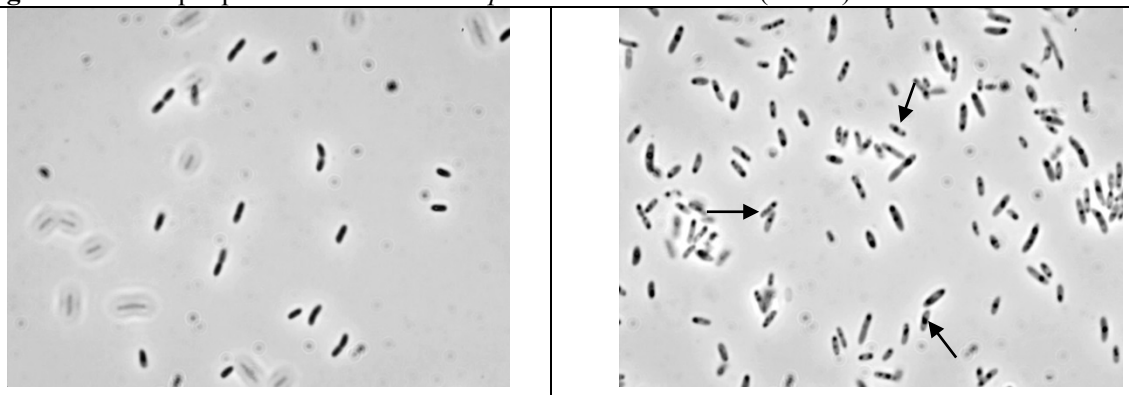

B. bronchiseptica 110H (pGLysivb) [Before lysis induction – 36°C]	*B. bronchiseptica* strain 110H (pGLysivb) [End of lysis and after inactivation with EI]

The arrows indicate the Bacterial Ghosts (BGs), EI; Ethyleneimine, pGLysivb; lysis plasmid under temperature inducible λPR_{mut} – c*I*857 promoter-repressor

In this study freeze-dried BGs has been substituted by a liquid formulation. After production, *Bb*BGs were stored at -20°C (~2 weeks). The vaccine was later thawed, reconstituted in dH_2O for final dosage and stored at +4°C until it was used for animal testing. A portion of this liquid formulation of *Bb*BG vaccine was used for monitoring vaccine stability and was found to be stable for several months at +4°C. This procedure was novel for BG vaccines and mimics veterinary practice to store vaccines in

liquid form which is ready to use. The *Bb*BG sample was stored at +4°C until administration. A portion of the final BG preparation was used for sterility test. No bacterial or fungal growth observed after 14 days of incubation in TSB enrichment medium at +36°C.

Vaccine safety and efficacy

All of the puppies were free from any *B. bronchiseptica* before they were entered into the study. The dogs stayed seronegative before the vaccination and the negative control group (T01) remained seronegative before the challenge, this was done through MAT antibody titers. It also showed a positive result in case of vaccinated group - T02 - T03 and T04. After the challenge all of the dogs in negative control group showed signs of disease (characterized by coughing and sneezing). No adverse reaction detected following the administration of either of the vaccines to any puppies in either group. There were no behavioral changes (e.g. listlessness, depression) or any abnormal elevated temperatures following vaccination. There were only two dogs with mild injection site reaction in groups - T02 (Bronchicine CAe) and T03 (*Bb*BG-7) respectively. These reactions occurred following the second vaccination. One animal died due to complications not related to the vaccination study. This animal belonged to the PBS negative control group.

The observation of animal was made to find any signs of tracheobronchitis. Animals were considered positive if any of the dogs had more than two days of coughing (not necessarily consecutive) during the 14 days of observation. In the group - T01 all of the remaining 7 puppies showed signs of tracheobronchitis whereas vaccinated group - T02 (Bronchicine CAe) and T03 (*Bb*BG-7) did not show sign of disease. The lower dose *Bb*BG-5 vaccinated group - T03 did not show any signs of protection and all of the puppies were positive for tracheobronchitis.

Both the spontaneous and induced coughing was monitored in the course of study. The number of days of spontaneous coughing was significantly affected by treatment group (P = 0.0003). Dogs in groups - T02 and T03 had significantly fewer days of coughing than dogs in group - T01 (control group). Dogs in group - T04 had more days of coughing than, dogs in group - T02 and was not statistically different than group - T01 (**Table 2**).

The scores for spontaneous coughing were summed per dog, and mean was calculated. A significant treatment group effect was detected (P = 0.0001). Groups - T02 and T03 had significantly lower total

scores than the negative control group (**Table 2**). Dogs in group - T04 had significantly higher scores than dogs in groups - T02 and T03. Treatment group - T01 and T04 were not statistically different. The mitigated fractions (MF) for spontaneous coughing were calculated. The MF is the probability that a vaccinated animal will have less severe disease across the observation period when compared to the negative control group. MF values in groups - T02 and T03, when compared to group - T01 were 0.7143 and 0.6964 respectively. Treatment group - T04 had a MF that was worse when compared to group - T01 (**Table 2**).

Induced coughing score (induced by mild laryngeal palpation) were significantly lower in group T02 and group - T03 when compared to values in control group - T01 or in group - T04. Similarly total clinical scores (post challenge) were lower in group T02 and T03 ranging between 1 – 0.5 respectively, as compared to values in group T01 which was around 8 (max score) and for T04 in range of 2 – 3.5. Other observed respiratory clinical signs were mucopurulent ocular and nasal discharge and sneezing. Only one dog had any recorded ocular or nasal discharge during the study. This dog was in treatment group - T04. Since serology and nasal shedding showed no discernable differences between any of the groups, the raw data is not shown here.

Table 2. *Summary of spontaneous coughing: duration and totaled scores (results for euthanized dogs entered as the max observed score (2))*

Treatment group	Duration (median number of days)	Scores totaled across Days 43 – 54 (mean)	Mitigated Fraction†† for total score (95% CI‡) (versus T01)
1	11.00	13.29	---
2	1.00*	1.75*	0.7143 (0.3618, 1.0000)
3	1.00*	2.25*a	0.6964 (0.3251, 1.0000)
4	7.00†	13.63†b	-0.2321 (-0.8350, 0.3708)
Overall treatment P-value	0.0003	0.0001	

††mitigated fraction = the probability that a vaccinate will be less affected by challenge than a non-vaccinate
*versus T01, P < 0.10
† versus T02, P < 0.10
‡Confidence interval
ab: among groups 2 – 4, values with no common letters are significantly different at P < 0.10

Discussion

This proof of concept study for testing of novel empty bacterial cell vaccine against virulent *Bordetella bronchiseptica* strain demonstrated well and confirms the previous claims of efficacious Bordetella vaccines in dogs [17-19, 41-44]. The challenge study did demonstrate efficacy of the *BbBG – 7* vaccine against the severe disease, comparable to the existing commercial; acellular vaccine Bronchicine CAe [45, 46]. The SC vaccination of the puppies with *BbBG – 7* vaccine resulted in substantive decrease in coughing (most common sign of Bordetella infection) when compared to the negative control group - T01.

Further, the *Bb*BG vaccine did demonstrate a dose dependent efficacy of the relatively lower dose (two log less of BG control) *Bb*BG – 5 vaccine which was not effective to protect animals from clinical disease. The *Bb*BG – 7 vaccine was used in concentrations up to 1 x 10^7, in comparison to *Bronchicine CAe* which is a purified extract of 3 x 10^8 *B. bronchiseptica* cells (Zoetis resource). There seems to be room for increasing the dose of *Bb*BG vaccine in a more extended dose finding study.

In vaccination studies routes of administration is highly debated topic and is often surrounded by controversies regarding the efficacy of parenteral, IN and oral Bordetella vaccination in dogs [45-51]. In one of the early studies [45] it has been shown that the dogs vaccinated subcutaneously with acellular vaccines showed higher serum concentration of *Bb*-reactive IgG when compared to IN vaccinated group in seropositive dogs. In later studies [47, 49], this claim has been contradicted and was shown that the oral and IN route activates better salivary and serum immunoglobulin responses in seronegative dogs. In a recent study [51], it was shown that the previous history of infection (seropositive dogs) attributes to a better and enhanced immune response in animals that are vaccinated subcutaneously with acellular vaccine.

In study presented, protection induced by parenteral administration of *Bb*BG in seronegative dogs was explored. From previous BG vaccine studies [31, 52-55], it is well established that BGs can be effectively administered through, oral, rectal, mucosal (eye), intranasal and parenteral routes, and conferred protective immunity in the vaccinated animals (mouse, rabbit, pigs, calves, etc.) against subsequent challenges. Since BGs are non-living cell envelops; it will also cater the reservation of scientists who believe that IN administration of live attenuated Bordetella vaccines may put the owners of pets and

veterinarians at risk of contracting Bordetella infection through shedding of bacterial droplets [8, 9, 11, 13, 56]. Non-living *Bb*BG vaccine is not able to induce infection in human recipients catching shedded vaccine material. Further BGs are shown to prevent bacterial colonization in a respiratory model [31, 32]. Pigs immunized either intramuscularly or aerogenically with *Actinobacillus pleuropneumoniae* (*App)* BGs prevented bacterial colonization in lungs when compared to formalin inactivated *App* vaccine. *Bordetella pertussis* (*Bp)* and *Bb* colonize the respiratory mucosa of humans and other mammals, respectively via their fimbriae *fim2, fim3, fimX and fimA* [57-60]. Besides several studies on role of fimbriae in colonization of *Bb* and *Bp* in respiratory mucosa, their precise role in pathogenesis of infection is yet to be concluded. It is due to this role that in some of the acellular Pertussis vaccines, *fim2* and *fim3* have been included [61]. Fimbriae and pili are well preserved in BGs, and are part of vaccine preparations as shown with toxin co-regulated pili in *Vibrio cholera* BGs and fimbriae in *E. coli* BGs [33, 62]. In any case, a vaccine able to prevent bacterial colonization and conferring immunity against disease is superior to any other vaccine which is directed against the toxin alone which causes the disease.

There is lot of resemblance among *Bb* and *Bp* vaccines, as both of the vaccines evolved from whole cell bacterins (past), to acellular or subunit products (current). This transition to acellular products was attributed to lower vaccine reactogenicity which is also of regulatory importance. The replacement of successful whole cell bacterins of *Bb* (dogs) and *Bp* (humans) with acellular vaccine was carried out to minimize the post vaccination reaction attributed to presence of high amounts of free lipopolysaccharides (LPS) in whole cell bacterins [63, 64]. However, later it was found out that acellular Pertussis vaccines are usually less potent than whole cell Pertussis vaccines, with some exceptions [65, 66]. The acellular Pertussis vaccines are alum based which promotes strong T helper type 2 (Th2), and T helper type 17 (Th17) antibody response, and lacks in producing cellular immunity linked to T helper type 1 (Th1) cells [67-71]. A recent review by *Higgs et.al.* [72] focuses for the need of Pertussis vaccine, that promote Th1 mediate cellular immune response, which is thought to be more efficient in clearing *Bp* from respiratory tract. It was also found out, that a novel Toll-like receptor (TLR2)-activating lipoproteins from *Bp* play an important role in activation of murine dendritic cells and macrophages and human mononuclear cells via TLR2 [73]. BGs are also known for stimulating both

cellular Th1 and humoral immune Th2 responses due to presence of essential structures on the cell surface [(74)].

In study presented, a whole cell envelope *Bb*BG vaccine, produced through proprietary method was used. This *Bb*BG vaccine exhibited similar safety profile like, commercially available acellular Bordetella vaccine, *Bronchicine CAe*®. BGs vaccine technology can also be used for production of other Bordetella species (*Bp, Bpp*) vaccines, for prevention of Whooping cough in humans. Whooping cough is considered to be reemerging disease by Centre for Disease control (CDC) and is mostly attributed towards use of acellular pertussis vaccines [(75)]. These *Bp*BG carries all essential surface structures that are necessary for triggering TLR mediated pathways, which is necessary for efficient clearance of *Bp* from respiratory mucosa. The BG technology has an edge over other vaccines because of its ease of production and being stable in freeze-dried (several years), and in liquid formulation up-to several months; GFP- reporter gene showed illumination under florescent microscope stored at +4°C after 6 months. There is a need for efficient and affordable Bordetella vaccines especially in developing countries where Bordetella is endemic and is a major cause of morbidity and mortality (up to 90% of *Bp* linked cases) in human populations [(76)]. BGs might be able to fill this gap.

Conclusion

The new *Bordetella bronchiseptica* BG vaccine tested in this study was found to be safe with a single small, transient injection site reaction after second vaccine dose administration. The challenge with virulent Bordetella strain was severe, as four dogs from placebo control and 3 dogs from *BbBG – 5* group required euthanasia due to severity of respiratory disease. Even though it was an over-challenge the *BbBG – 7* vaccine was found to be efficacious against CIRD caused by *Bordetella bronchiseptica*. It is worth mentioning here, that the tested commercial vaccine is a cellular antigen extract of at least 3 x 10^8 *Bb*. cells whereas, this newly tested *Bordetella* vaccine (*BbBG – 7)* contains 1 x 10^7 empty bacterial envelopes yet showing similar results in terms of safety and efficacy.

Acknowledgements

This study was conducted together with corporation of BIRD-C GmbH Co KG, Vienna, Austria and ELANCO a division of Animal Health of Eli Lilly, U.S.A.
The authors are thankful to Robin S. Readnour, Juan Escala, Frank Akosa Udeze and Gaofeng Lin of ELANCO Animal health for project support, and Laurie Larson, Patricia Sharp and Ronald D. Schultz of University of Wisconsin, for conducting animal study. The authors would also like to extend their thanks to Timo Langemann and Mascha Rauscher of BIRD-C, for production of BG vaccine.
This work was supported by the ELANCO Animal Health, Green Field, IN, U.S.A.

References

1. **Ford RB.** 2006. Canine infectius tracheobronchitis, p pp. 54–61. *In* Greene CE (ed), Infectious Diseases of Dog and Cat, Third Ed. ed. Saunders, ELSVIER, Philadelphia, PA, USA,.
2. **Ferry NS.** 1910. A preliminary report of the bacterial findings in canine distemper. Am Vet Rev **37:**499-504.
3. **Ferry NS.** 1911. Etiology of Canine Distemper. Journal of Infectious Diseases **8:**399-420.
4. **Ferry NS.** 1912. Bacillus bronchisepticus (bronchicanis): the cause of distemper in dogs and a similar disease in other animals. Vet J **68:**376-391.
5. **Ferry NS.** 1913. Bacteriology and control of acute infections in laboratory animals. The Journal of Pathology and Bacteriology **18:**445-455.
6. **Smith T.** 1913. Some bacteriological and environmental Factors in the Pneumonias of Lower Animals with Special Reference to the Guinea-Pig. The Journal of Medical Research **29:**291-324.295.
7. **Ferry NS.** Canine Distemper, p 80-88. *In* (ed), Vet. Med. Assoc.,
8. **Goodnow RA.** 1980. Biology of Bordetella bronchiseptica. Microbiol Rev **44:**722-738.
9. **Woolfrey BF, Moody JA.** 1991. Human infections associated with Bordetella bronchiseptica. Clin Microbiol Rev **4:**243-255.
10. **Bauwens JE, Spach DH, Schacker TW, Mustafa MM, Bowden RA.** 1992. Bordetella bronchiseptica pneumonia and bacteremia following bone marrow transplantation. Journal of Clinical Microbiology **30:**2474-2475.
11. **Gisel JJ, Brumble LM, Johnson MM.** 2010. Bordetella bronchiseptica pneumonia in a kidney-pancreas transplant patient after exposure to recently vaccinated dogs. Transpl Infect Dis **12:**73-76.
12. **Bjornstad ON, Harvill ET.** 2005. Evolution and emergence of Bordetella in humans. Trends Microbiol **13:**355-359.
13. **Gueirard P, Weber C, Le Coustumier A, Guiso N.** 1995. Human Bordetella bronchiseptica infection related to contact with infected animals: persistence of bacteria in host. Journal of clinical microbiology **33:**2002-2006.
14. **Anderton TL, Maskell DJ, Preston A.** 2004. Ciliostasis is a key early event during colonization of canine tracheal tissue by Bordetella bronchiseptica. Microbiology **150:**2843-2855.
15. **Bemis DA, Kennedy JR.** 1981. An improved system for studying the effect of Bordetella bronchiseptica on the ciliary activity of canine tracheal epithelial cells. J Infect Dis **144:**349-357.
16. **Mann P, Goebel E, Barbarich J, Pilione M, Kennett M, Harvill E.** 2007. Use of a genetically defined double mutant strain of Bordetella bronchiseptica lacking adenylate cyclase and type III secretion as a live vaccine. Infect Immun **75:**3665-3672.
17. **McCandlish IA, Thompson H, Wright NG.** 1978. Vaccination against canine bordetellosis using an aluminum hydroxide adjuvant vaccine. Res Vet Sci **25:**51-57.
18. **Shade FJ, Goodnow RA.** 1979. Intranasal immunization of dogs against Bordetella bronchiseptica-induced tracheobronchitis (kennel cough) with modified live-Bordetella bronchiseptica vaccine. Am J Vet Res **40:**1241-1243.

19. **Kontor EJ, Wegrzyn RJ, Goodnow RA.** 1981. Canine infectious tracheobronchitis: effects of an intranasal live canine parainfluenza-Bordetella bronchiseptica vaccine on viral shedding and clinical tracheobronchitis (kennel cough). Am J Vet Res **42:**1694-1698.
20. **Jalava K, Hensel A, Szostak M, Resch S, Lubitz W.** 2002. Bacterial ghosts as vaccine candidates for veterinary applications. J Control Release **85:**17-25.
21. **Lubitz W, Witte A, Eko FO, Kamal M, Jechlinger W, Brand E, Marchart J, Haidinger W, Huter V, Felnerova D, Stralis-Alves N, Lechleitner S, Melzer H, Szostak MP, Resch S, Mader H, Kuen B, Mayr B, Mayrhofer P, Geretschlager R, Haslberger A, Hensel A.** 1999. Extended recombinant bacterial ghost system. J Biotechnol **73:**261-273.
22. **Szostak MP, Hensel A, Eko FO, Klein R, Auer T, Mader H, Haslberger A, Bunka S, Wanner G, Lubitz W.** 1996. Bacterial ghosts: non-living candidate vaccines. J Biotechnol **44:**161-170.
23. **Szostak M, Lubitz W.** 1991. Recombinant Bacterial Ghosts as multivaccine vehicles p409-414. *In* Chanock R (ed), Vaccines 91 Modern Approaches to New Vaccines Including Prevention of AIDS, Cold Spring Harbor Laboratory Press.
24. **Lubitz P, Mayr UB, Lubitz W.** 2009. Applications of bacterial ghosts in biomedicine. Adv Exp Med Biol **655:**159-170.
25. Mayr B, Koller, V.J., Lubitz, P., Lubitz, W. 2008. Bacterial Ghosts as vaccine and Drug Delivery Platforms, Landes Bioscience, Austin.
26. **Witte A, Wanner G, Blasi U, Halfmann G, Szostak M, Lubitz W.** 1990. Endogenous transmembrane tunnel formation mediated by phi X174 lysis protein E. J Bacteriol **172:**4109-4114.
27. **Huter V, Szostak MP, Gampfer J, Prethaler S, Wanner G, Gabor F, Lubitz W.** 1999. Bacterial ghosts as drug carrier and targeting vehicles. J Control Release **61:**51-63.
28. **Paukner S, Kohl G, Jalava K, Lubitz W.** 2003. Sealed bacterial ghosts--novel targeting vehicles for advanced drug delivery of water-soluble substances. J Drug Target **11:**151-161.
29. **Witte A, Wanner G, Sulzner M, Lubitz W.** 1992. Dynamics of PhiX174 protein E-mediated lysis of Escherichia coli. Arch Microbiol **157:**381-388.
30. **Muhammad A, Champeimont J, Mayr UB, Lubitz W, Kudela P.** 2012. Bacterial ghosts as carriers of protein subunit and DNA-encoded antigens for vaccine applications. Expert Rev Vaccines **11:**97-116.
31. **Huter V, Hensel A, Brand E, Lubitz W.** 2000. Improved protection against lung colonization by Actinobacillus pleuropneumoniae ghosts: characterization of a genetically inactivated vaccine. J Biotechnol **83:**161-172.
32. **Hensel A, Huter V, Katinger A, Raza P, Strnistschie C, Roesler U, Brand E, Lubitz W.** 2000. Intramuscular immunization with genetically inactivated (ghosts) Actinobacillus pleuropneumoniae serotype 9 protects pigs against homologous aerosol challenge and prevents carrier state. Vaccine **18:**2945-2955.
33. **Eko FO, Mayr UB, Attridge SR, Lubitz W.** 2000. Characterization and immunogenicity of Vibrio cholerae ghosts expressing toxin-coregulated pili. J Biotechnol **83:**115-123.
34. **Langemann T, Koller VJ, Muhammad A, Kudela P, Mayr UB, Lubitz W.** 2010. The Bacterial Ghost platform system: production and applications. Bioeng Bugs **1:**326-336.
35. **Kovach ME, Elzer PH, Hill DS, Robertson GT, Farris MA, Roop RM, 2nd, Peterson KM.** 1995. Four new derivatives of the broad-host-range cloning vector pBBR1MCS, carrying different antibiotic-resistance cassettes. Gene **166:**175-176.
36. **Miller JF, Dower WJ, Tompkins LS.** 1988. High-voltage electroporation of bacteria: genetic transformation of Campylobacter jejuni with plasmid DNA. Proc Natl Acad Sci U S A **85:**856-860.
37. **EMA.** 1999. General Requirements for the Production and Control of Inactivated Mammalian Bacterial and Viral Vaccines for Veterinary Use. Association EM, http://ec.europa.eu/health/files/eudralex/vol-7/b/7blm2a_en.pdf.
38. Anonymous. 2011. Guid for the Care and Use of Laboratory Animals, Eighth ed, vol The National Acedemies Press, Washingtom, DC.
39. **Smith IM, Baskerville AJ.** 1979. A selective medium facilitating the isolation and recognition of Bordetella bronchiseptica in pigs. Res Vet Sci **27:**187-192.

40. **Barry AL.** 1972. Clinical specimens for microbiological examination., p 103-107. *In* Haeprich PD (ed), Infectious diseases: a guide to the understanding and management of the infectious process. ed. Harper & Row, New York.
41. **Bey RF, Shade FJ, Goodnow RA, Johnson RC.** 1981. Intranasal vaccination of dogs with liver avirulent Bordetella bronchiseptica: correlation of serum agglutination titer and the formation of secretory IgA with protection against experimentally induced infectious tracheobronchitis. Am J Vet Res **42:**1130-1132.
42. **Glickman LT, Appel MJ.** 1981. Intranasal vaccine trial for canine infectious tracheobronchitis (kennel cough). Lab Anim Sci **31:**397-399.
43. **McCandlish IA, Thompson H, Wright NG.** 1978. Vaccination against Bordetella bronchiseptica infection in dogs using a heat-killed bacterial vaccine. Res Vet Sci **25:**45-50.
44. **Shade FJ, VJ R.** 1982. Studies of a bacterin incorporating an extracted Bordetella bronchiseptica antigen for controlling canine bordetellosis. Vet Med Small Anim Clin **77:**1635-1639.
45. **Ellis JA, Krakowka GS, Dayton AD, Konoby C.** 2002. Comparative efficacy of an injectable vaccine and an intranasal vaccine in stimulating Bordetella bronchiseptica-reactive antibody responses in seropositive dogs. J Am Vet Med Assoc **220:**43-48.
46. **Ellis JA, Haines DM, West KH, Burr JH, Dayton A, Townsend HG, Kanara EW, Konoby C, Crichlow A, Martin K, Headrick G.** 2001. Effect of vaccination on experimental infection with Bordetella bronchiseptica in dogs. J Am Vet Med Assoc **218:**367-375.
47. **Laurie J. Larson, Bliss E. Theil, Patricia Sharp, Ronald D. Schultz.** 2013. A Comparative Study of Protective Immunity Provided by Oral, Intranasal and Parenteral Canine Bordetella bronchiseptica Vaccines. . Intern J Appl Res Vet Med **11:**153-160.
48. **Thomas JH, Dana S. Parker, Alan J. Hassall, Chiang Y-W.** 2011. Evaluation of Efficacy of Oral Administration of Bordetella bronchiseptica Intranasal Vaccine When Used to Protect Puppies from Tracheobronchitis Due to B bronchiseptica Infection. Intern J Appl Res Vet Med **9:**300-305.
49. **Davis R, Jayappa H, Abdelmagid OY, Armstrong R, Sweeney D, Lehr C.** 2007. Comparison of the mucosal immune response in dogs vaccinated with either an intranasal avirulent live culture or a subcutaneous antigen extract vaccine of Bordetella bronchiseptica. Vet Ther **8:**32-40.
50. **Gore T, Headley M, Laris R, Bergman JG, Sutton D, Horspool LJ, Jacobs AA.** 2005. Intranasal kennel cough vaccine protecting dogs from experimental Bordetella bronchiseptica challenge within 72 hours. Vet Rec **156:**482-483.
51. **Ellis J, Rhodes C, Lacoste S, Krakowka S.** 2014. Antibody responses to Bordetella bronchiseptica in vaccinated and infected dogs. Can Vet J **55:**857-864.
52. **Mayr UB, Kudela P, Atrasheuskaya A, Bukin E, Ignatyev G, Lubitz W.** 2012. Rectal single dose immunization of mice with Escherichia coli O157:H7 bacterial ghosts induces efficient humoral and cellular immune responses and protects against the lethal heterologous challenge. Microb Biotechnol **5:**283-294.
53. **Walcher P, Cui X, Arrow JA, Scobie S, Molinia FC, Cowan PE, Lubitz W, Duckworth JA.** 2008. Bacterial ghosts as a delivery system for zona pellucida-2 fertility control vaccines for brushtail possums (Trichosurus vulpecula). Vaccine **26:**6832-6838.
54. **Mayr UB, Haller C, Haidinger W, Atrasheuskaya A, Bukin E, Lubitz W, Ignatyev G.** 2005. Bacterial ghosts as an oral vaccine: a single dose of Escherichia coli O157:H7 bacterial ghosts protects mice against lethal challenge. Infect Immun **73:**4810-4817.
55. **Katinger A, Lubitz W, Szostak MP, Stadler M, Klein R, Indra A, Huter V, Hensel A.** 1999. Pigs aerogenously immunized with genetically inactivated (ghosts) or irradiated Actinobacillus pleuropneumoniae are protected against a homologous aerosol challenge despite differing in pulmonary cellular and antibody responses. J Biotechnol **73:**251-260.
56. **de la Torre MJ, de la Fuente CG, de Alegria CR, Del Molino CP, Aguero J, Martinez-Martinez L.** 2012. Recurrent respiratory infection caused by Bordetella bronchiseptica in an immunocompetent infant. Pediatr Infect Dis J **31:**981-983.
57. **Boschwitz JS, van der Heide HG, Mooi FR, Relman DA.** 1997. Bordetella bronchiseptica expresses the fimbrial structural subunit gene fimA. J Bacteriol **179:**7882-7885.

58. **Cuzzoni A, Pedroni P, Riboli B, Grandi G, de Ferra F.** 1990. Nucleotide sequence of the fim3 gene from Bordetella pertussis and homology to fim2 and fimX gene products. Nucleic Acids Res **18:**1640.
59. **Livey I, Duggleby CJ, Robinson A.** 1987. Cloning and nucleotide sequence analysis of the serotype 2 fimbrial subunit gene of Bordetella pertussis. Mol Microbiol **1:**203-209.
60. **Pedroni P, Riboli B, de Ferra F, Grandi G, Toma S, Arico B, Rappuoli R.** 1988. Cloning of a novel pilin-like gene from Bordetella pertussis: homology to the fim2 gene. Mol Microbiol **2:**539-543.
61. **Gustafsson L, Hallander HO, Olin P, Reizenstein E, Storsaeter J.** 1996. A controlled trial of a two-component acellular, a five-component acellular, and a whole-cell pertussis vaccine. N Engl J Med **334:**349-355.
62. **Montanaro J, Inic-Kanada A, Ladurner A, Stein E, Belij S, Bintner N, Schlacher S, Schuerer N, Mayr UB, Lubitz W, Leisch N, Barisani-Asenbauer T.** 2015. Escherichia coli Nissle 1917 bacterial ghosts retain crucial surface properties and express chlamydial antigen: an imaging study of a delivery system for the ocular surface. Drug Des Devel Ther **9:**3741-3754.
63. **Pittman M.** 1984. The concept of pertussis as a toxin-mediated disease. Pediatr Infect Dis **3:**467-486.
64. **Sato Y, Kimura M, Fukumi H.** 1984. Development of a pertussis component vaccine in Japan. Lancet **1:**122-126.
65. **J. Storsaeter, J. Wolter, Locht C.** 2007. *Pertussis* Vaccines, p 245-288. *In* Locht C (ed), *Bordetella* Molecular Microbiology. Horizon Biosciences, Norfolk, U.K.
66. **Klein NP, Bartlett J, Rowhani-Rahbar A, Fireman B, Baxter R.** 2012. Waning protection after fifth dose of acellular pertussis vaccine in children. N Engl J Med **367:**1012-1019.
67. **Ryan M, Murphy G, Ryan E, Nilsson L, Shackley F, Gothefors L, Oymar K, Miller E, Storsaeter J, Mills KH.** 1998. Distinct T-cell subtypes induced with whole cell and acellular pertussis vaccines in children. Immunology **93:**1-10.
68. **Ryan EJ, Nilsson L, Kjellman N, Gothefors L, Mills KH.** 2000. Booster immunization of children with an acellular pertussis vaccine enhances Th2 cytokine production and serum IgE responses against pertussis toxin but not against common allergens. Clin Exp Immunol **121:**193-200.
69. **Redhead K, Watkins J, Barnard A, Mills KH.** 1993. Effective immunization against Bordetella pertussis respiratory infection in mice is dependent on induction of cell-mediated immunity. Infect Immun **61:**3190-3198.
70. **Ausiello CM, Urbani F, la Sala A, Lande R, Cassone A.** 1997. Vaccine- and antigen-dependent type 1 and type 2 cytokine induction after primary vaccination of infants with whole-cell or acellular pertussis vaccines. Infect Immun **65:**2168-2174.
71. **Ross PJ, Sutton CE, Higgins S, Allen AC, Walsh K, Misiak A, Lavelle EC, McLoughlin RM, Mills KH.** 2013. Relative contribution of Th1 and Th17 cells in adaptive immunity to Bordetella pertussis: towards the rational design of an improved acellular pertussis vaccine. PLoS Pathog **9:**e1003264.
72. **Higgs R, Higgins SC, Ross PJ, Mills KH.** 2012. Immunity to the respiratory pathogen Bordetella pertussis. Mucosal Immunol **5:**485-500.
73. **Dunne A, Mielke LA, Allen AC, Sutton CE, Higgs R, Cunningham CC, Higgins SC, Mills KH.** 2015. A novel TLR2 agonist from Bordetella pertussis is a potent adjuvant that promotes protective immunity with an acellular pertussis vaccine. Mucosal Immunol **8:**607-617.
74. **Ebensen T, Paukner S, Link C, Kudela P, de Domenico C, Lubitz W, Guzman CA.** 2004. Bacterial ghosts are an efficient delivery system for DNA vaccines. J Immunol **172:**6858-6865.
75. **CDC.** 2002. PErtussis—united states, 1997-2000. JAMA **287:**977-979.
76. **Locht C.** 2008. A common vaccination strategy to solve unsolved problems of tuberculosis and pertussis? Microbes Infect **10:**1051-1056.

6 Material and Methods

6.1 Material

Chemicals, media, buffersand solutions are purchased from:
Carl ROTH (Karlsruhe, Germany), Merck (Darmstadt, Germany) or Sigma-Aldrich (a part of Merck, St. Louis, USA).

Materials for SDS-PAGE and Western blot are purchased from:
Thermo Fisher Scientific (Waltham, USA), Santa Cruz Biotechnology (Santa Cruz, USA) Carl Roth (Karlsruhe, Germany), Bio-Rad (Hercules,USA), GE Healthcare (Little Chalfont, UK).

All enzymes for DNA restriction, PCR and DNA ligation are purchased from:
Thermo Fisher Scientific (Waltham, USA), New England Biolabs (Frankfurt a. Main, Germany), or Promega (Mannheim, Germany).

6.2 Bacterial strains

Bacterial strains used in this study:

Escherichia coli K12 C2988J: *fhuA2* Δ(*argF-lacZ)U169 phoA glnV44 Φ80*Δ (*lacZ*)M15 *gyrA96 recA1 relA1 endA1 thi-1 hsdR17* (New England Biolabs, NEB,Germany) (used for cloning and E-lysis studies).

Escherichia coli JM109: endA1 glnV44 thi-1 relA1 gyrA96 recA1 mcrB$^+$ Δ(lac-proAB) e14- [F' traD36 proAB$^+$ lacI^q lacZΔM15] hsdR17($r_K^-m_K^+$) (NEB) (used for cloning).

Escherichia coli C41 (DE3): F – ompT hsdSB (rB- mB-) gal dcm (DE3) (Lucigen, Middelton, USA) (used for expression and E-lysis studies).
Bordetella bronchiseptica 110H-EL: used for BG production EI inactivation studies and vaccine production for kennel cough in dogs (provided by Elanco Animal Health, Eli Lilly, Indianapolis U.S.A.).

6.3 Growth media

Plate – Count agar

23.5 g L^{-1} (for determination of the cfu).

Vegetable variant of Luria-Bertani (LBv)

10.0 g L^{-1} soy peptone 5.0 g/l yeast extract and 5.0 g/l NaCl, adjusted to a pH of 7.4.

LBv- agar

10.0 g L^{-1} soy peptone 5.0 g/l yeast extract and 5.0 g/l NaCl) adjusted to a pH of 7.4; for agar plates 15 g agar/l is added.

Tryptose Phosphate broth – vegetable source (TPv) (Difco Laboratories)

supplemented with 0.004 g L^{-1} nicotinic acid, 0.02 g L^{-1} $FeSO_4 7.H_2O$ and 0.02 g L^{-1} ascorbic acid.

Tryptose Phosphate Agar (TPA) (Difco Laboratories, US)

6.4 Antibiotics

Antibiotics were added to a final concentration of: 100µg ampicillin ml^{-1}, 20µg gentamycin ml^{-1}, 50 µg kanamycin ml^{-1}.

6.5 Buffers & Solutions

50 % Glycerin

Mix 25 ml 100 % glycerin with 25 ml dH_2O and sterilize by autoclaving.

Saline Medium

8.5 g NaCl per 1l dH_2O.

GelRed staining solution

Mix 15 µl of GelRedTM nucleic acid gel stain (10000X in water (No. 41003) from Biotium), 5 ml 1M NaCl and 45 ml dH_2O.

MOPS I

10.47 g MOPS (100mM), 5.15 g $CaCl_2$ x 2 dH_2O (70 mM) and 0.6 g $RbCl_2$ (10mM) dissolve in 400 ml dH_2O, adjust pH to 6.5 with KOH fill up to 500 ml with dH_2O and autoclave.

MOPS II

10.47 g MOPS (100mM), 0.74 g $CaCl_2$ x 2 dH_2O (10mM), 0.6 g $RbCl_2$ (10mM) dissolve in 400 ml dH_2O, adjust pH to 7.0 with KOH and fill up to 500 ml with dH_2O and autoclave.

PonceauS

0.2 g PonceauS, 3 g trichloric acetic acid, fill up to 100 ml with dH_2O

1xNuPage® Sample Buffer

Mix 6.5 ml PBS, 2.5 ml NuPage® LDS Sample Buffer (4x) and 1 ml NuPage® Reducing Agent (10x).

10x PBS

137 mM NaCl, 2.7 mM KCl, 10 mM Na_2HPO_4, 2 mM KH_2PO_4 800 mL dH_2O, adjust pH to 7.4 with HCl and fill up to 1 l with dH_2O.

TBS

6.05 g Tris and 8.76 g NaCl in 800 ml of dH_2O, adjust pH to 7.5 with 1 M HCl and make volume up to 1 l with H_2O.

TBST

TBS with 0.05 % Tween-20.

6.6 Cloning

All reactions were performed according to the manufacturer's instructions.
All synthetic DNA sequences were ordered at Eurofins Genomics (Ebersberg, Germany).
All primers were obtained from Microsynth AG (Balgach, Switzerland).
For final confirmation of the correct plasmid inserted sequence, plasmid preparations were send to Microsynth AG for sequencing.

6.7 PCR

PCR reactions were performed by using the Bio-Rad iCycler-system, according to the instruction manual. Material for PCR reactions were purchased from Thermo Fisher Scientific (Waltham, USA). PCR-reactions were performed according to instruction notes.

6.8 CaCl2 / RbCl2 competent cells

30 ml of LBv-medium was inoculated with an overnight grown bacterial culture to an OD_{600} of 0.05. The culture was incubated at 35°C under continuous shaking until an OD_{600} of ~ 0,5 was reached. The culture was pelleted by centrifugation for 10 minutes at 4 ° C and 3000 x g. The pellet was resuspended in 6 ml MOPS I and placed for 10 minutes on ice. The cells were pelleted again and resuspended in 6 ml MOPS II and placed on ice for 30 minutes. Afterwards, the cells were centrifuged for 10 minutes at 4 ° C and 3000 x g and resuspended in 480 µl MOPS II and 180 µl of 50% glycerol and placed on ice for 10 minutes. Aliquots were made in 100 µl portions and frozen at -80 °C.

6.9 Transformation of CaCl2 / RbCl2 competent cells

5 µl containing 10-100 ng of plasmid DNA were pipetted into the 100 µl aliquot of competent cells and placed for 30 minutes on ice. Subsequently, a heat shock at 35°C (for lysis plasmid pGLysivb) or 42°C (for all other plasmids used in this study) was performed for 2 minutes and incubated for 5 minutes on ice. Following that, 700 µl LBv-medium was added to the cells and incubated at 35°C with agitation. After regeneration, the transformed cells were plated on agar plates containing the corresponding antibiotics and incubated over night at 35°C.

6.10 Growth and E-lysis of ice nucleation active bacteria

E. coli C41 harboring pBINP and E-lysis plasmid were grown in LBv supplemented with suitable antibiotics and 0.2 % L-arabinose at 23°C to induce constitutive expression of the ice nucleation protein sequence under control of P_{BAD}. When the culture reached an optical density at 600 nm (OD_{600}) of 0.6 E-mediated lysis was initiated. Expression of gene *E* in lysis plasmid pGLysivb was induced by a temperature up-shift of the growing cultures from 23°C to 42°C. Whereas the expression of gene *E* from lysis plasmid pGLMivb in cultures kept at 23°C was induced with 0.5 mM isopropyl-D-1-thiogalactopyranoside (IPTG). After the completion of E-lysis process, the cell harvest was washed four times with 1x Vol. of sterile de-ionized water (dH_2O) by centrifugation and suspended in 1x Vol of sterile dH_2O.

6.11 Expression- and lysis-study in small scale

Experiments were carried out in nose flasks with 30 ml LBv supplemented with appropriate antibiotics. Growth medium was inoculated with the bacterial overnight culture to an OD_{600} of 0.05. The nose flasks were incubated at 30°C (if not indicated otherwise) with agitation. Genes under control of P_{BAD} were expressed by the addition of 0.2 % L-arabinose to the growth medium, whereas genes under control of P_{lac} or P_{tac} were expressed by adding 0.5 mM isopropyl-D-1-thiogalactopyranoside (IPTG) to the culture. Expression of gene *E* in lysis plasmid pGLysivb was induced by a temperature up-shift of the growing cultures to 42°C. During growth, expression and lysis of the bacterial cultures was monitored by measuring OD_{600}, determining cfu and light-microscopic (Leica DM R microscope, Leica Microsystems) analysis.

6.12 Monitoring and determination of E-lysis efficiency

The BG production was monitored by light-microscopy (Leica DM R microscope, Leica Microsystems), by checking the optical density at 600nm (OD_{600}) and fluorescence-activated flow cytometry according to Langemann et *al.* .[44,45] Flow cytometry (FCM) was performed using a CyFlow® SL flow cytometer (Partec) with a 488-nm blue solid-state laser. The membrane potential-sensitive dye DiBAC4(3) (abs./em.: 493/516 nm, FL1,) was used for the evaluation of cell-viability. Fluorescent dye RH414 (abs./em. 532/760 nm) was used for staining phospholipid membranes and discriminating non-cellular background. 1 ml samples were diluted to provide appropriate cell counts and stained with 1.5 µl DiBAC4(3) (0.5mM) and 1.5 µl RH414 (2 mM), both from AnaSpec. Collected data was analyzed using FloMax V 2.52 (CyFlow SL; Quantum Analysis) and presented as 2D density dot plots illustrating forward scatter (FSC) against DiBAC fluorescence signal (FL1, DiBAC). To determine the colony forming units (cfu) during growth and lysis of *E. coli* C41 expressing INP bacterial samples were collected at different time points, diluted with saline and 50 µl samples were plated as triplicates on Plate Count Agar (Carl Roth) using a WASP spiral plater (Don Whitley Scientific). The plates were incubated at 36°C overnight and analyzed the next day using ProtoCOL SR 92000 colony counter (Synoptics Ltd). Lysis efficiency (LE) is defined as ratio of BGs after complete lysis to total cell counts and can be calculated by using following equation:

$$LE = \left(1 - \frac{cfu_{(t)}}{cfu_{(t_0)}}\right) \times 100\%$$

where t_0 is the time point of lysis induction (LI) and t is any time after LI.

6.13 β-propiolactone-treatment after E-lysis process

After the completion of E-lysis process, the cell harvest was washed four times with 1x Vol. of sterile de-ionized water (dH_2O) by centrifugation (5000 x g, at 4°C) and suspended in 1x Vol of sterile dH_2O. To inactivate any surviving E-lysis escape mutants from BG production, 0.17 % (v/v) of the DNA-alkylating agent β-propiolactone (BPL, 98.5 %, Ferak, Berlin, Germany) was added to the washed harvest and kept for 120 min at 23°C with agitation. This mixture was washed twice with 1x Vol. of sterile dH_2O and once with ROTISOLV® water (Carl Roth) and finally resuspended in 1/10x Vol. ROTISOLV®.

6.14 Ethyleneimine-treatment after E-lysis process

After completion of E-mediated lysis, the bacterial culture was washed (4x) with 1 x Vol. sterile dH_2O by centrifugation (5000 x g, at 4°C) or TFF. Different concentrations (10 mM, 8 mM, 6 mM, 4 mM, 3mM, 2 mM, 1mM) of Ethyleneimine (final concentration, Ethyleneimine stock conc. 186mM) (0,8% EI in 1% KOH, Ferak, Berlin Germany) was added to the washed harvest and kept for 120 min and

360 min, respectively at 35°C. Every hour EI treated bacteria were checked for viability by plating 100µl of serial 10-fold dilutions (pure, 10^{-1}, 10^{-2}, 10^{-3}) of the bacteria on TPv agar plates in duplicate. EI inactivation efficiency (IE) was calculated analog to LE described in chapter 6.11. Afterwards EI was inactivated by adding 10% (Vol. of used EI) 1 M Na-thiosulfat to the EI-treated harvest and kept for 30 min at 35°C and washed twice with 1x Vol. of sterile dH_2O and once with ROTISOLV®.

6.15 Mid-scale *B. bronchiseptica* BG production

The medium scale fermentation of *B. bronchiseptica* 110H was performed in a Labfors 3 fermenter (Infors Ag, Bottmingen, Switzerland) with a working volume of 4 liters. Medium scale fermentation was performed in TPv supplemented with gentamycin at 20 mg / L. Five mL of 30 hours culture of *B. bronchiseptica* 110H (carrying lysis plasmid pGLysivb) was used to prepare 200 mL pre-culture (35°C for 12 – 14 hours). This pre-culture with the OD_{600nm} of 1.15 was used to inoculate the fermenter containing 3.8 L of TPv to get starting OD_{600nm} of 0.052. The cells were grown to OD_{600} of ~0.5 at 35°C and the lysis was induced by temperature upshift to 44°C. The lysis was complete after 420 min and subsequently lysed cells were washed to get rid of the cytoplasmic contents using 4 L of sterile dH_2O using a Tangential Flow Filtration (TFF) module (0.2µm cut-off, GE healthcare) for 60 min. This was accomplished by matching the flow of media out of the TFF module with the same amount of dH_2O pumped into the fermenter. During the course of fermentation following parameters were documented: temperature, flow, stirrer, pH, pO_2, foaming and pumps for acid and base. Antifoam-A (Sigma) was added via sterile septum. After the completion of washing, the broth was concentrated to approximately 200 mL in TFF module (0.2 µm cut, GE, healthcare) and flushed from the module with ~200 mL sterile dH_2O into the "inactivation bottle" to get a final volume of ~400 mL (conc. I).

Due to regulatory requirements for veterinary vaccines by United States Department of Agriculture (USDA) and European Medicines Agency (EMA), the remaining un-lysed cells or escape mutants are inactivated / killed by one of the prescribed chemical procedures [(1)]. To fulfill the above requirement, ethyleneimine (EI) was used. A final concentration of 20 mM EI (FERAK, Berlin) was added to conc. I and incubated for 3 hrs with slight agitation at 35°C (2 mM, if calculated for initial volume of 4 liters before concentration). Samples for cfu count and microscopy were drawn hourly and the inactivation activity was halted by addition of 1 M sodium thiosulfate, at 10% of initial volume of EI used and kept for another 30 min at 35°C, while shaking. The inactivated sample was washed with 4 liters of sterile dH_2O using a fresh TFF module (sterile 0.2 µm cut-off, GE, healthcare). This was accomplished by matching the flow of media out of the TFF module, with the same amount of dH_2O pumped into the inactivation bottle. Later the broth was concentrated to ~200 mL, before being flushed out of the module with ~200 mL sterile dH_2O to bring the volume to ~400 mL (conc. II). This sample was stored

at -20°C for approx. 15 days, and was later thawed, and resuspended in dH_2O for final dose defining and shipped in liquid form at +4°C, for animal experiments.

6.16 Sterility testing of BGs

Full inactivation efficiency and sterility of BG products (after inactivation of E-lysis escape mutants) is tested in triplicates. For each set 100 µl and 200 µl were plated on LBv agar and inoculated in 5 ml LBv, respectively, and incubated overnight at 35°C.

6.17 Protein sample preparation

1 ml of bacterial culture was pelleted and diluted with 1x sample buffer according to the culture OD_{600}:

OD_{600} *x 250 = Volume of 1x sample buffer*

The bacterial pellet was resuspended in 1x sample buffer and mixed well, boiled for 10 minutes and centrifuged for 3 minutes at maximum speed. The supernatants (15-20 µl) were loaded on the gel.

6.18 Protein sample preparation of lysed culture

1 ml of bacterial culture was pelleted and diluted with 1x sample buffer according to the culture OD_{600}:

OD_{600} *(at lysis induction) x 250 = Volume of 1x sample buffer*

The bacterial pellet was resuspended in 1x sample buffer and mixed well, boiled for 10 minutes and centrifuged for 3 minutes at maximum speed. The supernatants (15-20 µl) were loaded on the gel.

6.19 Gel-Electrophoresis of proteins

The proteins were separated by using the NuPage® Bis-Tris Electrophoresis System (Invitrogen, Paisley, UK) according to the manufacturer's instructons. 15-20 µl of prepared protein samples and 5 µl of molecular weight protein marker (Bio-Rad) were loaded on the gel and run for approximately 90 minutes at 100 Volt.

6.20 Production of antibodies

N-terminal His-tagged INP lacking the N-terminal domain (H-NINP) was expressed from pBH-NINP in *E. coli* C41and H-NINP affinity purification of the protein was performed under denaturing conditions by using a nickel- agarose column (QIAGEN) according to the manufacturer's instructions.

With this protein fraction custom made INP specific polyclonal serum was produced by Moravian Biotechnology in rabbits after 4 rounds of immunization.

6.21 Western blot

All materials for Western-blot were purchased from Invitrogen™ (Thermo-Fischer) and Carl Roth (Karlsruhe, Germany) if not indicated otherwise. The proteins were transferred to a 0.45 µm pore size nitrocellulose membrane (GE Healthcare) by using the XCell II™ Blot Module according to the manufacturer's instructions. The efficiency of protein transfers and location of the protein marker is checked by Ponceau S staining. The membrane was placed in TBST with 5 % milk powder overnight at 4°C. All washing steps were performed 3 x 5 minutes in TBST. Immunodetection was performed using mouse anti-His antibodies (1:500 in TBST) (Thermo-Fischer) followed by α-mouse IgG-HRP (GE Healthcare). Detection was performed with an Amersham ECL Western blot detection kit (GE Healthcare) and developed with ChemiDoc™ XRS (Bio-Rad).

6.22 Production of INP antibodies

N-terminal His-tagged INP lacking the N-terminal domain (H-NINP) was expressed from pBH-NINP in *E. coli* C41. H-NINP affinity purification of the protein was performed under denaturing conditions by using a nickel- agarose column (QIAGEN) according to the manufacturer's instructions. With this protein fraction custom made INP specific polyclonal serum was produced by Moravian Biotechnology in rabbits after 4 rounds of immunization.

6.23 Ice-nucleating activity measurements

The ability to nucleate ice formation was measured by droplet freezing assay using a modified device based on a method of Vali.[2] The cooling unit was constructed with the help of instruction notes by Quick-Ohm (Quick-Ohm Küpper). Hence, to detect ice nuclei in the suspensions to be tested (each suspension was adjusted to a concentration of 5x 10^8 cells ml^{-1} determined by FCM) active at lower temperatures, a series of tenfold dilutions from each suspension (ranging from 5 x 10^8 cells ml^{-1} to 5 x 10^4 cells ml^{-1}) was tested resulting in respective ice nucleus spectrum. Forty-five 10 µl droplets if not indicated otherwise of each dilution were distributed on a sterile aluminum plate coated with a hydrophobic film. The plate surface was washed with aceton before coating and flushed with a stream of filtered air before the sample droplets were placed. The plate was surrounded by styrofoam and covered by a plexiglas plate for isolation. The temperature of the working plate was decreased by two in series circuited two-stage Peltier elements of the type TEC2-127-63-04, controlled by a QC-PC-C01C temperature controller (Quick-Ohm Küpper). The temperature controller was energized by a 10

kΩ potentiometer (M22S-R10K, Eaton). To measure the surface temperature of the plate a small precision temperature sensor TS□NTC□103A (B+B Thermo – Technik) was affixed, which is connected to the controller and the controller-display QC-PC-D-100 (Quick-Ohm Küpper). The plate surface can be cooled by the Peltier elements to a maximum temperature of -24.5°C. The temperature variation of the plate surface determined by a Voltcraft PL-120 T1 thermometer and a type K temperature sensor (1xK NL 1000, B+B Thermo – Technik) was ± 0.4°C. Samples were tested for its ice nucleation activity from -2 to -13°C at a constant rate of 0.5 or 1°C decrements. After a 30 sec dwell time at each temperature the Plexiglas plate was removed and the number of frozen droplets was recorded by a Panasonic Luminex DMC-FS3 digital camera. The different samples were compared by the median freezing temperature (T_{50}), which represents the temperature where 50 % of all droplets are frozen. The T_{50} was calculated with the equation reported by Kishimoto et al. [3]

$$T_{50} = \frac{T_1 + (T_2 - T_1)(2^{-1}n - F_1)}{(F_2 - F_1)}$$

where F1 and F2 are the number of frozen drops at temperature T1 and adjacent temperature T2, and are just below and above 50 % of the total number of tested drops (n).

The cumulative number N(T), of ice nuclei ml^{-1}active at a given temperature was calculated by an analogical variant of the equation of Vali [2] reported by Govindarajan and Lindow:[4]

$$N(T) = -\ln(f) \times \frac{10^D}{V}$$

where f = fraction of droplets unfrozen at temperature T, described as total number of droplets used divided by unfrozen droplets (N_0/ N_U), V = volume of each droplet used (10 µl), D = the number of 1:10 serial dilutions of the original suspension. N(T) was normalized for the number of cells present in each suspension to obtain the nucleation frequency (NF) per cell by dividing ice nuclei $^{-ml}$ through cell density ($cell^{-ml}$)[5] .

6.24 References

1. **EMA.** 1999. General Requirements for the Production and Control of Inactivated Mammalian Bacterial and Viral Vaccines for Veterinary Use. Association EM, http://ec.europa.eu/health/files/eudralex/vol-7/b/7blm2a_en.pdf.
2. **Vali G.** 1971. Quantitative Evaluation of Experimental Results an the Heterogeneous Freezing Nucleation of Supercooled Liquids. Journal of the Atmospheric Sciences **28:**402-409.
3. **Kishimoto T, Yamazaki H, Saruwatari A, Murakawa H, Sekozawa Y, Kuchitsu K, Price WS, Ishikawa M.** 2014. High ice nucleation activity located in blueberry stem bark is linked to primary freeze initiation and adaptive freezing behaviour of the bark. AoB Plants **6:**
4. **Govindarajan AG, Lindow SE.** 1988. Size of bacterial ice-nucleation sites measured in situ by radiation inactivation analysis. Proc Natl Acad Sci U S A **85:**1334-1338.
5. **Kassmannhuber J, Rauscher M, Schöner L, Witte A, Lubitz W.** 2017. Functional Display of Ice Nucleation Protein InaZ on the Surface of Bacterial Ghosts. Bioengineered doi:10.1080/21655979.2017.12847120-0.

7 Appendix

7.1 Summary of produced BG constructs

Graphic summary of the different BG-constructs carrying INP and truncated versions of INP in **Fig. 7.1.**

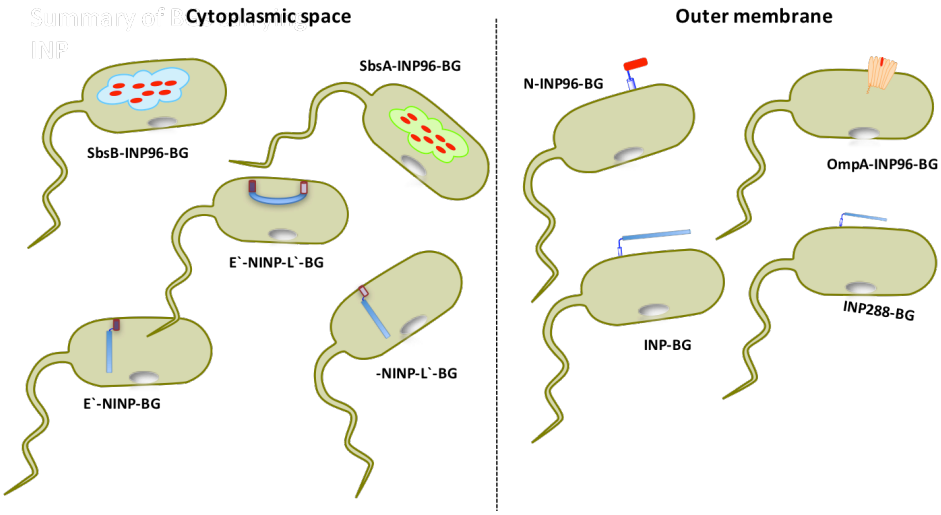

Figure 7.1. Summary of INP and truncated INP location in different domains of the BG envelope

7.2 Supplementary data for chapter 2.1

Supplementary data for the construction of the cooling device described in chapter 2.3 are illustrated in **Fig. 7.2**.

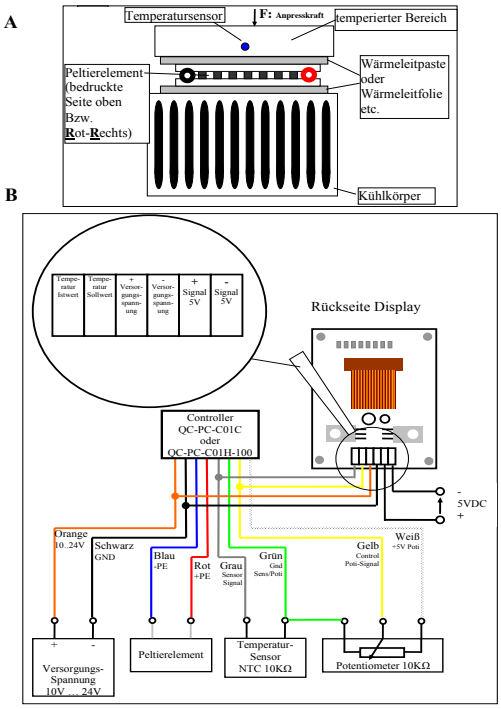

Figure 7.2. Instruction notes of Quick-Ohm (Quick-Ohm Küpper, Wuppertal, Germany) for construction of a cooling-device. **A**. Fundamental basic construction of the cooling-device. **B.** Graphic representation of the electric construction. (http://www.waermemanagement.com)

Pictures (**Fig. 7.2.1 and Fig. 7.2.2**) of the described cooling device used for droplet freezing assays.

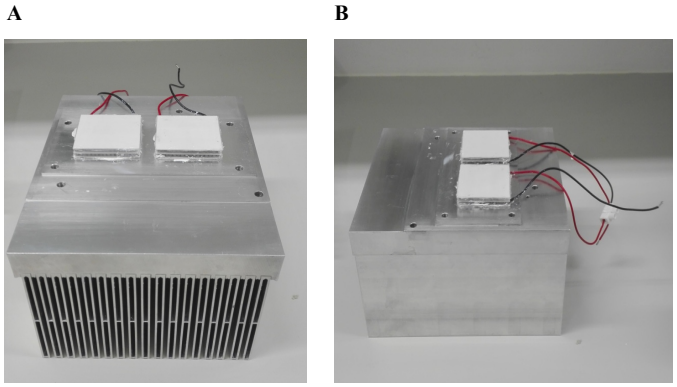

Figure 7.2.1 Photo-graphic pictures of the two-stage Peltier elements fixed with thermally conductive paste on the heat sink. A. Frontal view of the heat sink. B. Side view of the heat sink and the two in series circuited two-stage Peltier elements.

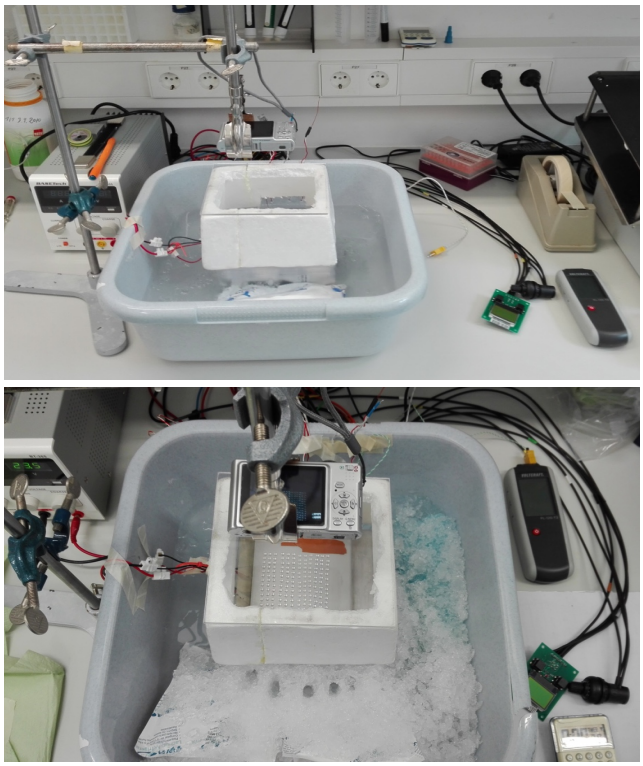

Figure 7.2.2. Photo-graphic pictures of the cooling-device used for the droplet-freezing assay

Captured photos during a droplet-freezing assay are shown in **Fig. 7.2.3.**

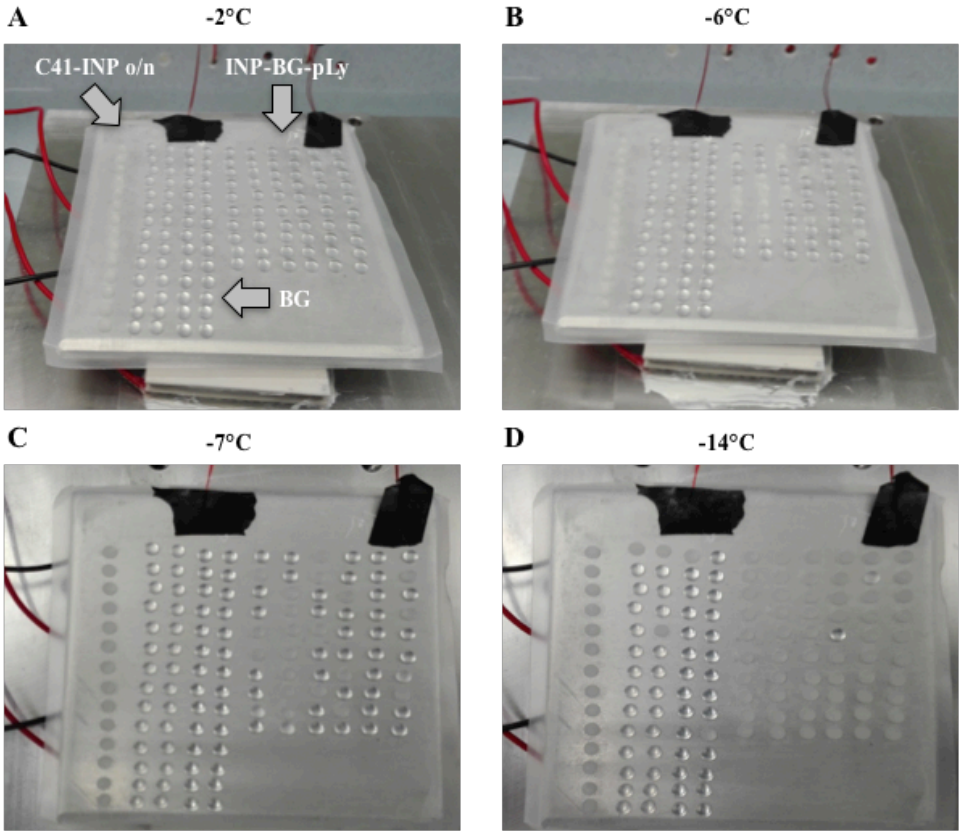

Figure 7.2.3. Photo-graphic pictures of a droplet-freezing assay. All used samples were resuspended in ROTISOLV® water and adjusted to a concentration of 5x 10^8 cells ml^{-1}. C41-INP o/n: one lane of 14 droplets on the very right side of the aluminum plate; BGs: four lanes of 14 droplets; INP-BGs-pLy: six lanes of 10 droplets. A. Aluminum plate was cooled to -4°C. B. Aluminum plate was cooled to -6°C. C. Aluminum plate was cooled to -7°C. D. Aluminum plate was cooled to -13°C. Liquid-droplets appear transparent, frozen-droplets appear translucent.